

#### 6 October 2025

# JERA Nex bp Comments on the Taranaki VTM Project

1. Contact Details									
Please ensure that you have authority to comment on the application on behalf of those named on this form.									
Org	anisation name (if relevant)	JE	RA Nex	bp					
Firs	t names								
Last	t name								
Pos	ition	Co	ountry N	Manager, Aotearoa New Zealand					
Pos	tal address								
Pho	ne number								
	ail (a valid email address enables us to naunicate efficiently with you)								
2.	We will email you draft conditions of consen	t for	your co	mment					
×	I can receive emails and my email address correct	is	I cannot receive emails and my postal address is correct						
3.	Please select the effects (positive or negative	e) tha	) that your comments address:						
$\boxtimes$	Economic Effects	$\boxtimes$	Sedimentation and Optical Water Quality Effects						
$\boxtimes$	Effects on Coastal Processes		Benth	ic Ecology and Primary Productivity Effects					
	Fished Species		□ Seabirds						
	Marine Mammals		Noise	Effects					
Human Health Effects of the Marine Discharge Activities			☑ Visual, Seascape and Natural Character Effects						
	Air Quality Effects		Effect	s on Existing Interests					
×	Other Considerations (please specify):								

Our comments are provided in the following pages.



#### **Taranaki VTM Project**

#### **Executive Summary**

These comments respond to an application by Trans-Tasman Resources Limited (*TTR*) for marine consents under the Fast-track Approvals Act 2024 to authorise a seabed mining project in the Taranaki Bight.

JERA Nex bp urges the Panel to decline the application on the basis that the economic benefits are not necessarily regionally or nationally significant, and in any event are outweighed by the adverse impacts. In particular, the likely loss of the nascent offshore wind industry for New Zealand and the adverse geotechnical impacts (not to mention the adverse environmental impacts which will be well addressed by others). The adverse impacts of TTR's Taranaki VTM project, including the impact of offshore wind projects not being able to proceed in the best sites of the South Taranaki Bight, are significant and out of proportion to the regional and national benefits thought to be offered by the proposed Taranaki VTM project. Critically, we believe the adverse impacts of the Taranaki VTM project cannot be corrected by modifying the application, and nor can they be avoided, remedied, mitigated, offset or otherwise compensated for by way of conditions of consent.

It is clear from the Taranaki VTM application that there are a number of significant adverse environmental impacts that would result from the project and we understand these will be addressed in detail by other concerned parties. Therefore, our comments primarily focus on the adverse economic and geotechnical impacts that would arise from the inability for offshore wind projects to proceed in the same, or a proximate, location as the project, which also happens to be the best location for offshore wind.

Principally, those impacts are:

- (a) the foregone electricity generation and decarbonisation resulting from offshore wind;
- (b) the foregoing, or loss of, the much more significant regional and national economic benefits that would flow from the construction and long-term operation of offshore wind projects and associated infrastructure (e.g. transmission and port upgrades); and
- (c) the significant risk of flow liquefaction that is likely to result from seabed mining of the type proposed by TTR for the Taranaki VTM project, rendering it impracticable and unsafe for jack-up vessels to operate in the same or proximate marine environments, whether for offshore wind purposes or for oil & gas purposes.

We elaborate on each of these points below.

We also urge the Panel to examine closely the claimed economic benefits of the Taranaki VTM Project, which we consider are significantly overstated. We have serious reservations as to whether the economic benefits claimed in respect of the Taranaki VTM Project are either regionally or nationally significant, for the reasons enunciated in the submission provided to the Panel by Taranaki Offshore Partnership. We endorse the contents of that submission but, as the material is already before the Panel, we do not repeat it here.



#### Introduction to JERA Nex bp

JERA Nex bp greatly appreciates the opportunity to provide comments on the Taranaki VTM Project and its implications on the offshore wind industry in Taranaki.

JERA Nex bp, headquartered in London with offices globally and a team of around 700 employees, is one of the world's largest offshore wind companies, with a significant portfolio of high-quality development projects and operating assets. This includes around 1GW of current net generating capacity, a 7.5GW development pipeline and an additional 4.5GW of secured leases. JERA Nex bp was specifically conceived as an offshore wind joint venture between JERA (incorporating specialist Belgian offshore wind developer Parkwind) and bp. Its ambition is to safely deliver the abundant, clean, secure and affordable energy the world needs as part of a competitive and sustainable global industry.

Our comments are made from the perspective of an experienced offshore wind developer who has developed, financed, and operated offshore since 2010. JERA Nex bp has built and operates seven offshore wind farms close to Belgium, Germany, UK, and Taiwan, with one of Japan's first offshore wind farms (Ishikari Bay) commissioned last year.

JERA Nex bp aspires to build a 500MW to 1GW offshore windfarm in New Zealand, to be operational by mid-2030. It wants to work in partnership with iwi and hapū, local communities, and selected experienced energy sector participants. As JERA Nex bp progresses its preliminary discussions and investigations, it is building strategic alliances that will benefit the eventual offshore project or projects in which it invests for the long-term benefit of Aotearoa New Zealand.

An example is the memorandum of understanding (*MOU*) signed with Meridian Energy to explore offshore wind generation in New Zealand waters. Efforts will focus principally on the Taranaki coast and will build on work already undertaken by JERA Nex bp, including engagement with stakeholders as well as the iwi of Taranaki.

#### **General comments**

JERA Nex bp is concerned that the approval of a seabed mining project in the South Taranaki region could fundamentally jeopardise any investment in New Zealand's emerging offshore wind industry.

#### The offshore wind opportunity for Taranaki and New Zealand

Seabed mining does not co-exist with offshore wind anywhere else in the world.

Offshore wind projects are long-term investments which require significant de-risking through the development phase. With the material risk that seabed mining creates, offshore wind investor confidence would be substantially impacted by the granting of approvals for such mining activities in South Taranaki.

Offshore wind will provide broader and longer-term economic development, increased energy security and supply, and a transition pathway for Taranaki's existing offshore energy workforce, infrastructure and supply chain. These will not be able to be achieved if the Taranaki VTM project proceeds. In short, the granting of the Taranaki VTM consents would jeopardise and potentially stop our investment, and the investment of others, in offshore wind in this location.

Offshore wind is a critical tool for New Zealand to reach its decarbonisation commitments, it can co-exist with other ocean-based activities such as customary, recreational and commercial fishing and aquaculture, and it is a mature technology which will support New Zealand's growing demand for renewable electricity. The last



significant scale generation built was the Clyde Dam in 1990. Continuing population growth, increased electrification and AI are strong trends that will see New Zealand's electricity supply under significant pressure in the 2030s unless there is significant generation built at scale.

South Taranaki offers a number of strategic advantages for offshore wind development:

- 1. World class wind resource; high average wind speeds resulting in a 75% higher energy yield than other sites on the west coast of the North Island.
- 2. Relatively shallow water depths and favourable seabed conditions for monopile foundations, the most cost-effective foundation type for offshore wind.
- 3. The above factors mean that the Pātea shelf off South Taranaki delivers the lowest levelised cost of energy (*LCOE*) of any offshore wind site in New Zealand and is, therefore, the most commercially attractive. There are other potential sites around New Zealand, but at this stage the LCOE they are likely to offer is unlikely to be attractive enough to warrant investment.
- 4. Access to nearby deepwater port infrastructure in New Plymouth.
- 5. Access to an experienced local offshore workforce and service industry.
- 6. Close proximity to existing 220kV transmission lines.

According to the recent Offshore Wind National Impact Study undertaken by PwC at the request of a number of businesses interested directly or indirectly in the offshore wind opportunity for New Zealand (including JERA Nex bp and several other offshore wind developers), New Zealand's offshore wind industry has the potential to:

- 1. generate between \$12b and \$94b¹ of Gross Domestic Product (*GDP*) over the life of the projects, half of which will be concentrated during the construction phase, and the other half during operations. By 2050, the economic impact of offshore wind could be as large as that of the oil and gas sector;
- 2. directly result in the abatement of 18 to 30% of New Zealand's energy emissions by 2050;
- 3. create 5,000 to 22,000³ jobs during the build-out phase, and 620 to 3,900 ongoing jobs during operations;
- 4. play a critical role in ensuring reliable electricity supply in the context of predicted demand growth; and
- 5. result in important benefits for our electricity system with more stable generation profiles when compared to other renewable generation, including improved output in winter months.<sup>4</sup>

The very wide range here is attributable to differences between the various projects then being planned by offshore wind developers, which were of differing size and scale, some also including offtake use by way of hydrogen production (in other words, the economic benefits of the offtake side were also included). We believe the realistic benefits are more likely to be at the lower end of the PwC range and flow from co-creation of new large scale industrial demand in the Taranaki region as well as electrification of existing industry and transport.

Similarly, emissions abatement depends on the use of the electricity generated.

Projected job numbers differ significantly depending on what the offshore wind plus end use project look like.

National Impacts Report: New Zealand Offshore Wind Industry (Final Embargoed - 20 March 2024)



#### Multiple benefits of offshore wind during energy transition

New Zealand requires significant new investment in renewable electricity generation to:

- 1. ensure reliable, resilient, affordable and sustainable energy supply to New Zealand households and prevent further de-industrialisation, build business confidence; promote investment in industry; and job retention and growth; and
- 2. decarbonise our economy to meet our 2050 net-zero commitments.

Recent studies by MBIE and PWC<sup>5</sup> estimate that New Zealand's electricity demand is set to grow significantly from 42TWh currently to as much as 110TWh. In order to meet this demand, new renewable generation capacity needs to be built at a rate of over 1,000MW per year.

Transpower's more conservative projections still require 500MW of new generation to be added each year until 2050 to meet the net zero target (to around 70TWh). New generation is happening but not fast enough. Since 2020 only 1.2GW of new generation has been built, half the necessary rate, according to Transpower. This, together with the rapid decline in gas available for electricity generation, has contributed to medium-term supply pressure, and prices on the forward electricity contracts market have roughly doubled over the last six years, from around \$90 MWh in 2019 to \$180 MWh today.

The availability of high-quality onshore wind sites in New Zealand is expected to lessen over the next decade. The best onshore locations are already under agreement, consented, under development, or built. As developers move to more marginal sites with lower wind speeds and more complex consenting requirements, the LCOE for onshore wind is expected to rise or plateau. Widespread deployment of onshore wind and grid-scale solar could lead to a lessening of 'social licence' for sufficient new generation to meet demand growth and decarbonisation goals. In contrast, offshore wind continues to benefit from rapid technological innovation, scale efficiencies, and maturing global supply chains — driving costs down and narrowing the LCOE gap with onshore alternatives.

This shift significantly strengthens the long-term economic case for offshore wind, particularly for large-scale, high-capacity projects like ours proposed in South Taranaki. In terms of capacity, PWC's report estimates that offshore wind could contribute from 2 to 15 GW by 2050 to help meet demand (by comparison, New Zealand's current midwinter peak load is 7 GW).

To help meet higher peak loads and rising electricity volumes, offshore wind is expected to play a critical role in our energy future due to the following strong advantages:

- 1. the ability to build projects at scale to rapidly ramp-up new generation;
- 2. higher capacity factors than other renewables, supplying more reliable electricity to the market, and in a way that complements onshore wind;
- 3. a winter-weighted generation profile, helping to ensure NZ has electricity supply when we need it most; and

https://www.mbie.govt.nz/dmsdocument/26911-interim-hydrogen-roadmap-pdf – figures based on Base Case scenario; https://www.pwc.co.nz/pdfs/2024/national-impacts-report-new-zealand-offshore-wind-industry-mar-2024.pdf - figures based on Electrification Plus scenario



4. the ability to mitigate impacts on communities and land use through its distant, offshore location.

#### Jera Nex bp's proposed \$5bn Taranaki wind farm would create jobs, enhance energy security

Over the past three years, JERA Nex bp has invested considerable time and capital investigating the development of a large-scale wind farm off the coast of South Taranaki. If delivered, it would become one of New Zealand's largest power stations. Our proposed 1GW project would generate a mean annual output of 4,620 GWh, similar to Manapōuri, more than double the Clyde Dam (2,160GWh) and more than all existing onshore wind farms combined in 2024 (3,920 GWh).

A highly productive offshore wind farm would have significant energy security benefits by preserving water stored in hydro schemes for when it is needed in dry years. If coupled with new flexible industrial offtakes, our project would provide significant demand response capacity – similar to the arrangement Meridian has with the Tiwai Aluminium Smelter. This offtake helped New Zealand get through the energy shortage of 2024.

In terms of economic gains, New Zealanders would benefit from \$5 billion in private sector investment and spending of around \$100 million annually on operations. This would support the Taranaki regional economy and create hundreds of high-value local jobs.

A number of international developers have been actively investigating offshore wind projects in Taranaki since 2021. Collectively, they have invested tens of millions of dollars in progressing project studies, engaging with the Government's emerging regulatory regime, and hiring local resources. However, several developers have already exited the country, with one saying that risk from seabed mining was a driver of the decision.<sup>6</sup>

#### Compatibility of offshore wind and seabed mining

Seabed mining in the Taranaki Bight would significantly hinder offshore wind development in South Taranaki on both technical and environmental grounds, resulting in a substantial lost opportunity impact.

#### Offshore wind assets cannot be built within an operational seabed mining project

A seabed mining project will significantly disrupt the seabed floor, up to a depth of 11 metres. Offshore wind turbines and electrical cables could not be constructed in the same location as an active seabed mining operation, resulting in the unavailability of that zone for offshore wind generation.

This means that the best zone in the country (due to the high wind speed and shallow waters) is unavailable for development.

For a long time after mining activities have ceased, offshore wind assets can not be built in an area which was previously subject to seabed mining.

There are no international precedents for offshore wind projects being built on areas previously subject to seabed mining. To supplement its own internal assessments, JERA Nex bp commissioned Fugro NV<sup>7</sup> to undertake a qualitative study to determine potential geotechnical and geomorphological effects associated with the seabed mining activities, and how they may affect development of an offshore wind farm in the area.

BlueFloat Energy withdraws from offshore wind projects in New Zealand citing regulatory uncertainty | 4C Offshore News

Fugro NV is a world-leading Dutch geotechnical consultancy with significant expertise in the offshore New Zealand environment.



Fugro, which has supported design of our offshore wind farms around the world, also undertook detailed geotechnical design of the Kupe platform under the former company Advanced Geomechanics, so it has good knowledge of the seabed characteristics in South Taranaki.

Please refer to Fugro's report in Appendix 1.

Key findings from section 2 of the report are:

- 1. Fugro determined that very loose tailings backfill from seabed mining are unlikely to densify (consolidate) under ambient wave conditions (i.e. the sea state present most of the time).
- 2. However, under storm conditions (e.g. one-year return or longer) and seismic conditions, the soil will be prone to liquefaction. The approximately 10 m of backfilled sediment is anticipated to liquefy to a depth of about three meters under a one-year return period storm and completely liquefy over the full back-fill depth under a 10 year storm. Earthquakes with 200-year (DLE) and 2,000-year (RIE) return periods are also expected to completely liquefy the backfilled sediment.
- 3. Flow liquefaction implies an almost complete loss of strength where the soil can transition to a state where it may 'flow' like a viscous fluid down slopes (similar to an underwater landslide/debris flow).
- 4. Liquefaction would be a serious risk and could compromise any infrastructure encountered (platform or turbine foundations, cables, pipelines, wells).
- 5. It would pose a serious hazard to any jack-up vessel servicing the area (see section 2.4 and Figure 1 below). Jack-up vessels equipped with heavy lift cranes are typically used to construct, maintain and decommission offshore infrastructure (ORE and oil & gas). Fugro notes the significant risk, and potential catastrophic consequences, of flow liquefaction should a vessel attempt to jack up on undensified tailings. This has not been recognised in the OCEL (2015) report 'Implications of Loose Tailings Seabed Material on Future Jack-Up Deployment in the South Taranaki Bight'.
- 6. Over the long term (i.e. geological time scales encompassing many millennia), it is anticipated that repetitions of large storm and seismic events will eventually densify the sediments to a state similar to their current in situ condition.
- 7. Given the above, if seabed mining activities proceed, it is highly unlikely offshore wind farms could be built in that same area for the foreseeable future.





Figure 1: A Jack-up vessel constructing an offshore wind turbine generator.

We have concerns, based on the findings presented by Fugro, that the material presented to the Panel by TTR is not necessarily complete or reliable.

#### Offshore wind assets may not be able to be built in areas adjacent or proximate to seabed mining permits

Fugro's analysis also determined that flow liquefaction can affect sites *outside* the mining area. In the event of seismic or storm conditions (e.g. 1 year return or longer), the soil can transition to a state where it may 'flow' like a viscous fluid (similar to an underwater landslide) down slope from the mining area. This could compromise any infrastructure or jack-up installation vessels operating in neighbouring areas.

While it is difficult to define a fixed minimum buffer distance due to variable seabed conditions, our studies suggest that areas downslope from mining operations are at greater risk of sediment movement and structural instability. As a result, ORE developers may be forced to site projects closer to shore (up slope from the mining area), increasing visual impacts and potentially conflicting with sensitive marine areas, as well as reducing the chance of those projects clearing a final investment decision. Flow liquefaction pathways affecting adjacent areas of the EEZ are indicated on Figure 2 below.



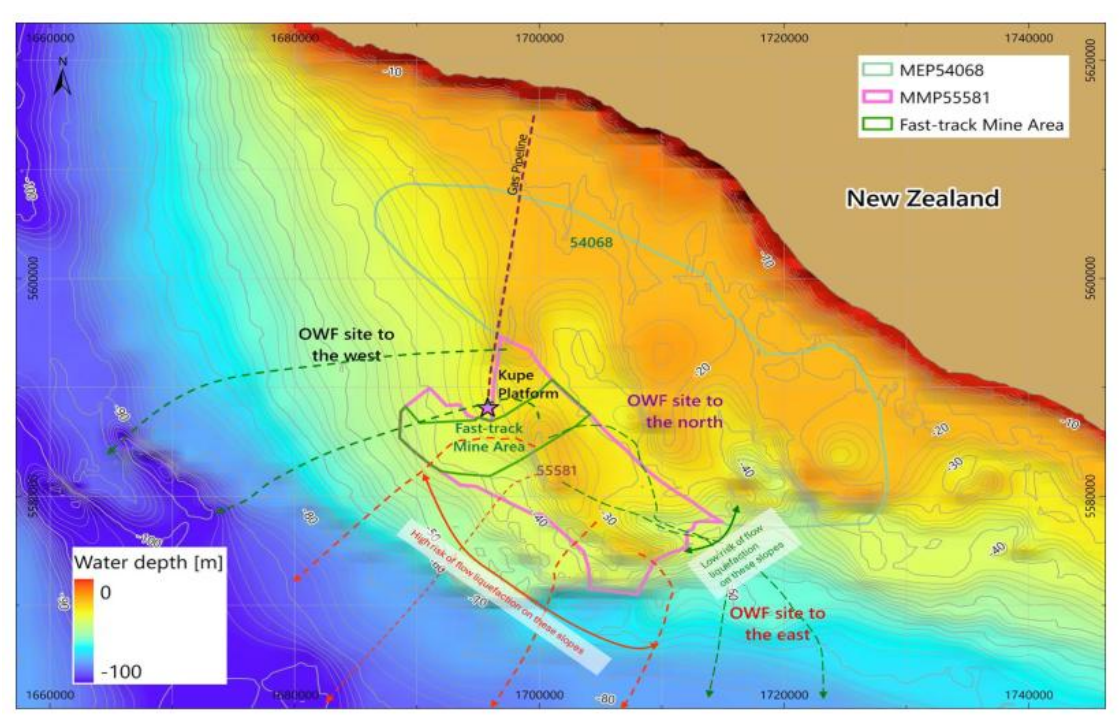


Plate 14: Potential Flow Paths from Seabed Mining Zone - Bathymetry

Figure 2: High risk (red) and low risk (green) flow paths of tailings debris initiated by flow liquefaction.

Figure 3 below shows the flow liquefaction pathways as they would affect the Kupe petroleum platform, potentially jeopardising any future development, servicing or decommissioning activity.

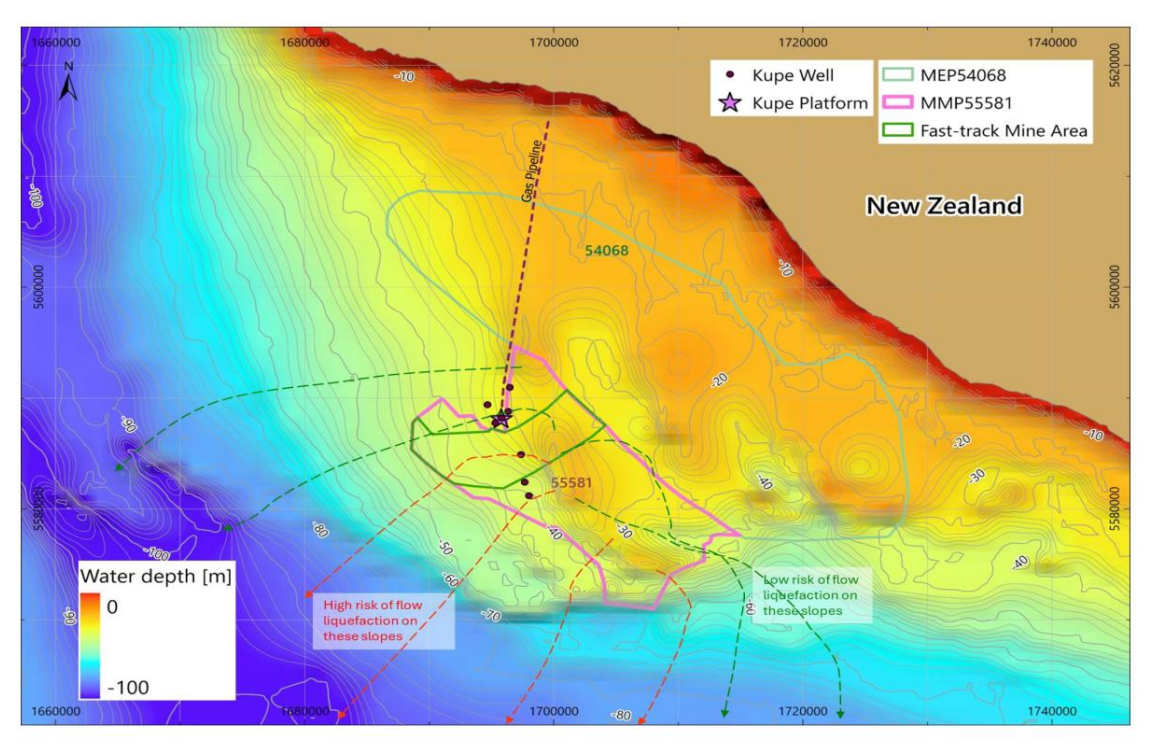


Plate 19: Potential Flow Paths from Seabed Mining Zone Around Existing Kupe Infrastructure

Figure 3 Liquefaction pathways.

Moreover, seabed mining in the South Taranaki Bight will result in adverse impacts on local ecological receptors in that region. Any other project development in the region – for example, our windfarm – when undertaking



an impact assessment and seeking a consent, will need to consider the cumulative effects of their own project and the seabed mining activity. While offshore wind development by itself may result in an acceptable level of impact, the prior existence of a seabed mining project could jeopardise the ability of offshore wind in the broader region to obtain a consent, due to consideration of cumulative effects. To be clear, this would not represent a risk only to offshore wind projects proposed in the exact same area as seabed mining, but also to any offshore wind projects proposed in the broad vicinity of the seabed mining activity. In summary, cumulative effects are another adverse impact that will deter offshore wind.

For all the reasons above, the granting of a consent to seabed mining projects in the South Taranaki Bight would significantly jeopardise any ongoing investment in South Taranaki offshore wind projects, due to the long-term technical and consenting constraints that would result from seabed mining potentially going ahead. Offshore wind projects are long-term investments which require significant de-risking through their development phase. With the material risks that potential seabed mining would create, offshore wind investor confidence would be substantially impacted by the granting of approvals to seabed mining activity in South Taranaki.

#### **Economic review**

While we acknowledge that seabed mining could generate its own economic benefits for New Zealand, we strongly encourage the Panel to commission its own review of TTR's material, especially in relation to jobs created. JERA Nex bp is aware of the review of economic benefits carried out by the Taranaki Offshore Partnership, as presented to the Panel, and endorses the outcomes of that study. In particular:

- The economic benefits of the Taranaki VTM Project are materially overstated and unlikely to be regionally or nationally significant.
- NZIER's analysis uses a static input-output (I-O) model to estimate the proposal's gross economic impacts. This approach is insufficient for a large, first-of-its-kind, capital-intensive proposal with material supply-side constraints and high delivery risk.
- The NZIER Report also inflates the proposal's likely economic benefits by including so-called induced impacts, which largely cancel out. Omitting them reduces the proposal's estimated economic impacts on GDP and employment by between 22% and 29%.
- Project deliverability risk is very high, in our view, but this is not captured in the NZIER report. TTR's
  challenging financial position, its lack of proven domestic operating capability, and the technical, regulatory,
  and social-licence hurdles associated with the Taranaki VTM Project materially diminish its likely benefits.
- The NZIER report's labour market assumptions are also optimistic. The Taranaki VTM project relies on specialised marine and mining support roles in a region with thin existing capacity; displacement of other activity and wage pressure are likely but are not captured by NZIER.

In addition, as explained above, we consider potential opportunity costs are material. We also point out that the NZIER report assesses economic impacts, whereas the criterion under the Act refers to economic benefits: in a national economic cost-benefit analysis, the two are not the same, and jobs can be regarded from an economic perspective as a cost, not a benefit. Jobs have an opportunity cost, unless there is substantial and involuntary unemployment in the economy. The true net economic benefits from a project are the sum of consumer and producer surplus (economic value added) created by the project.



#### Conclusion

Offshore wind is a critical tool for New Zealand to deploy in reaching its international decarbonisation commitments and is able to co-exist with other ocean-based activities such as customary, recreational and commercial fishing and aquaculture. It is a mature technology successfully deployed and being delivered today by JERA Nex bp in several other jurisdictions, it will assist significantly through scale to meet growing domestic electricity demand. In addition, offshore wind provides a strong opportunity for broader and longer-term economic development and jobs, increases energy security and supply, and provides a pathway for Taranaki's offshore energy workforce, infrastructure and supply chain.

The offshore wind industry is growing globally at a rapid pace with multiple jurisdictions competing for investment. Approval of the Taranaki VTM project would send a strong negative signal to not only global offshore wind developers but also to international supply chains and financial lenders with potential implications beyond Taranaki.

Thank you for the opportunity to provide these comments. Please contact us if you have questions or require more information on any aspect of our views. Finally, we would welcome the opportunity to speak to our comments if the Panel is minded to hold a hearing on the application.

Yours sincerely,



Country Manager New Zealand



Appendix 1: Report AGR-2269 Rev 0 by Fugro Australia Pty Ltd dated 16 September 2025: Qualitative Assessment on Co-existence of Seabed Mining and OWF Development, South Taranaki OWF

Please see attached PDF copy.



# Qualitative Assessment on Coexistence of Mining and OWF Development, South Taranaki OWF

Report | Offshore New Zealand

TANFU-GTS-TNO-2000-01

AGR-2269 Rev 0 | 16 September 2025 Issue for Use

**JERA NEX BP** 



# **Document Control**

## **Document Information**

Project Title	Report
Document Title	Qualitative Assessment on Coexistence of Mining and OWF Development, South Taranaki OWF
Fugro Project No.	273310
Fugro Document No.	AGR-2269
Issue Number	Rev 0
Issue Status	Issue for Use
Fugro Legal Entity	Fugro Australia Pty Ltd
Issuing Office Address	Level 1, Fugro Building, 1060 Hay Street, West Perth, WA 6005, Australia

# **Client Information**

Client	JERA NEX BP
Client Address	Sint-Maartenstraat 5, 3000 Leuven Belgium
Client Contact	
Client Document No.	TANFU-GTS-TNO-2000-01-Coexistence Of Mining And OWF Development

# **Document History**

Clien Issue	Issue	Date	Status	Comments on Content	Prepared By	Checked By	Approved By
00	Α	29Aug 2025	For Review	Awaiting client comments	SL/CO/BS/MC	CE/BS	SL
01	0	9 Sept 2025	For Use	-	SL/CO	CE/BS	SL
01b	0	16 Sept 2025	For Use	-	SL	CE/BS	SL





# **Executive Summary**

An offshore wind farm development planned by Jera Nex BP for the South Taranaki Bight, offshore New Zealand is located in an area of the seabed that is adjacent to a proposed seabed mining zone. The proposed seabed mining would involve extracting soils up to a depth of 11 m and processing the sediment to extract heavy minerals – expected to be around 10% of the mined sediment – and then discarding the remaining sediment into the mined pits.

At the request of Jera Nex BP, Fugro have undertaken qualitative assessments of potential geotechnical and geomorphological issues associated with the seabed mining activities that may have a negative effect on the offshore wind farm development. Note that the analysis reported in this report applies to both the area proposed in the Fast Track, Taranaki VTM application and the wider area covered by Minerals Mining Permit 55581(see Plate 14), which is assumed to be mined in a similar manner.

The main aspects considered were:

- Potential for liquefaction of the backfilled sediment in the mined pits, either from storm or seismic activity.
- Whether ambient metocean conditions could densify the backfill sufficiently such that if the sand did liquefy, it would not trigger a debris runout event.
- Potential for a heightened risk of scouring and seabed mobility within the offshore wind farm area.

It should be appreciated that the current assessment is based on regional geotechnical data available to Fugro, which has been collected from a limited part of the mining site. It is possible that other geotechnical conditions are also present, which could result in different conclusions to those presented below.

Fugro's geotechnical assessment indicates a strong likelihood that the backfilled sediment in the mined pits will be in a very loose state, with no reliable densification occurring over the operational timeframe of the offshore wind farm. Consequently, the approximately 10 m of backfilled sediment is anticipated to liquefy to a depth of about 3 m under a 1-year return period storm and completely liquefy over the full back-fill depth under either a 10- or 100-year storm. Earthquakes with 200-year (DLE) and 2,000-year (RIE) return periods are also expected to completely liquefy the backfilled sediment.

Given the very loose state of the backfill, there is a strong likelihood that should liquefaction occur, it will manifest as flow liquefaction where the material will have the potential to flow long distances, similar to a viscous fluid with very low strength. The seabed gradients at the site are very gentle (less than 2 degrees) but are considered sufficient to accelerate the flow mass such that a debris flow runout event may occur.

The topography of the site is such that a runout event is most likely to travel in either a westerly or south-westerly direction. Fugro's flow path assessment suggests that a flow event towards an OWF



site to the North of the mining site or an OWF site to the West of the mining site is unlikely, but that there is potential for flow events towards an OWF site to the East of the mining site. These risks may be mitigated by establishing mining exclusion zones between the proposed mining zone and the OWF sites. In lieu of detailed runout modelling, we cannot define how far such runout events might extend, but in lieu of such assessments we suggest a provisional exclusion zone comprising the entire western quarter of OWF site to the east of the mining area.

An observational strategy may also be considered, comprising CPT testing of the post-mined sediment to verify the density state of the backfilled sand. Follow-up CPTs at defined intervals could then be used to assess the real-world densification rate. If positive results are obtained these could be used to justify an easing of any precautionary restrictions initially imposed on the seabed mining operations.

Jack-up operations within the OWF sites would generally be subject to the same risks and impacts from the seabed mining as the OWF infrastructure. However, operating a jack-up directly on top of undensified mining backfill is not recommended since this presents a significant risk of storm or seismic-induced flow liquefaction failure. This could lead to catastrophic collapse and total loss of the jack-up rig.

Beyond the risks of flow liquefaction induced runouts into the proposed OWF areas, Fugro does not perceive any geotechnical issues that necessitate significant buffer zones between the proposed OWF and mining zones. In such cases, a minimum acceptable buffer zone can be adopted that is sufficient to permit any jackup rigs required for OWF construction and support operations to always have all their feet resting entirely on in situ unmined soil. It is suggested that recommendations are sought from relevant jack-up operators as to how far this zone should extend from the OWF infrastructure. Fugro's geomorphological assessment has investigated the sediment dynamics in the South Taranaki Bight, focusing on the implications of offshore mining activities and wave-induced transport processes within designated Areas of Interest (AOIs). The shoreline and seabed are highly mobile due to a wave-dominated sediment transport regime, with bidirectional longshore drift primarily toward the southeast. Surface sediments are routinely mobilised under typical wave conditions, while storm waves and rare tidal currents (≥1-year return) may resuspend sediments even at deeper AOI locations. In situ sediments have high specific density owing to heavy minerals. Despite having a lower specific density, laboratory testing suggests dumped mining sediments are expected to exhibit similar seabed mobility susceptibility, with larger fines content and potentially subject to flocculation. Disruption of surficial crusts, reefs, and hard grounds may enhance vulnerability to sediment movement and ripple formation, although large sediment waves are considered unlikely due to modest tidal currents.



# **Contents**

Exec	cutive Summar	/	
1.	Introduction		1
1.1	Project Backg	round	1
1.2	Data Source		1
1.3	Scope of Wor	k	2
1.4	Use of Report		4
2.	Geotechnical	Qualitative Assessment	5
2.1	Properties of	Pre-Mined and Post-Mined Sediments	5
	2.1.1 Specif	ic Gravity, G₅	5
	2.1.2 Grain	Size Distributions	5
	2.1.3 Relativ	ve Density	5
	2.1.4 Draina	age and Consolidation	6
2.2	Potential Liqu	efaction and Densification of Post-mined Material	7
	2.2.1 Flow L	iquefaction Versus 'Cyclic Mobility' Liquefaction	7
		sment Under Ambient and Storm Metocean Conditions	8
	theore depth deploy very u appro	aside, we note that engineered techniques such as vibro-compaction may be tically feasible to densify the post mined tailings over their full depth in wat sup to 50 meters. However, this would require specialised vibroflot equipmed from barges or jack-up platforms (but see Section 2.4). We consider that nlikely to be economically or practically viable at the scale required in this case. 10 million cubic metres of densified soil for each 1 km <sup>2</sup> of mined Assessment of Seismic-Induced Liquefaction	ter ent it this is
2.3		y Considerations	15
2.5	•	ple of Flow Liquefaction on Very Gentle Slope, Palu Earthquake, Indonesia	15
	•	pecific Risk of Flow Failures and Runouts	16
2.4		Jack-up Operability	17
		ssion on Static Penetration Depths Within Mining Site	20
2.5		and Recommendations – Geotechnical Assessment	20
3.	Geomorphol	ogical Qualitative Assessment	23
3.1	Background		23
3.2	Regional Con	text	23
	3.2.1 Geolo	gical Settings and Sedimentary Environment	23
	3.2.2 Ocean	ography and Sediment Dynamics	24
3.3	Sediment Mo	bility	25
	3.3.1 Critica	I Bed Shear Stress	25
	3.3.2 Poten	tial for Sediment Mobility	27
3.4	Conclusions a	and Recommendations – Geomorphological Assessment	28
4.	References		30



33

**List of Plates** 



# **Tables in the Main Text**

Table 1.1: A Summar	y of Relevant Documents	for the Current Stu	ıdv

1

Table 3.1: Geotechnical parameters for in situ materials and materials originating from the iron sand extraction process

Table 3.2: Metocean data and corresponding induced shear stress for different design criteria at Kupe platform (ASR, 2004)

# **Abbreviations**

AOI	Areas of Interest
CFD	Computational Fluid Dynamics
СРТ	Cone Penetration Test
CRR	Cyclic Resistance Ratio
CSR	Cyclic Stress Ratio
DLE	Ductility Level Earthquake
ISO	International Organization for Standardization
NZ	New Zealand
O&G	Oil and Gas
OSS	Offshore Sub-Station
OWF	Offshore Wind Farm
PGA	Peak Ground Acceleration
RIE	Rare Intensity Earthquake
STB	South Taranaki Bight
WTG	Wind Turbine Generator



# 1. Introduction

## 1.1 Project Background

Jera Nex BP is planning an offshore wind farm (OWF) development in the South Taranaki Bight, offshore New Zealand (NZ). Meanwhile, the NZ government is considering allowing seabed mining activities and OWF development to coexist in the same region, adjacent to each other but not within the same area. The seabed mining involves extracting soils up to 11 m below the surrounding seabed, retaining about 10% for its iron ore content, and backfilling approximately 90% of the remaining soils into the mined pits.

Jera Nex BP has requested Fugro to perform a qualitative assessment to assess a potential buffer zone between the two activities from geotechnical and geomorphological perspectives (related to WTG and OSS foundations). The key questions to be addressed are:

- What is considered a safe buffer from the seabed mining operation to safely develop, construct, operate, and decommission the OWF? A nominal 500m buffer zone may be considered as a starting point based on regulations from other parts of the world.
- Will the backfilled materials have the potential to liquefy under an earthquake or wave action, subsequently triggering retrogressive slope failure at the mining pits and/or mass transport deposits that could compromise the nearby wind turbine generator (WTG) foundations?
- Will seabed mining potentially worsen scouring and seabed mobility within the OWF area, given that the backfilled materials are expected to be looser than their original state?
- Are there any other potential impacts throughout the project life cycle? (from site investigation, construction, operation, to decommissioning)

#### 1.2 Data Source

A summary of the data sources relevant to the current study is presented in Table 1.1.

Table 1.1: A Summary of Relevant Documents for the Current Study

Year	Document Titles	Relevance to Study		
2025	Request for quotation, co-existence with seabed mining at South Taranaki wind farm	Project Scoping and Background Information		
2016	Impact Assessment - South Taranaki Bight Offshore Iron Sand Extraction and Processing Project" and "Appendices to Impact Assessment - South Taranaki Bight Offshore Iron Sand Extraction and Processing Project	Assessment of properties of post- mined material, Assessment of geological, oceanographic and morphodynamical environment,		
2019	Implications of Loose Tailings Seabed Material on Future Jack- up Deployment in the South Taranaki Bight	Jack-up operability in adjacent to		
2025	Taranaki VTM Project – Fast-track act application: Section 5.14.4 Jack -up Deployment Impacts	or on the mining site.		



Year	Document Titles	Relevance to Study			
2004	Kupe Metocean Design Criteria - Environment Statistics for Design	Assessment of the percentage of exceedance of certain current and			
2022	Metocean DataCube for the South Taranaki Bight, New Zealand	wave magnitudes			
2004	Geotechnical Report - KUPE South Field Development Geotechnical Investigation, Offshore New Zealand	A			
2022	Recommendation for the Exemption of CPT Acquisition at Kupe Wellhead Platform Area Phase 2 Development Drilling Programme-Geotechnical Properties of the Seabed	Assessment of properties of in-situ pre-mined material.			

# 1.3 Scope of Work

The following activities were conducted:

#### A. Literature Review:

Fugro will review a list of relevant documents as described in Section 1.2.

#### B. Geotechnical Qualitative Assessment:

Fugro will provide qualitative geotechnical assessments including:

- a. Review the material properties of the in-situ material and assess potential properties of the resulting backfill material.
- b. Discuss liquefaction potential and densification of the in situ and backfilled materials when subjected to day-to-day and storm condition wave actions and seismic events (to support the arguments made, simple hand calculations will be made of induced shear stresses across the backfill thickness under different levels of wave loading and seismic events which may densify or liquefy the backfill).
- c. Using the results from a), review metocean data and potential seismic events and discuss potential for wave or seismic-induced liquefaction or densification of the backfill material.
- d. Discuss potential for retrogressive slope failure at the perimeter boundary of the mining pit and impacts to the nearby offshore wind farm. Given that the seabed elevation of an OWF site to the East of the mining site is lower than the mining sites, discuss the potential for soil flow from the mining pits into an OWF site to the East of the mining site.
- e. A nominal buffer zone of 500m will be initially considered and discussion may include if this buffer zone can be lesser or higher.
- f. Comment on the implications of operating a jack-up vessel on or adjacent to a premined site.

#### C. Geomorphological Qualitative Assessment:

- Fugro will review the physical geological, oceanographic and morpho-dynamical environment of the Study area, based on the review of previous studies including the NIWA Phase 2 report by Hume et al. (2013; updated 2015) and the TTR (Trans-Talisman Resources) Impact Assessment report from 2016.
- 2. Fugro will review the Metocean data from global and regional hindcast models to inform on the percentage of exceedance of certain current and wave magnitudes.



- 3. Fugro will review the presence of existing seabed bedforms for instance in the form of erosional ridges nearshore trending to depositional further offshore, documented in relevant literature. The abovementioned reviews aim to inform on an understanding of the regional processes considering tidal currents, waves and storms that govern sediment mobility.
- 4. Fugro will assess the susceptibility to sediment mobilisation by establishing critical Shield exceedance curves for representative sediment sizes, the properties of the preexisting seafloor and the estimated disposed mining spoils.
- 5. The anticipated patterns of future evolution will be discussed, in light of the dominant directions of tidal currents and waves, as well as the topology of the coastal shelf and seabed gradients in the area bordering the planned mining area and the wind development area.
- 6. Conclusions regarding the risks for the wind farm development will be drawn to assist with the definition of a safe separation distance from the competing mining activities, as well as recommendations for site investigations, monitoring, and further studies.



## 1.4 Use of Report

This Report and its contents have been prepared for the purposes set out in the agreed scope of work, which forms part of the contract between Fugro and JERA NEX BP in relation to the qualitative study on the coexistence of seabed mining and offshore windfarm development. This Report and its contents are provided solely for the use of JERA NEX BP for the agreed purpose and are not to be used or relied on outside of that purpose. The Report is to be read and used in its entirety and in the context of the methodology, procedures and techniques used, and the circumstances and constraints under which the report was written. Sections or parts of the Report should not be read or relied upon out of context.

The technical work has been conducted, and this Report has been prepared, based on the assumptions identified in the Report and, where indicated in the Report, on information and data supplied by others. Fugro accepts no liability for any omission or inaccuracy in the information or data supplied by JERA NEX BP or its agents.



# 2. Geotechnical Qualitative Assessment

# 2.1 Properties of Pre-Mined and Post-Mined Sediments

#### 2.1.1 Specific Gravity, G<sub>s</sub>

Regional measurements of the in-situ specific gravity over the upper 10 m of the seabed show a reduction from approximately  $G_s = 2.9$  at the seabed surface to around  $G_s = 2.7$  at a depth of z = 10 m (see Plate 1a). These are higher than the specific gravity of silica sand ( $G_s = 2.65$ ) by up to 10%, indicating the presence of higher density minerals and is consistent with the 10% by volume of material expected to be retained during mining.

As the mining process is expected to retain the higher density portion of the excavated sand, it is reasonable to assume that the redeposited backfill material with have a specific gravity close to that of silica sand, i.e.,  $G_s = 2.65$ .

#### 2.1.2 Grain Size Distributions

Regional measurements of particle size distribution for the upper 10 m of the seabed are presented on Plate 2 and indicate that the in situ material within this depth range can be classified as a fine sand, with a medium particle size ( $d_{50}$ ) in the range from 0.15 to 0.22 mm, 10% passing particle size ( $d_{10}$ ) from 80 to 150  $\mu$ m and a fines content of approximately between 2% and 4%.

According to HR Wallingford (2014), the mined sediment is expected to undergo a series of processing steps. Initially, particles larger than 3.5mm are removed, followed by a two-stage magnetic separation process that eliminates non-magnetic materials. The remaining sediment is then split into coarse and fine fractions, with the coarse portion directed to a milling machine for grinding.

Since approximately 90% of the mined material is expected to be redeposited, the redeposited material is anticipated to contain a higher fines content than the in-situ material. Whilst there are insufficient data available to quantify how this might change the particle size distribution, a higher fines content will have the effect of reducing  $d_{10}$ , which would in turn reduce the in situ permeability, as discussed further in Section 2.1.4.

#### 2.1.3 Relative Density

Interpretation of cone penetration test data at the Kupe development (AG, 2004) suggests the in-situ sediment exhibits a high relative density state, with  $D_r > 85\%$ . This very dense sand state is consistent with void ratio (e<sub>0</sub>) measurements, typically ranging from 0.6 to 0.8 over the upper 10 m of the soil profile, and also with measured peak friction angles, exceeding 40 degrees.

Descriptions of the sediment processing (in the Trans-Tasman Resources, TTRL Offshore Irons Sand Project Description) indicate that redeposition of the backfilled sand would involve



discharging the sand through a 'disposal pipe' from a height of around 4 m above the redeposited surface. Relative density is expected to be very low for deposition in water and independent of fall height as: 1) terminal velocity is reached very quickly and 2) terminal velocity is much lower due to (water) drag acting on falling soil particles. This assumption is consistent with laboratory experience preparing pluviated sand samples (Lagioia et al. 2006; Raghunandan et al., 2012). Fugro's assessment is that the backfilled material will likely be at a very low initial relative density state, taken here as  $D_r = 0.2$ .

Assessment of the regional in-situ data indicates minimum and maximum void ratios of  $e_{min}$  = 0.65 and  $e_{max}$  = 1.0 (see Plate 1b). For the current assessment, the initial void ratio of the backfilled sand is therefore assumed to be as shown on Plate 1c, reducing from e = 0.93 ( $D_r = 0.2$ ) at the surface of the backfilled sand (z = 0 m) to e = 0.89 ( $D_r = 0.31$ ) at the base of the backfilled sand (z = 10 m). This slight increase in relative density with depth is due to densification associated under the overburden stress imposed by the overlying sand.

The average specific volume of the backfill is estimated as 1.91 as compared to 1.7 for the insitu soil at 85% relative density. This means the soil will 'bulk up' by around 12%, which exceeds the 10% initial volume removed. Hence, the backfilled seabed is likely to be at a very similar (slightly higher) level as compared to the pre-mined in-situ seabed.

#### 2.1.4 Drainage and Consolidation

As discussed in AG (2004), regional measurements of permeability in the upper 10 m of the seabed are typically in the order of  $k = 2 \times 10^{-5}$  m/s. This is consistent with permeability assessment using Hazen's formula (Equation 2.1), which is often used to assess the likely permeability based on particle size distribution data.

$$k = C_k d_{10}^2$$

Equation 2.1

where the constant,  $C_k = 8$  to 12 (mms)<sup>-1</sup> for clean sands. Adopting a median  $C_k = 10$  (mms)<sup>-1</sup> results in an estimated permeability in the range,  $k = 2.3 \times 10^{-5}$  m/s to  $6.4 \times 10^{-5}$  m/s, which agrees well with the measured,  $k = 2 \times 10^{-5}$  m/s (particularly as permeability is subject to very high variation; generally, at least one order of magnitude can be expected).

As noted in Section 2.1.2, the proposed mining processes involve grinding, such that the redeposited sediment will have a higher fines content than the in-situ sediment. Although it is unclear as to the amount of material that would be subjected to grinding, a conservative estimate of 10% is all that would be needed to significantly alter the permeability, as permeability is strongly dependent on  $d_{10}$ . Particle size distributions of sand recovered from the site and subjected to grinding (as reported in HR Wallingford, 2014) indicate  $d_{10}$  of around 10 microns, which all other things being equal, could reduce permeability by 100-fold to  $k = 2 \times 10^{-7}$  m/s.

In contrast, the decreasing density will tend to increase the permeability. Following Kozeny-Carman (Carrier III, 2003), k may be considered approximately proportional to  $e^3/(1+e)$ .



Hence, for the anticipated change in average void ratio, the permeability may be anticipated to increase by a factor of 2 from the in-situ to backfill condition, all other things being equal.

The proposed mining and redeposition processes are also anticipated to reduce the post-mined constrained modulus (M) of the sediment. Typically for coarse-grained materials, constrained modulus is approximately 4-5 times the measured cone resistance (q<sub>c</sub>) (Lunne et. al.,1997). A reduction of the relative density of sediments from 85% to 20% in the mining process would therefore imply a reduction of M by at least 4-5 fold.

Combining the overall net increase in permeability with the reduction in bulk modulus, the coefficient of consolidation ( $c_v$ ) of the post-mined sediments would then be at least 200 – 250 times lower than for the in-situ sediments.

Whilst the inclusion of plastic fines (i.e. derived from clay minerals) into the soil matrix generally reduces the risk of liquefaction, the same is not generally true for non-plastic fines, such as those anticipated to be created from grinding the in-situ sand. In fact, the opposite can be expected; the reduction in coefficient of consolidation caused by adding fines will impede drainage, such that any reduction in soil strength due to excess pore pressure development will persist for a longer duration, thereby increasing the risk of a liquefaction event under application of lower frequency cyclic shear stresses (such as induced by waves).

## 2.2 Potential Liquefaction and Densification of Post-mined Material

### 2.2.1 Flow Liquefaction Versus 'Cyclic Mobility' Liquefaction

One of the most critical aspects in cyclic soil testing is to investigate whether soil liquefaction may occur, and if so, what type of liquefaction can be expected (see Lam, et. al. 2023; Lam, et. al. 2025). Generally, typical offshore subsea sediments will have been subjected to waveinduced cyclic loading of various magnitudes over geological time scales, leading to progressive densification over time. Such sediments may also have been over-consolidated via erosion and soil 'ageing'. Such soils generally exhibit a specific type of liquefaction termed 'cyclic mobility'. Cyclic mobility can be illustrated conceptually in a cyclic simple shear test, as for instance shown on Plate 3a. It is a progressive cycle-by-cycle accumulation process of excess pore pressure and shear strain leading to an incremental reduction in soil stiffness. Upon soil 'liquefaction', the excess pore pressure momentarily equals the total mean stress (i.e. the mean effective stress is zero) and the soil loses its shear stiffness. However, it can regain stiffness and strength once shearing past the neutral stress position, due to the intrinsically dilative nature of the material at such low effective stresses. During a post-cyclic shearing phase, the majority of the original soil strength can generally be re-mobilised, and the 'damage' is reversible once the excess pore pressure dissipates. Hence, while cyclic mobility does not usually have much impact on the soil 'strength' the large reduction in stiffness can nevertheless result in the development of large permanent settlements and tilts of any foundation systems sitting on the soil. On a sloping seabed, cyclic mobility would be expected to cause down-slope lateral spreading, but not catastrophic slope failures.



The second type of cyclic liquefaction is exhibited by inherently loose sandy soil that substantially contract and generate very high excess pore pressure during monotonic shear, with no/ minimal large strain dilative phase. This causes the effective stresses to reduce close to zero and stay at very low levels. This condition is termed "flow liquefaction" and is illustrated on Plate 3b. With this scenario, the initial cycling process is very similar to its cyclic mobility counterpart, however, upon 'liquefaction', the soil exhibits a 'brittle' contractile failure that involves a significant reduction in both soil strength and stiffness. The post-cyclic monotonic strength is often close to zero in this case. The sudden decrease in strength associated with flow liquefaction may be so large that essential static shear stresses (e.g. those required to sustain a sloping seabed, or to support the static weight of a structure) can no longer be supported. In this case, catastrophic failure of seabed slopes and collapse of structures and foundations can be anticipated. Identification of the potential for any flow liquefaction-prone material is therefore a critical task.

For the reasons discussed below such sediments are not normally encountered offshore, except in a potential surficial and thin layer of mobile sediment. However, we anticipate that redeposited mining tailings will initially be in a very loose state, as discussed in Section 2.1.3, and hence assessment of flow liquefaction is a critical risk.

Cyclic shear stresses induced within the seabed – either from a storm or from a seismic event are the mechanism that may trigger flow liquefaction. Over the geological time scale relevant to deposition of in-situ sediment (i.e. many millennia), it can be expected that there will have been numerous storm events that will have densified (and potentially liquefied) the sediment to its current in situ state, which regional data indicates to be very dense. However, these time scales are several orders of magnitude longer than the operating life for an OWF, such that the only densification that can reliably be assumed to occur in the redeposited backfill is that associated with wave-induced shear stresses imparted from ambient metocean conditions. Rare storm or seismic events may induce liquefaction in the backfilled sand, so the key question in this case is whether prior ambient metocean conditions will have reliably densified the sediment sufficiently such that the resulting liquefaction will manifest as cyclic mobility instead of flow liquefaction. The former is not expected to have a negative impact on the proposed OWF development, as it is expected to only cause local ground settlement, but not a slope failure with a run-out event. In contrast, the latter may result in a run-out event that could have a significant impact on the OWF development, depending on the likely direction of the run-out and on the residual strength of the liquefied sediments.

#### 2.2.2 Assessment Under Ambient and Storm Metocean Conditions

#### 2.2.2.1 Metocean Conditions

Available metocean data for the location shown on Plate 4 (which is in the proximity of the Kupe well head platform at a water depth of 35 m) are reported in ASR (2004) and Oceanum (2022). ASR (2004) report data from short-term waverider buoy measurements at the Kupe platform over the period July to September 2004 in addition to presenting



statistical data from hindcast modelling. The Oceanum (2022) study provides statistical data from hindcast modelling over a 21-year period (1999-2019), validated by comparing significant wave heights produced by the hindcast model with measurements from the Kupe well head platform over the period 2010-2021.

Statistical distributions for both datasets are provided on Plate 5 and are seen to be generally consistent. The Oceanum (2022) statistical data are used here to inform the likely ambient metocean conditions for the OWF development. These are considered more representative of the ambient metocean conditions at the site as they pertain to a much longer monitoring period and represent the observed wave height measurements at the Kupe platform.

Wave statistical data from Oceanum (2022) are summarised in Table 2.1, which indicates the most prevalent 'ambient' annual wave conditions comprise significant wave heights in the range,  $H_s = 1 - 2$  m with peak wave periods in the range,  $T_p = 12 - 15$  s, and waves with  $H_s = 2 - 3$  m and  $T_p = 6 - 8$  s.

Metocean data for storm conditions with 1-, 10- and 100-year return periods are taken from ASR (2004), and are described by the following combinations of significant wave height and peak wave period:

- 1-year return period  $H_s = 5.5$  m,  $T_p = 8.8$  s;
- 10-year return period  $H_s = 7.3$  m,  $T_p = 10.7$  s;
- 100-year return period  $H_s = 9.3$  m,  $T_p = 11.7$  s.

#### 2.2.2.2 Assessment of Wave-induced Liquefaction

The potential for wave-induced liquefaction has been assessed by considering the cyclic shear stresses induced by wave action and comparing these to the magnitude of cyclic shear stress that could be expected to initiate liquefaction. The latter, termed the cyclic resistance ratio (CRR), is assessed as a function of the expected cone resistance, q<sub>c</sub>, of the backfilled sand based on published relationships and regional data. In lieu of measured data in the post-mined backfill, an appropriate cone resistance has been estimated using the correlation proposed by Baldi et al. (1986), corrected to obtain the equivalent cone resistance, q<sub>c1</sub>, at a reference overburden pressure equal to 100 kPa:

$$q_{c1} = \frac{1.8}{0.8 + (\sigma'_{VO}/100)} q_c$$

Equation 2.2

Both the expected cone resistance,  $q_c$ , and the corrected cone resistance,  $q_{c1}$  are presented against depth on Plate 6.

The cyclic stress ratio (CSR =  $\tau/\sigma'_{v0}$ ) induced by wave action is calculated as a function of wave height, wave period and depth below the seabed using the standard equations for periodic loading of a homogenous elastic seabed, based on linear wave theory (e.g. see Ishihara and Yamazaki, 1983).



Plate 7 presents the corrected cone resistance,  $q_{c1}$ , (which is a proxy for depth) as a function of the cyclic stress ratio (CSR =  $\tau/\sigma'_{v0}$ ) induced under the peak stresses that may be expected during the most onerous ambient metocean condition (Case 6 in Table 2.2) and for each of the three design storm scenarios (1-yr, 10-yr and 100-yr RP; Table 2.3).

Plate 7 also shows the cyclic resistance ratio (CRR), defined as the critical normalised cyclic shear stress at which liquefaction may be expected to initiate. Plate 7 includes a limiting CRR criteria derived from the regional Kupe cyclic simple shear tests (for 20 cycles of two-way loading at a shear strain of 15%; AG,  $2004^{1}$ ). However, it should be appreciated that the Kupe cyclic simple shear tests were performed on samples with an average relative density,  $D_r = 75\%$  (and hence reflect rather high  $q_{c1}$ ) and are therefore heavily extrapolated for the much lower  $q_{c1}$  expected for the mined backfill.

For comparison, Plate 7 also includes the CRR design criteria from Stark and Olsen (1995) for clean silica sand, which are derived from onshore field observed cases of seismic-induced liquefaction in soils with a wide range of relative density.

Although there are no cyclic test results for Kupe sands at the very low relative density expected in the backfilled state, a large database of cyclic triaxial test data has been summarised in Jefferies and Been (2016) (presented here on Plate 7a), which provides useful guidance. Specifically, these tests indicate that a CRR of 0.08 may be assumed as a credible lower bound for triggering liquefaction (which would manifest as flow liquefaction at such low densities). This lower limit of CRR = 0.08 is therefore also included on Plate 7b.

The factor of safety against wave-induced liquefaction may be calculated as  $F_{w-l} = CRR/CSR$ . For the current assessment, the limiting CRR criterion has been defined as per Plate 7b, with a lower bound CRR = 0.08 up to a corrected cone resistance,  $q_{c1} = 3.9$  MPa and then with CRR increasing linearly with  $q_{c1}$  at higher corrected cone resistances, following the Kupe simple shear profile. The maximum corrected cone resistance is estimated as  $q_{c1} = 4.1$  MPa in the backfilled sand (using Baldi et al., 1986) at a relative density,  $D_r = 0.2$  and at the maximum backfill depth of 10 m (see Plate 6). As a result, the lower bound CRR = 0.08 effectively applies to almost the entire depth of backfilled sand.

Depth profiles of calculated  $F_{w-l}$  are presented on Plate 8, which shows a minimum factor of safety under ambient conditions of  $F_{w-l} = 1.83$  at the seabed, increasing to  $F_{w-l} = 3.69$  at the base of the backfilled sand. In contrast, under 1-year storm conditions the factor of safety against wave-induced liquefaction is estimated to be less than unity up to z = 3.1 m, and less than unity over the entire 10 m backfill depth for 10-year or 100-year return period storms. Hence, it can be concluded that the upper 3 m of sediment may be expected to liquefy

**fucko** 

<sup>&</sup>lt;sup>1</sup> Real seas will impose continuous cyclic loading on the seabed. However, when assessing liquefaction risk, it is found that only the few largest cycles associated with any metocean condition will control the soil response and drainage of accumulated excess pore pressures between cycles means that the soil only 'remembers' the load cycles imposed upon it for short periods of time. Fugro's experience indicates that in clean sands, an equivalent number of cycles (each of the maximum induced by a specific sea state) of around 3 to 5 is reasonable, and this might increase to around 20 cycles for finer grained materials, such as expected for the mined backfill.

during a 1-year return period storm, while the entire 10 m of backfill sediment may be expected to liquefy during 10-yr or 100-yr return period storms.

The liquefaction scenarios described above are only strictly applicable if the specified return period event is the first significant storm event that occurs post-backfilling. Any sediment that does not 'flow away' will reconsolidate and progressively move to a denser state after each successive storm event and hence will exhibit a progressive enhancement in liquefaction resistance during any future events. This does not mean that liquefaction cannot occur after the first major storm event, but it does mean that the risk (and consequences) of the most dangerous type of flow liquefaction is reduced. In the unlikely event that the first major storm were a 10-yr or 100-yr RP storm event (or anything in between), the volume of likely liquefied deposit is anticipated to be more than 3 times greater than resulting from a 1-yr storm. The larger liquefied masses associated with these longer return period events can be expected to increase the risk of the liquefied mass gaining sufficient momentum to trigger and propagate a full flow event with a significant runout distance. The above assessment of CRR is based on clean sands with minimal fines. As noted in Section 2.1.2 and Section 2.1.3, the proposed mining activity involves grinding of the mined sediment, such that the redeposited material will have a higher fines content. However, since the resulting ground fines are anticipated to be non-plastic, this is unlikely to significantly enhance the cyclic resilience. Nevertheless, a higher fines content will act to inhibit drainage of any accumulated excess pore pressures, which increases the risk of liquefaction (albeit we have already accounted for this in selecting N=20, as discussed above).



Table 2.1: Annual joint probability distribution (%) of significant wave height, H<sub>s</sub>, and peak spectral wave period, T<sub>p</sub> (Oceanum, 2022)

									т	(a)								
Hs									l p	(s)								Total
(m)	3.0-4.0	4.0-5.0	5.0-6.0	6.0-7.0	7.0-8.0	8.0-9.0	9.0-10.0	10.0-11.0	11.0-12.0	12.0-13.0	13.0-14.0	14.0-15.0	15.0-16.0	16.0-17.0	17.0-18.0	18.0-19.0	>19.0	
0.0-0.5	0	0	0	0	0	0	0	0.02	0.07	0.08	0.01	0	0.01	0.01	0	0.01	0	0.21
0.5-1.0	0.05	0.13	0.08	0.04	0.17	0.19	0.26	0.7	2.02	3.44	3.09	1.36	0.69	0.54	0.13	0.14	0.02	13.05
1.0-1.5	0.04	0.56	1.31	0.76	0.62	1.02	0.89	1	2.15	4.79	5.43	3.37	1.76	1.3	0.32	0.27	0.11	25.7
1.5-2.0	0	0.25	1.88	2.77	1.4	1.27	1.68	1.41	1.48	2.51	3.29	2.37	1.38	0.91	0.25	0.13	0.11	23.09
2.0-2.5	0	0.03	0.67	2.78	2.34	1.13	1.14	1.3	1.27	1.4	1.52	1.3	0.75	0.57	0.14	0.07	0.11	16.52
2.5-3.0	0	0	0.13	1.01	2.3	0.99	0.83	0.92	0.92	0.96	0.75	0.54	0.45	0.3	0.04	0.03	0.04	10.21
3.0-3.5	0	0	0.02	0.2	1.27	0.88	0.57	0.49	0.6	0.66	0.45	0.29	0.15	0.1	0.02	0.01	0	5.71
3.5-4.0	0	0	0	0.03	0.4	0.6	0.32	0.25	0.32	0.41	0.3	0.19	0.08	0.04	0.02	0	0	2.96
4.0-4.5	0	0	0	0	0.08	0.33	0.24	0.16	0.15	0.17	0.16	0.12	0.06	0.01	0	0	0	1.48
4.5-5.0	0	0	0	0	0	0.09	0.14	0.09	0.07	0.1	0.08	0.05	0.03	0	0	0	0	0.65
5.0-5.5	0	0	0	0	0	0.02	0.06	0.02	0.03	0.02	0.03	0.02	0.01	0	0	0	0	0.21
5.5-6.0	0	0	0	0	0	0	0.03	0.01	0.01	0.02	0.01	0.01	0.01	0	0	0	0	0.1
6.0-6.5	0	0	0	0	0	0	0	0.01	0	0	0.01	0	0	0	0	0	0	0.02
6.5-7.0	0	0	0	0	0	0	0	0	0	0	0	0	0	0	0	0	0	0
Total	0.09	0.97	4.09	7.59	8.58	6.52	6.16	6.38	9.09	14.56	15.13	9.62	5.38	3.78	0.92	0.66	0.39	99.91



Table 2.2: Metocean cases – ambient sea states

Metocean case no.	Water depth, d (m)	Peak wave period, T <sub>p</sub> (s)	Significant wave height, H₅ (m)	Maximum wave height, H <sub>max</sub> (m)	Wavelength, L (m)	Wave number, λ (m)	Mudline Peak normalised cyclic shear stress, τ <sub>mud</sub> /σ' <sub>vo</sub> (-)
1	35	15.0	2.0	3.72	248.8	0.025	0.039
2	35	12.0	2.0	3.72	186.2	0.034	0.041
3	35	15.0	1.0	1.86	248.8	0.025	0.019
4	35	12.0	1.0	1.86	186.2	0.034	0.021
5	35	13.5	2.0	3.72	217.9	0.029	0.040
6	35	8.0	3.0	5.58	97.7	0.064	0.044
7	35	6.0	3.0	5.58	39.0	0.112	0.015
8	35	8.0	2.0	3.72	97.7	0.064	0.029
9	35	6.0	2.0	3.72	56.2	0.112	0.010

Table 2.3: Metocean cases – storm conditions

Return period (years)	Water depth, d (m)			Maximum wave height, H <sub>max</sub> (m)	Wavelength, L (m)	Wave number, λ (m)	Mudline Peak normalised cyclic shear stress, τ <sub>mud</sub> /σ' <sub>vo</sub> (-)
1	35	8.8	5.5	10.2	116.1	0.054	0.095
10	35	10.7	7.3	13.6	157.1	0.040	0.148
100	35	11.7	9.3	17.2	180.1	0.035	0.191



#### 2.2.2.3 Assessment of Wave-induced Densification

As discussed in the previous section, wave-induced liquefaction appears unlikely for ambient conditions but quite likely under storm conditions, even for a 1-year return period storm. That assessment was undertaken assuming that water-pluviated backfill would lead to an initial relative density,  $D_r = 0.2$ , with the overburden stress increasing the density state to a maximum  $D_r = 0.31$  at a depth, z = 10 m.

In concept, ambient wave loading has the potential to increase the density of backfilled sand (thereby increasing the  $q_{c1}$  of the backfill), which would then increase the limiting CRR required to initiate liquefaction. Considering the maximum CSR produced under ambient conditions (Case 6, CSR = 0.044) relative to the adopted minimum CRR = 0.08, implies an  $F_{w-1}$  = 1.8 at the seabed, increasing to over 3.5 at the base of the backfill (see Plate 8). In lieu of site-specific data, the potential associated volumetric strain under these conditions may be estimated from published correlations between FoS and post-liquefaction volumetric strain, as for example shown on Plate 10 (Ishihara, 1993). From these correlations, a volumetric reconsolidation strain of about  $\varepsilon_v$  = 0.1% could be expected with an  $F_{w-1}$  of 1.8, with  $\varepsilon_v$  of essentially zero for  $F_{w-1}$  of 3.5. Even for the former case, this could be expected to increase the relative density by a mere 1%, which is very unlikely to materially influence the liquefaction performance of the backfill material and hence is very unlikely to be sufficient to transition the soil response from catastrophic flow-liquefaction to the much less risky cyclic-mobility.

It can therefore be concluded that no reliable densification of the mined backfill can be assumed prior to application of a significant design storm event (e.g. 1yr RP or greater), and hence the latter can be considered a high risk of initiating a flow liquefaction event.

As an aside, we note that engineered techniques such as vibro-compaction may be theoretically feasible to densify the post mined tailings over their full depth in water depths up to 50 meters. However, this would require specialised vibroflot equipment deployed from barges or jack-up platforms (but see Section 2.4). We consider that this is very unlikely to be economically or practically viable at the scale required in this case (i.e. approx. 10 million cubic metres of densified soil for each 1 km<sup>2</sup> of mined area).

#### 2.2.3 Assessment of Seismic-Induced Liquefaction

As the proposed seabed mining and OWF zones are in areas where seismic activity is to be expected, a simple free-field seismic analysis has been undertaken to provide a preliminary assessment of the susceptibility of the backfilled sand to liquefaction during a seismic event. This analysis has considered earthquake return periods of 200 years (ductility level earthquake – DLE) and 2,000 years (rare intensity earthquake – RIE). AG (2004) provides estimated peak ground acceleration (PGA) for these return periods; PGA = 0.28g for the 200-year return period event and PGA = 0.48g for the 2,000-year return period.

Cyclic shear stresses due to a seismic event can be linked to the horizontal peak ground acceleration using the simplified approach outlined in Seed and Idriss (1971). This calculates



the applicable cyclic stress ratio (CSR) as a function of the total vertical stress,  $\sigma_{vo}$ , the effective vertical stress,  $\sigma'_{vo}$ , a magnitude weighting factor, MWF, and a factor that varies with depth to account for the flexibility of the soil column. The MWF allows consideration of earthquakes of different magnitudes but appropriate earthquake magnitudes for the DLE and RIE are not currently available for the proposed mining and OWF sites. In lieu of such data, appropriate magnitudes have been estimated empirically, using the approach presented in Wald et al. (1999), as 7.3 for the DLE and 8.1 for the RIE.

Liquefaction resistance during a seismic event may be defined using the same cyclic resistance ratio (CRR) that was used to assess liquefaction under wave-induced seabed shear stresses, as discussed in Section 2.2.2.2 and shown on Plate 7.

Factors of safety against liquefaction during an earthquake are calculated in the same way as for wave-induced liquefaction, i.e.  $F_{s-l} = CRR/CSR$ .  $F_{s-l}$  is plotted against depth for both the DLE and RIE earthquakes on Plate 9. For both cases, liquefaction is predicted for the entire 10 m depth of backfilled sand, with an average  $F_{s-l} = 0.24$  calculated for the DLE event, reducing to  $F_{s-l} = 0.11$  for the RIE event.

# 2.3 Slope Stability Considerations

#### 2.3.1 Example of Flow Liquefaction on Very Gentle Slope, Palu Earthquake, Indonesia

Flow liquefaction can occur irrespective of ground slope, but a mass run-out event, triggered by flow liquefaction, requires a non-zero seabed gradient. Seabed runout events are generally undetected as they are underwater, typically becoming evident as historic events during site investigations. However, onshore flow liquefaction events have been witnessed and are often well documented. A particularly interesting example is the flow liquefaction triggered by the Palu earthquake in Indonesia in 2018, as described and interpreted in numerous publications (e.g., Miyajima et al. 2019; Gallant et al., 2020; Kiyota et al., 2020; Jalil et al., 2021; Mason et al., 2021). This case study may be relevant to the proposed OWF development as the upper 10 m of the sediment at Palu was at a very low initial relative density with a fines content of between 20% and 40% (which may be similar to the backfilled sand after grinding) and is an area with a similar seismic risk.

A 7.5 (moment magnitude) earthquake at Palu on 28 September 2018 triggered flow liquefaction, causing sediment to travel downslope over distances of up to 3 km (Kiyota et. al., 2020). The sediment flowed as a viscous fluid with a very low residual strength (Mason et. al., 2021), causing very significant damage and loss of life. As shown on Plate 11 to Plate 13, the average gradient along the flow paths was between 0.5° and 1.2°, indicating that liquefied sediments with very low residual strengths can flow over very shallow slopes.

One key differentiator is that the onshore flow at Palu was exacerbated by the water table, which was inclined and ran parallel to the slope, which decreases the overall stability of the slope. This differs from the seabed situation, where the water table is level and of course, lies well above the seabed. On the other hand, the upper parts of an underwater slide may



become entrained in water in a very diffuse state and the resulting dilute turbidity current may travel much longer distances than a much denser onshore flow.

#### 2.3.2 Site-Specific Risk of Flow Failures and Runouts

#### 2.3.2.1 Impact on OWF Development

The likelihood that a flow liquefaction-triggered runout event may travel into the proposed OWF zones has been assessed by considering the location of the proposed seabed mining zone in relation to the proposed OWF development sites and the seabed gradients. Plate 14 shows the interpreted bathymetry in this region, which translates to seabed slopes in the range 0 - 2°, as shown on Plate 15.

Potential flow paths are also shown on Plate 14 and Plate 15, with the most probable indicated by the red dashed lines, and the less probable indicated by the green dashed lines. The red flow paths propagating south and west from the higher regions (i.e. shallower water) of the mining area are considered to represent a much greater risk of triggering a flow failure event. The risk of initiation along the red paths is increased compared to the green paths due to the presence of local higher seabed gradients at the initiation points. Along the red paths, these gradients are considered sufficient to potentially enable the initial acceleration required to initiate a flow failure, whereas on the green paths, the slopes are considered too shallow to initiate a significant flow failure.

Fugro's experience from assessment of iron tailings runout events indicates that residual strengths during a debris flow may be as low as 70 Pa (i.e. 0.07 kPa). As shown on Plate 16, this is consistent with theoretically calculated residual sediment strengths, that may be achievable for very loose sediments, as considered applicable to the mined backfill.

The thickness of liquefied sediment that can retain (or regain) static stability is a function of both the slope angle and residual strength. Simple static stability calculations to show the influence of these parameters are summarised on Plate 17. This plate presents results that consider slope angles in the range 0 - 2° and residual strengths in the range 50 to 200 Pa. At a slope angle of 0.5° it can be observed that a runout flow would be expected to regain static stability once the flowing sediment has thinned to a thickness of 0.7 m, assuming a residual strength of 50 Pa. This increases to 2.7 m assuming a residual strength of 200 Pa. At a steeper slope angle of 2°, the corresponding stable runout thickness decreases to 0.17 m and 0.67 m for residual strengths of 50 Pa and 200 Pa, respectively. The smaller stable runout thickness calculated along steeper slopes indicates that any flow would need to travel further from its source in order to thin sufficiently to regain static stability.

These calculations demonstrate the potential susceptibility of even very gentle slopes to a post-flow liquefaction runout event. The momentum of the already accelerated runout sediment was not included in these simple calculations, which means that, in practice, even greater downslope movements would be required to halt a sediment flow.



While soil drainage might traditionally quickly strengthen and stabilise the soil, this may not be the case for already energised liquefied sediments. This reflects that once the excess pore water pressure within the accelerated flow has built up, the continuous shearing action within the flow may hinder excess pore pressure dissipation, thereby preventing an increase in strength that could suppress the flow.

Based on the foregoing, it is concluded that flow failures are unlikely to initiate and propagate towards the east and south-east into an OWF site to the north of the mining zone or south-west into an OWF west of the mining zone, due to the very gentle seabed gradients. In contrast, flow failures along the red flow paths present a credible risk of a runout into an OWF site to the east of the mining site, due to steeper slopes at the initiation point.

To alleviate the risks posed by potential runouts toward an OWF site to the East of the mining site, an exclusion zone, as shown via the deep blue shaded area on Plate 18, may be established in the southeast corner of the proposed seabed mining area. By avoiding mining of these steeper south-facing slopes, the risk of a flow liquefaction-initiated runout towards the south is negated.

If this proposed exclusion area were mined instead, a substantial volume of loose sediment may be deposited and this could undergo flow liquefaction in the event of a significant storm or seismic event. In lieu of detailed runout modelling, we cannot define how far such a runout might extend, but in lieu of such assessments we consider this should be considered to pose a significant hazard to the entire western quarter of the OWF site to East of the assumed mining area.

#### 2.3.2.2 Impact on Existing Kupe Infrastructure

A preliminary assessment of potential runout paths from the proposed fast-tracked mine area has also been conducted, with a specific focus on the existing Kupe subsea infrastructure. The results of this assessment are presented on Plate 19. Provided locations of the Kupe platform, wells and flowlines in the vicinity of, or within, the proposed fast-tracked mining area are presented on this plate. As previously, higher probability flow failure paths are indicated with red dashed lines while less likely flow paths are denoted with green dashed lines. Due to the very shallow seabed gradients at potential initiation points, it appears that only a low-probability flow path propagating northeast and then southwest, could potentially run into the existing Kupe platform. However, to the south a number of wells and associated flowlines are located in line with the red high-probability flow paths. To properly quantify the risk and impact on the Kupe project offshore infrastructure, detailed quantitative runout modelling would be required for debris flows originating from the mining area along these critical flow path.

## 2.4 Discussion on Jack-up Operability

As discussed in Section 2.2.2, Fugro have assessed the likelihood that initially (very) loose tailings backfill at South Taranaki may densify under ambient wave conditions (i.e. the range



of sea state that will be present for almost all the time). It was concluded that significant densification is unlikely to occur under ambient conditions. However, under storm conditions (e.g. 1-year return or longer) and seismic conditions, it is anticipated that the soil will ultimately densify, but will also first be prone to liquefaction. This is particularly likely during seismic events, which are of very short duration compared to storms, and hence the tailings are not expected to undergo any densification during such events (but may do so after).

Over the long term (i.e. geological time scales encompassing many millennia), it is anticipated that repetitions of such storm and seismic events will eventually densify the sediments to a state similar to their current in situ condition. However, over the short and finite life of OWF or existing O&G infrastructure, densification is likely to be slow and irregular and hence the tailings backfill can be expected to remain in a loose or very loose state for a long time (potentially the lifetime of such facilities).

As mentioned in Section 2.2.1, liquefaction can be divided into two types: 1) cyclic mobility and 2) flow liquefaction. Even the dense in situ soil may be subject to cyclic mobility-type liquefaction during a seismic event. In this condition, the soil temporarily loses stiffness, but if strained sufficiently will recover its original strength. A loss of stiffness of this type is not without consequences for a jack-up placed on such soil. In particular, this has the potential to cause quite large leg settlements (e.g. see Erbrich et al. (2020a and b)). However, ultimately the soil strains will be limited and so will be the settlements. Notwithstanding, the structural integrity of a jack-up subject to such conditions would need to be confirmed.

In contrast, flow liquefaction implies (at the extreme) an almost complete loss of strength – after an initial peak strength is passed, the soil can transition to a state where it may 'flow' like a viscous fluid. The response in this case is very brittle. A seismic or storm event may cause the peak strength to be exceeded and once this has occurred, the soil will transition to a state with small to negligible strength. Considering a jack-up placed on such soil, it can be expected that if flow liquefaction were initiated, the bearing capacity below the leg would transition to a low level. It is unlikely that this will be sufficient to support the weight of the jack-up rig and hence catastrophic sinking of the leg under the applied dead weight of the jack-up rig could then be expected, with total loss of the rig likely.

Soil that is initially 'dense' (i.e. the in-situ soil) is expected to undergo cyclic mobility type liquefaction. However, loose and very loose soils (i.e. un-densified tailings) can be anticipated to exhibit flow liquefaction.

The significant risk of (and potential catastrophic consequences of) flow liquefaction in the un-densified tailings has not been recognised in the OCEL (2015) report that considers jack-up operations in a post-mined environment at South Taranaki. Liquefaction potential is given cursory consideration, with a specific claim that while 'liquefaction' (of unspecified type) might occur in the post-mined tailings in the free-field, consolidation under the jack-up weight will mitigate this risk for the jack-up. This conclusion is incorrect and unsafe. In fact,



the opposite is true – consolidation under the jack-up weight increases the risk of a brittle flow liquefaction-type failure.

A technical explanation for this critical conclusion is provided below

- Liquefaction of sandy soils is well described using a state parameter approach and a critical state framework (Jefferies and Been, 2016) as shown on Plate 20. A negative state parameter defines a dilative soil while a positive state parameter defines a contractive soil.
- 2. The critical state line defined in void ratio versus mean effective stress space divides soils that contract when subject to shearing versus those that dilate. Dilation always leads to 'cyclic mobility' type liquefaction, while contraction can (under some conditions) cause flow liquefaction. Even in the absence of full flow liquefaction, shallow foundations on contractive soils (e.g. spudcans) will have undrained bearing capacity lower than the drained bearing capacity, which can still be highly problematic during a seismic event, unless considered very carefully (e.g. see Erbrich et al. (2020a and 2020b)).
- 3. Plate 20 illustrates why consolidating the soil under the jack-up dead weight does not mitigate the risk of brittle flow liquefaction type failure.
- 4. In this example, before the jack-up weight is applied to the soil (i.e. Point A), the undensified tailings have a slightly positive state parameter. The monotonic undrained stress-strain response for such a soil element is also shown. This reflects a brittle response, with a peak strength first mobilised, followed by some post-peak strain softening (i.e. brittle behaviour) to the critical state strength. Since the in-situ stresses are very low, both the peak strength and post-failure critical state strength are very small in this case (the latter being close to zero).
- 5. Once the jack-up weight is applied (i.e. Point B), the void ratio of the un-densified tailings will reduce a little. However, the application of dead weight to sand is generally an ineffective way of changing the density very much. Only vibrations/ cyclic loading can effectively densify sand. Hence, due to the relative slope of the consolidation curve and the critical state line, the state parameter is likely to become significantly more positive after consolidation compared to before.
- 6. It can be seen that the post-consolidation peak strength has increased, as has the post-failure critical state strength. However, the critical state strength under the jack-up weight is now a smaller percentage of the peak than under in situ stress conditions (i.e. the response is more brittle). In addition, and most critically, the weight of the jack-up imposes a relatively large static shear stress in the soil. In contrast, the static shear stress in the free field is very low, being just that imposed by the natural seabed slope.
- 7. If a seismic (or even a storm) event induces an undrained shear stress in the soil that exceeds the peak strength, or if accumulation of strain under repeated cyclic loads leads to an intersection of the stress-strain path with the post-peak monotonic response, then failure is likely to be triggered. This is because, once this state is reached, the post-peak critical state strength must be greater than the imposed static shear stress under the jack-up weight. Given the high positive state parameter that we anticipate would apply at



- this stage, this condition is unlikely to be met. Hence, the jack-up leg will likely plunge down, with potential for a resulting total loss of the rig (albeit noting that the total plunge would be limited to the spudcan not penetrating significantly below the base of the mined tailings see further discussion below on this).
- 8. The exact state parameter of the un-densified tailings immediately after mining can only be speculated at this stage. However, we anticipate that it would be positive and potentially significantly more positive than shown in the example presented here. A more positive initial state parameter can only make things worse. Only when the state parameter of the post-mine tailings has become significantly negative (due to densification under wave and seismic-induced cyclic loading) will it be possible to safely mitigate the scenario outlined here.

#### 2.4.1 Discussion on Static Penetration Depths Within Mining Site

The OCEL (2015) report suggests that static penetration of a typical spudcan into undensified tailings would be in the order of 6 m at the widest section. If this were the case, then a flow liquefaction-induced leg plunge might be limited to circa 4 m, assuming a maximum thickness of 10 m of un-densified tailings. Plausibly, this might be survivable for a jack-up rig, depending on its operational configuration at the time of the EQ or storm, albeit major structural damage is still likely. However, our review does not support such a deep spudcan penetration. OCEL (2015) has used friction angles for loose and very loose sands as suggested in an outdated recommended practice (SNAME, 2002). Contemporary practice should be in accordance with ISO-19905-1 (2023), which does not suggest such low values. Instead, it is noted that back analysis of spudcan penetrations tends to suggest operational friction angles that are close to, or a bit larger than, the critical state friction angle. For all predominantly silica sands (including those anticipated at South Taranaki) the critical state friction angle would be in the order of 30 to 33 degrees. Due to the potentially very loose state, leading to enhanced compressibility compared to denser sands, the 'apparent' operational friction angle (i.e. that required to make the classical bearing capacity formula work in more compressible soil) may be reduced a little. However, we do not envisage a scenario where this could be less than 25 degrees. Adopting this friction angle, we anticipate that the widest spudcan section of a typical O&G spudcan is unlikely to penetrate more than 2 m. This scenario is much more critical than that envisaged by OCEL (2015), with a potential leg plunge of circa 8 m in the event of flow liquefaction. We do not envisage that leg plunges of this magnitude could be survivable for any jack-up rig.

#### 2.5 Conclusions and Recommendations – Geotechnical Assessment

The qualitative/ semi-quantitative geotechnical assessment presented in this report indicates that under the metocean conditions anticipated at the proposed OWF and seabed mining sites, and given the very loose density state of the backfilled sand, the following may apply:



- Wave-induced liquefaction under a 1-year return period storm may occur in the upper 3 m of backfill, while 10-year and 100-year return period storms may liquefy the full 11 m thickness of the post-mined tailings.
- Ambient metocean conditions are not expected to significantly densify the backfill material. As a result, any subsequent liquefaction event is expected to manifest as flow liquefaction, posing a high risk of runout events.
- Significant seismic events (200 yr RP to 2000 yr RP) are also expected to extensively liquefy the mined backfill and probably also the in-situ soil. However, 'safe' cyclic mobility type liquefaction can be expected for the latter, while 'unsafe' flow liquefaction can be expected for the former.
- Owing to the very low-density state of the backfill, the residual strength of the liquefied silty sand, coupled with unfavourable drainage conditions, is likely to be very low. This significantly elevates the risk of debris flow runouts even on a very gently sloping seabed.
- Bathymetric data show seabed gradients ranging from 0° to 2°, which, at the upper end, are sufficient to initiate acceleration of low-strength sediments into a flow failure event.
- Analysis of site topography suggests that potential flow events would most likely
  propagate west and south-east from the high points of the mined area. Without
  mitigation, there remains a credible risk of a flow event propagating southeast from
  the proposed seabed mining zone into the SW corner of an OWF site to the East of
  the mining site.

To mitigate the risk of a flow liquefaction-initiated run-out event impacting an OWF site to the East of the mining site, Fugro recommends the establishment of a mining exclusion zone in the southeast of the proposed mining area. This exclusion zone, illustrated by the blue shaded area on Plate 18, delineates where mining should be prohibited.

To evaluate the risk and impact of potential run-outs towards the existing Kupe subsea infrastructure, including wells, platform and flowlines, Fugro recommend that quantitative modelling of debris flow runout and impacts should be conducted.

An observational strategy may also be considered, comprising CPT testing of the post-mined sediment to verify the density state of the backfilled sand. Follow-up CPTs at defined intervals (e.g. 1 year) could then be used to assess the real-world densification rate resulting from ongoing ambient metocean conditions and any storms or earthquakes that may have occurred. Such an observational approach may be used to inform an ongoing updated flow liquefaction risk assessment, which could be used to ease any precautionary restrictions that are initially imposed on the seabed mining operations.



In lieu of any site-specific laboratory data for the assumed low-density backfill material, the assessments outlined in this report are based on Fugro's experience and public domain literature references. Further validation of these findings could be achieved through a programme of cyclic simple shear tests on example tailing samples conducted at a range of low relative density states. Such tests would provide a more reliable site-specific basis for:

- Establishing the threshold cyclic resistance ratio relevant for the low-density state of the backfill
- Quantifying the volumetric strain (resulting in densification) associated with the magnitudes of cyclic stress ratios imposed under ambient metocean conditions.
- Beyond the risks of flow liquefaction induced runouts into the proposed OWF areas,
  Fugro does not perceive any geotechnical issues that necessitate significant buffer
  zones between the proposed OWF and mining zones. In such cases, a minimum
  acceptable buffer zone can be adopted that is sufficient to permit any jackup rigs
  required for OWF construction and support operations to always have all their feet
  resting entirely on in situ unmined soil. It is suggested that recommendations are
  sought from relevant jack-up operators as to how far this zone should extend from
  the OWF infrastructure.



### 3. Geomorphological Qualitative Assessment

#### 3.1 Background

This section reviews the regional morpho-dynamics and seabed mobility context in the South Taranaki Bight (STB), along with the potential implications of collocating offshore sand extraction with other marine uses, particularly offshore wind farms (OWFs). It synthesises findings from previous regional oceanographic studies, sediment transport modelling, and scientific literature, and is conducted to support the analytical estimation of expected seabed mobility. Plate 21 presents the bathymetry and seabed gradients over the area of study for sites A and B, along with delineations of potential seabed mining permits currently undergoing a fast-track approval process.

#### 3.2 Regional Context

The STB, located on the west coast of New Zealand's North Island, is a dynamic marine environment shaped by complex geological and oceanographic processes. The region is underlain by sedimentary formations derived from both terrestrial and marine sources, with coastal erosion and riverine input contributing to a diverse sediment regime (NIWA, 2011). Oceanographically, the STB is influenced by the D'Urville Current (Plate 22 & Plate 23), which transports nutrient-rich waters from the west into the Bight, supporting high biological productivity and complex ecological interactions<sup>2</sup> (Carter & Heath, 1975; Carter et al., 1998). Currents in the area are predominantly wind-driven and exhibit strong seasonal variability, with sediment transport generally moving in a south-easterly direction from Cape Egmont toward the Kapiti Coast (NIWA, 2011). These physical processes are critical to understand the environmental dynamics of the STB and form the foundation for assessing the impacts of any proposed marine activities in the region.

#### 3.2.1 Geological Settings and Sedimentary Environment

The STB is a shore-connected Holocene sand prism that is up to 20 m thick at the coast and extends seaward to approximately 22 – 29 km offshore. At the seaward limit the sand prism thins to a transgressive erosional surface, delineated by coarse-grained lag deposits (TTR, 2016; NIWA, 2015a).

#### 3.2.1.1 Coastal Dynamics and Morphology

The Taranaki Peninsula shoreline (from Opunake to Inaha) is characterised by (eroding) cliffs and rocky, wave-cut intertidal platforms with a thin veneer of sand or gravelly sand, cobbles or boulders.

Further South (around Patea), the shoreline consists of almost continuous near-vertical, 30 – 50 m tall, sedimentary seacliffs (resulting from continual tectonic uplift) (NIWA, 2015b). While



<sup>&</sup>lt;sup>2</sup> Project Reef South Taranaki

measurements of coastline retreat rates are not recorded over the entire STB coast, active erosion is regularly observed and/or expected along cliffs comprising soft sedimentary material, capped in places by resistant materials (Plate 24).

Sandy beaches are located at the base of the cliffs, and in small re-entrants. The beach profile data show there is a very high flux of sand both across shore and longshore through the system. The beach elevation goes up and down 1 to 2 m and the beach face shows excursions back and forth of about 10 – 40 m over time scales of weeks and months (NIWA, 2015b). Storm events cause erosion, while calmer periods allow beach rebuilding.

#### 3.2.1.2 Sediment Properties

Medium-coarse sands and gravelly sands forming the beaches have as their primary source river inputs and cliff erosion (providing the coarser material), and sand being fed in from the sea (NIWA, 2015b).

Under water, STB sediments are fine, well-sorted volcanic sands with high specific gravity due to heavy minerals. The coastal iron sands along the west coast of the North Island are primarily derived from Taranaki volcano andesites (NIWA, 2011). For the current study, properties of superficial and natural sediments are sourced from the Geotechnical Investigation Report (Advanced Geomechanics, 2004) conducted for the Kupe platform located at ~6 km from the southwest corner of OWF site to the North of the mining site. Particle size distribution of superficial sediments shows very small fines content and a median particle diameter of 0.22 mm (Plate 25). The specific gravity decreases from 2.87 at seafloor to a constant value of 2.73 from 10 m bsf.

#### 3.2.2 Oceanography and Sediment Dynamics

STB continental shelf exhibits complex bathymetry due to shoals, namely Patea Bank, Graham Bank, and Rolling Ground, having a large influence on the oceanography (NIWA, 2011). The sediment budget is influenced by inputs from cliff erosion, river discharge, and longshore transport (NIWA, 2015b).

Morphodynamical processes and sediment mobility over the STB area are reported to be mainly driven by wave action, with regular waves frequently resuspending mud down to ~15 m water depth near Whanganui-Manawatu and storm events able to resuspend sediment down to 150 m water depth (NIWA, 2015b). The largest wave heights are encountered off the western end of the Taranaki Peninsula with decreasing values further south in more sheltered areas (NIWA, 2015b).

Plate 26 presents the distributions of significant wave heights and depth-averaged sea currents for the location of the Kupe platform in the vicinity, taken as a preliminary representative for the project area for the present study.

In the nearshore zone, the orientation of the coast relative to the predominant WSW incident wave direction (Plate 27) results in the longshore bidirectional sediment transport, with a



predominant direction towards the southeast from Opunake to south of Wanganui River (NIWA, 2011).

The zone is characterised by erosional bedforms in the form of rock outcrops, ancient buried valleys or exposed mudstone platforms (TTR, 2016; NIWA, 2011; NIWA, 2015a; Plate 28). Further offshore, seabed stirring by waves entrains seabed sediments that can then be advected by currents mostly coast-parallel, with only moderate cross-shore transport (NIWA, 2015b). The seafloor is dominated by depositional bedforms generated by storms (NIWA, 2015a). It includes sand waves, iron sand ridges, sand ribbons and mega ripples. The ridges can be up to 12 m high, several hundred meters wide and several kilometres long, aligned sub-parallel to the shoreline on a relatively flat seafloor at depths up to 50 m. Their probable formation dates from 9,000 to 12,000 years old (NIWA, 2015a). Smaller active bedforms upon the old depositional bedforms, and persistent down to water depths larger than 50 m, suggest strong oscillatory currents approaching 1 m/s during storm events (NIWA, 2015a).

#### 3.3 Sediment Mobility

Sediment mobility refers to the capacity of sediment particles to be entrained, transported, and redeposited by fluid motion, primarily driven by waves, tides, and currents in marine environments. The initiation of sediment movement depends on the balance between hydrodynamic forces exerted by the flow and the resisting forces due to gravity, cohesion, and friction. This balance is often quantified using the Shields parameter, which relates the bed shear stress to the gravitational force acting on a particle. Sediment can be transported as bedload, where particles roll or slide along the seabed, or as suspended load, where finer particles are lifted into the water column.

#### 3.3.1 Critical Bed Shear Stress

Sediment transport occurs when the bed shear stress associated to currents and/or waves exceeds a critical value for incipient motion of sediment particles. It depends on factors such as particle size, density, and fluid properties. Typically, this threshold value is obtained by the formula of (Soulsby & Whitehouse, 1997) defining the critical shear stress or in its dimensionless form, Shields parameter, i.e. the critical dimensionless shear stress beyond which sediment motion is initiated. The expected critical shear stresses corresponding to insitu cohesionless surface sediments and sediments arising from the iron sand extraction process are reported in Table 3.1.

#### 3.3.1.1 Natural Sediments

Considering a median particle diameter of 0.22 mm and a specific gravity of 2.87, the critical bed shear stress associated to the superficial sediment layers naturally present over the STB is estimated at  $\sim$ 0.18 Pa.



#### 3.3.1.2 Sediments Arising from Iron Sand Extraction Process

Details on the iron sand extraction process, and properties of the material expected to be returned to the seabed after extraction, is not fully confirmed. The output of sediments resulting from the extraction of iron sand is expected to be divided into two groups: sediment in the sand size fraction or coarser, anticipated to deposit proximally on the seabed behind the crawling mining processing facility, and the fraction of finer sediment (produced by the grinding/de-oring process) that is susceptible to prolonged suspension and dispersion during the redeposition phase. This latter suspended source of fine sediment (grain size less than 0.09 mm) was firstly assessed to have a critical shear stress for mobility in the order of 0.1 Pa (NIWA, 2013), which is significantly less than the initial in-situ sediment, rendering the deposit more prone to scouring and mobility. However, subsequent laboratory tests by HR Wallingford have suggested that the critical shear stress required to resuspend material resulting from the iron sand extraction process is in the range between 0.2 Pa and 0.3 Pa (HR Wallingford, 2015), a difference which they attribute to flocculation, among others. This would make the sediments resulting from the extraction process almost indistinguishable from the in-situ materials in terms of susceptibility to mobility. It is worth noting that the origin and history of these samples remain unclear, and the specific way they will be deposited following iron sand extraction with respect to the disregarded coarser fraction has not been fully defined. Therefore, any conclusions regarding their mobility should be interpreted with caution. Also, noting that the depth of extraction at the front mining face amounts to well over 10 m, it is emphasized that the extraction and redeposition process would suppress any presence of an locally armoured (coarser) or hardened layer at the seafloor, by which the very shallow seafloor sediment would have gained a greater resistance to mobility than the sediment layers immediately underlaying the surface. The redeposited sediment would also initially be in a very loose state. Altogether, enhanced susceptibility of the disposed sediment from the mining process to mobility under the action of currents and waves is likely.

Table 3.1: Geotechnical parameters for in situ materials and materials originating from the iron sand extraction process

Conditions	Median Particle Diameter [mm]	Specific Gravity [-]	Critical Shear Stress [Pa]
In situ (Kupe) <sup>(1)</sup>	0.22	2.87	0.18 <sup>(2)</sup>
Arising from iron sand extraction process <sup>(3)</sup>	<0.08	2.66-3.11	0.2-0.3 <sup>(4)</sup>

- (1) Superficial conditions from Sample 1 at 0.38 m (Advanced Geomechanics, 2004)
- (2) Computed using an empirical equation (Soulsby & Whitehouse, 1997)
- (3) From three samples originating from the west coast of New Zealand at depths > 2 m arising from the iron sand extraction process. Sent by TTR to HR Wallingford for laboratory analysis (HR Wallingford, 2015)
- (4) Obtained from laboratory tests (HR Wallingford, 2015)



#### 3.3.2 Potential for Sediment Mobility

Sediment mobility in this study is evaluated using analytical formulations, specifically those developed by Summer and Fredsøe (2002), which are widely recognised in scientific literature and regulatory practice for assessing sediment transport under wave and current conditions. These equations provide reliable estimates of sediment mobility thresholds and transport rates based on hydrodynamic parameters and sediment characteristics. However, when higher precision or site-specific detail is required (particularly in complex or sensitive environments), Computational Fluid Dynamics (CFD) modelling may be employed to simulate the patterns of currents and waves, and associated sediment transport pathways, with greater fidelity.

In the present work, current-induced sediment mobility is evaluated by applying a logarithmic velocity profile in the immediate vicinity of the seabed, accounting for bed boundary layer, while a 1/7th power law is adopted to model the velocity distribution from 1 meter above the bed to the sea surface. For wave-induced shear stress, the approach involves calculating the near-bed orbital motion of water particles, with linear wave theory providing the theoretical basis for estimating the associated hydrodynamic forces. The shear current- and wave-induced shear stresses presented in the following are computed considering in-situ cohesionless materials. It is important to note that this mobility analysis is restricted to areas where unconsolidated sediments are present and does not apply to locations characterised by surficial crusts, hardgrounds, or reef structures, where sediment entrainment would largely be inhibited under the considered hydrodynamic conditions.

#### 3.3.2.1 Extreme Sea State

Extreme sea states are metocean conditions generally derived using design criteria based on typical return periods, which consider the likelihood of extreme conditions. The metocean conditions corresponding to different return periods at the Kupe platform are retrieved from (ASR, 2004) and summarised in Table 3.2. The results indicate that sediments are mobilised under both wave and current forcing across all considered return periods. While the current-induced shear stress alone may marginally exceed the critical threshold for sediment motion (particularly at low return periods for sediments arising from the iron sand extraction with a critical shear stress up to 0.3 Pa), it is likely that such exceedance is not sustained long enough to result in significant or widespread sediment transport. However, the combined shear stress from waves and currents consistently surpasses the critical value.

This strongly suggests that sediment mobility occurs at the site, even for the smallest return period considered (1 year). Wave-induced shear stresses are in the order of 5 times greater than current-induced shear stresses, confirming a wave-dominated sedimentary environment. For return periods greater than 1-year, combined bed shear stresses are over an order of magnitude greater than critical values. Widespread sediment redistribution is therefore expected during storm events.



Table 3.2: Metocean data and corresponding induced shear stress for different design criteria at Kupe platform (ASR, 2004)

Return Period	1	5	10	25	50	100
Current velocity (1 m asb) [m/s]	0.48	0.64	0.71	0.79	0.85	0.92
Peak period [s]	8.82	9.70	10.66	10.66	11.72	11.72
Sign. wave height [m]	5.49	6.75	7.33	8.06	8.64	9.27
Current-induced shear stress* [Pa]	0.33	0.58	0.71	0.88	1.02	1.20
Wave-induced shear stress* [Pa]	1.26	2.45	3.54	4.18	5.57	6.30
Combined shear stress* [Pa]	2.86	5.42	7.43	8.90	11.36	12.98

<sup>\*</sup>Induced shear stresses are computed using analytical formulas of Summer and Fredsøe (2002), considering the in-situ cohesionless sediments at Kupe platform water depth (~34 m)

#### 3.3.2.2 Normal Sea State

Normal sea states correspond to conditions regularly encountered during a typical year. Exceedance and joint probability distribution tables for currents and waves were retrieved from (Oceanum, 2022) and used to compute the percentage of critical shear stress exceedance for currents (Plate 29a) and waves (Plate 29b) during a typical year. The mobility threshold represented as the orange area on Plates corresponds to shear stresses comprised between 0.18 Pa (critical shear stress for in-situ material) and 0.3 Pa (highest critical shear for processed resuspended material). The green area corresponds to live-bed conditions, while the red area corresponds to a lack of sediment mobility.

The analysis suggests that currents induce sediment mobility for around 1% of the time during a typical year (Plate 29a), while waves are susceptible to inducing mobility for up to 60% of the time (Plate 29b). Plate 30 presents bed shear stress associated to variable wave height  $H_s$  and peak period  $T_p$  (left plot) along with  $H_s$ - $T_p$  joint probabilities (right plot) (Oceanum, 2022). The plates also show reported mobility thresholds (red and green lines, respectively for 0.18 and 0.3 pa critical shear stress). It is noted that the high percentage exceedance under normal waves is attributed to the longer modal peak wave period under normal conditions compared to the peak period reported for extreme conditions.

### 3.4 Conclusions and Recommendations – Geomorphological Assessment

A qualitative assessment of the seabed and coastal geomorphology has been conducted to assess expected sediment dynamics at proposed offshore wind farm (OWF) and seabed mining sites in the South Taranaki Bight. This study specifically focuses on the implications of offshore mining activities and sediment mobility within the designated Areas of Interest (AOIs). By examining the interaction between hydrodynamic forces and sediment characteristics, the following conclusions can be drawn from the study:

 The South Taranaki Bight features an actively changing shoreline and a mobile seabed, governed by a wave-dominated sediment transport regime that results in bidirectional longshore drift, predominantly directed toward the southeast;



- Under normal conditions, waves are capable of mobilising surface sediments across the range of water depths representative of the Areas of Interest (AOIs), while storm waves have the potential to resuspend sediments at even greater depths;
- Tidal currents under typical conditions are not expected to induce sediment movement at the AOI depths; however, currents associated with return periods of one year or greater are likely to do so;
- In situ shallow sediments exhibit high specific gravity due to the presence of heavy minerals;
- The specifics of the mining process and its effects on the characteristics and grain size distribution of the dumped sediment are not fully documented. Nonetheless, the dumped sediment is anticipated to contain a higher proportion of fines due to the grinding process and to exhibit a comparatively lower specific density. Despite this, the range of critical shear stress required to initiate sediment mobility for both the in situ cohesionless surface sediments and the dumped loose sediments resulting from the iron sand extraction process is expected to be similar. Laboratory tests conducted by HR Wallingford (2015) indicate that the higher fines content and tendency toward flocculation in the processed material result in a comparable susceptibility to mobility;
- The mining process may also lead to the destruction of patches of surficial crust or hard grounds and reefs, rendering these areas more vulnerable to sediment movement and the formation or migration of sediment ripples and mega ripples. However, the formation of large sediment waves appears unlikely given the magnitude of tidal currents at the site.

While these findings provide a preliminary understanding of sediment dynamics in the South Taranaki Bight and particularly in relation to mining activities, further investigation is needed to validate and refine these preliminary insights. It is particularly recommended to:

- Acquire more detailed insights into the bathymetry and morphology of the seafloor;
- Characterise the nature of surface and subsurface sediments.



#### 4. References

Advanced Geomechanics (2004) "Geotechnical Investigation Interpretative Report, Kupe Development, New Zealand", Report prepared for Origin Energy, Report No. AGR-1328 Rev 0.

ASR (2004) "Kupe Metocean Design Criteria: Environmental Statistics for Design", Report prepared for Origin Energy Resources (Kupe) Limited, Report No. 5510-02 Rev 0.

Baldi, G., Bellotti, R., Ghionna, V., Jamiolkowski, M. and Pasqualini, E. (1986) "Interpretation of CPTs and CPTUs; 2nd part: drained penetration of sands", Proceedings of the Fourth International Geotechnical Seminar, Singapore, 143-156.

Carrier III W. D. (2003). "Goodbye, Hazen; Hello, Kozeny-Carman", Journal of Geotechnical and Geoenvironmental Engineering, 129(11), pp. 1054-1056

Carter, L., and Heath, R. A. (1975). Role of mean circulation, tides, and waves in the transport of bottom sediment on the New Zealand continental shelf. New Zealand journal of marine and freshwater research, 9(4), 423-448.

Carter, L., Garlick, R. D., Sutton, P.(1998). Ocean Circulation New Zealand. NIWA Chart Miscellaneous Series 76.

Erbrich C., Lee KK., Lam, S., Tho KK., Galanes Alvarez H. and Ramadhan A (2020a). 'Earthquake Soil-Structure Interaction Assessments of Jack-up Modu for Tangguh development – Part 2', proc ISFOG 2020, Austin, Texas.

Erbrich C., Lee KK., Lam, S., Tho KK., Galanes Alvarez H. and Ramadhan A (2020b). 'Earthquake Soil-Structure Interaction Assessments of Jack-up Modu for Tangguh development – Part 3', proc ISFOG 2020, Austin, Texas.

Gallant, A.P., Montgomery, J., Mason, H.B., Hutabarat, D., Reed, A.N., Wartman, J., Irsyam, M., Simatupang, P.T., Alatas, I.M., Prakoso, W.A. and Djarwadi, D. (2020). The Sibalaya flowslide initiated by the 28 September 2018 MW 7.5 Palu-Donggala, Indonesia earthquake. Landslides, 17(8), pp.1925-1934.

HR Wallingford (2014) "Support to Trans-Tasman Resources: Laboratory testing of Sediments", Report prepared for Trans-Tasman Resources, DDM7316-RT002-R01-00, October, 2014.

HR Wallingford (2015). Source terms and sediment properties for plume dispersion modelling. Report No. RT004.

Ishihara, K. (1993). Liquefaction and flow failure during earthquakes. Géotechnique, 43(3), pp.351-451.



Ishihara K. and Yamazaki A. (1983). "Wave Induced Liquefaction in Seabed Deposits of Sand", Seabed Mechanics Symposium Proceedings, International Union of Theoretical and Applied Mechanics, Union of Geodesy and Geophysics.

ISO 19905-1 (2023) "Petroleum and Natural Gas Industries — Site-Specific Assessment of Mobile Offshore Units Part 1: Jack-Ups".

Jalil A., Fathani T.F., Satyarno I. and Wilopo W. (2021). Liquefaction in Palu: the cause of massive mudflows. Geoenvironmental Disasters. 8:21. https://doi.org/10.1186/s40677-021-00194-y.

Jefferies and Been (2015). 'Soil Liquefaction – a Critical State Approach, 2nd Ed', CRC Press, Taylor and Francis.

Kiyota, T., Shiga, M., Mori, K., Katagiri, T., Furuichi, H. and Setiawan, H. (2025). Triggering mechanism of long-distance flow-type landslides caused by 2018 Sulawesi Earthquake, Indonesia. Soils and Foundations, 65(1), p.101544.

Lagioia, R., Sanzeni, A. and Colleselli, F. (2006). Air, water and vacuum pluviation of sand specimens for the triaxial apparatus. Soils and foundations, 46(1), pp.61-67.

Lam, S.Y., Erbrich, C. and Lee, K. (2023). Seismic Modelling of Foundations Supporting Wind Turbines in Liquefiable Soils. Proceedings of OSIG 2023. 12<sup>th</sup> September,2023, London. pp. 1138-1145. https://doi.org/10.3723/UTXA2791

Lam, S.Y., Erbrich, C., Ingarfield, S., Xie, Y. and Zhao, L. (2025). A cyclic design framework for assessing seismic stability of submarine slopes. Themed Paper. Proceedings of ISFOG 2025. July, 2025, Nantes, France. PP.196. Doi: 10.53243/ISFOG2025-456.

Lewis, K.B. (1979). A storm-dominated inner shelf, western Cook Strait, New Zealand. Marine Geology 31, 31–43.

Lunne, T., Powell, J.J.M. and Robertson, P.K. (1997). Cone Penetration Testing in Geotechnical Practice. 1<sup>st</sup> Edition. Spon Press.

Mason, H.B., Montgomery, J., Gallant, A.P., Hutabarat, D., Reed, A.N., Wartman, J., Irsyam, M., Simatupang, P.T., Alatas, I.M., Prakoso, W.A. and Djarwadi, D. (2021). East Palu Valley flowslides induced by the 2018 MW 7.5 Palu-Donggala earthquake. Geomorphology, 373, p.107482.

Miyajima, M., Setiawan, H., Yoshida, M., Ono, Y., Kosa, K., Oktaviana, I.S., Martini and Irdhiani (2019). Geotechnical damage in the 2018 Sulawesi earthquake, Indonesia. Geoenvironmental Disasters, 6(1), p.6.

NIWA (2011). South Taranaki Bight Factual Baseline Environmental Report, Report No. WLG2011-43.



NIWA (2013). South Taranaki Bight Iron Sand Extraction Sediment Plume Modelling - Phase 3 studies. Report No. WLG2013-36.

NIWA (2015a). Geological Desktop Study. Report - Active Permit areas 50753 (55581), 54068 and 54272, South Taranaki Bight. Report No. WLG2013-44.

NIWA (2015b). Coastal stability in the South Taranaki Bight – Phase 2. Report No. HAM2013-082.

Oceanum (2022) "Metocean DataCube for the South Taranaki Bight, New Zealand", Report No. TN22-08 Rev 0.

OCEL (2015) 'Implications of Loose Tailings Seabed Material on Future Jack-Up Deployment in the South Taranaki Bight'.

Raghunandan, M., Juneja, A. and Hsiung, B. (2012). Preparation of reconstituted sand samples in the laboratory. International Journal of Geotechnical Engineering, 6(1), pp.125-131.

Seed, H.B. and Idriss, I.M. (1971) "Simplified procedure for evaluating soil liquefaction potential", Journal of Soil Mechanics and Foundation Div., ASCE, Vol. 97, No. 9.

Soulsby, R. L., and Whitehouse, R. J. (1997). Threshold of sediment motion in coastal environments. Pacific Coasts and Ports' 97: Proceedings of the 13th Australasian Coastal and Ocean Engineering Conference and the 6th Australasian Port and Harbour Conference; Volume 1, (p. 145).

Stark, T.D. and Olson, S.M. (1995) "Liquefaction resistance using CPT and field case histories", Journal Geotech. Eng Div., ASCE, Vol. 121, No. 12, 856-869.

Sumer, B. M. and Fredsøe, J. (2002). The mechanics of scour in the marine environment (Vol. 17). World Scientific Publishing Company.

TTR (2016). South Taranaki Bight Offshore Iron Sand Extraction And Processing Project – Impact Assessment.

Vaid, Y.P. and Negussey, D. (1984). "Relative Density of Pulviated Sand Samples". Soils and Foundations. Vol. 24, No. 2, June 1984.

Verruijt, A. (1995). Computational geomechanics (Vol. 7). Springer Science & Business Media.

Wald, D.J., Quitoriano, V., Heaton, T.H., and Kanamori, H. (1999) "Relationship between peak ground acceleration, peak ground velocity and modified mercalli intensity in California", Earthquake Spectra, Vol. 15, No. 3, 557-564.



### **List of Plates**

Plate 1: Measured and Interpreted Soil Properties at Kupe	34
Plate 2: Particle Size Distributions of In-situ Sediment	35
Plate 3: Cyclic Mobility and Flow Liquefaction	36
Plate 4: Reference Location for Metocean Statistical Data	37
Plate 5: Statistical Metocean Data	38
Plate 6: Estimated Cone Resistance Profile for Backfilled Sand	39
Plate 7: Liquefaction Potential for Ambient and Storm Conditions	40
Plate 8: Factor of Safety Against Wave-induced Liquefaction	41
Plate 9: Factor of Safety Against Seismic Liquefaction	42
Plate 10: Assessment of Post-liquefied Volumetric Strain (after Ishihara, 1993)	43
Plate 11: 2018 Palu Earthquake – Flow Liquefaction at Petobo (runout 1)	44
Plate 12: 2018 Palu Earthquake – Flow Liquefaction at Petobo (runout 2)	45
Plate 13: 2018 Palu Earthquake – Flow Liquefaction at Petobo (runout 2)	46
Plate 14: Potential Flow Paths from Seabed Mining Zone - Bathymetry	47
Plate 15: Potential Flow Paths from Seabed Mining Zone - Seabed Gradient	48
Plate 16: Residual Strength of Liquified Sands (after Jefferies and Been 2016)	49
Plate 17: Stable Sediment Thickness and Seabed Gradient	50
Plate 18: Proposed Mining Exclusion Zone	51
Plate 19: Potential Flow Paths from Seabed Mining Zone Towards Existing Kupe Infrastructure	52
Plate 20: Loose Tailings Stress-strain Responses and Stress Paths With and Without Soil Consolidati	
	53
Plate 21: Seabed Mining Zone – Bathymetry and Seabed Gradient	54
Plate 22: Surface Current, Oceanic fronts & Main Water Masses	55
Plate 23: Outline of Main Elements of Abyssal Circulation	56
Plate 24: Shoreline stability in the South Taranaki Bight in historical times NIWA, 2015b)	57
Plate 25: Particle size distribution curves (Advanced geomechanics, 2004)	58
Plate 26: Significant Wave Height & Depth-averaged Current	59
Plate 27: Spatial Distribution along Isobath of Mean Wave Energy Flux	60
Plate 28: Summary of Bedforms	61
Plate 29: Seabed Shear Stress Exceedance Curve	62
Plate 30: Wave-induced Bed Shear Stress & Joint Probability of Significant Wave Height and Period	63



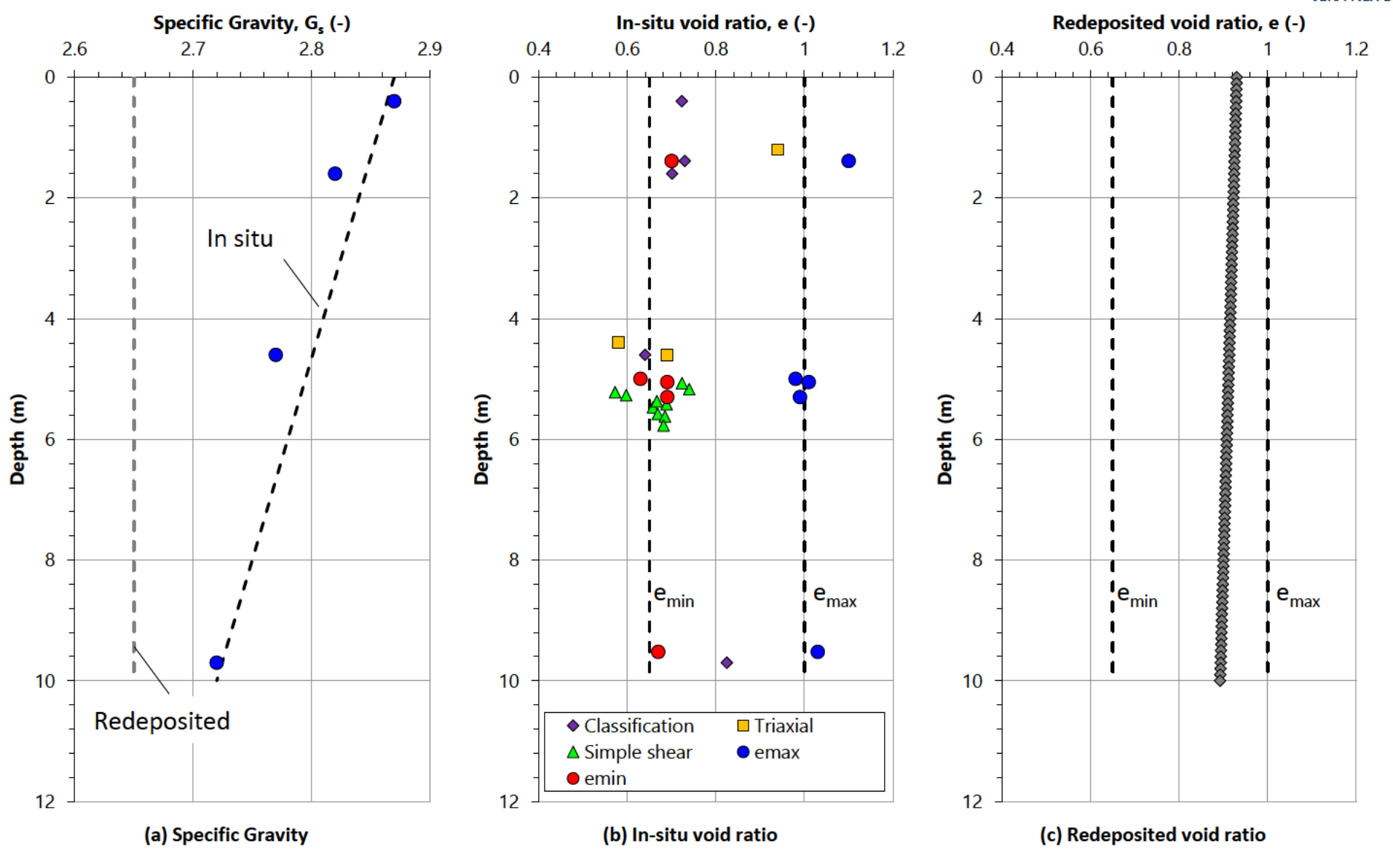


Plate 1: Measured and Interpreted Soil Properties at Kupe



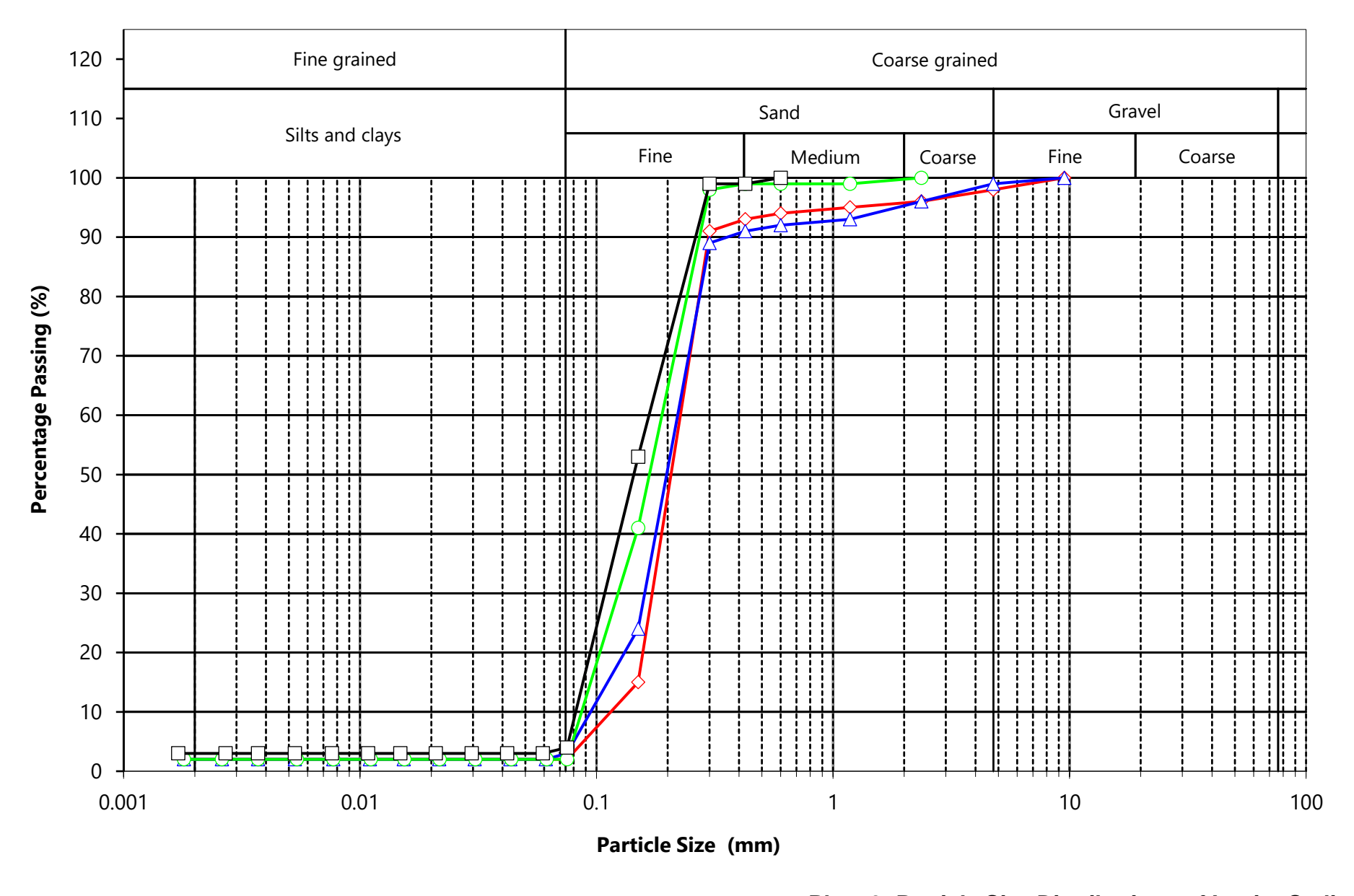
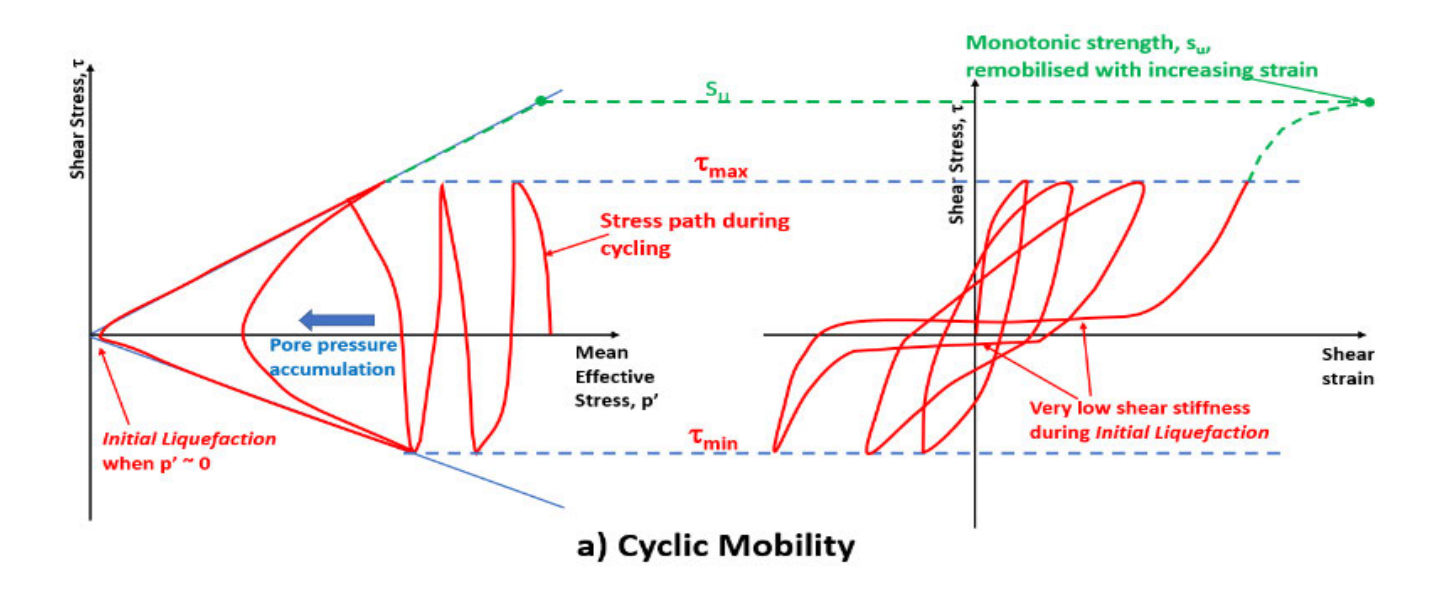


Plate 2: Particle Size Distributions of In-situ Sediment





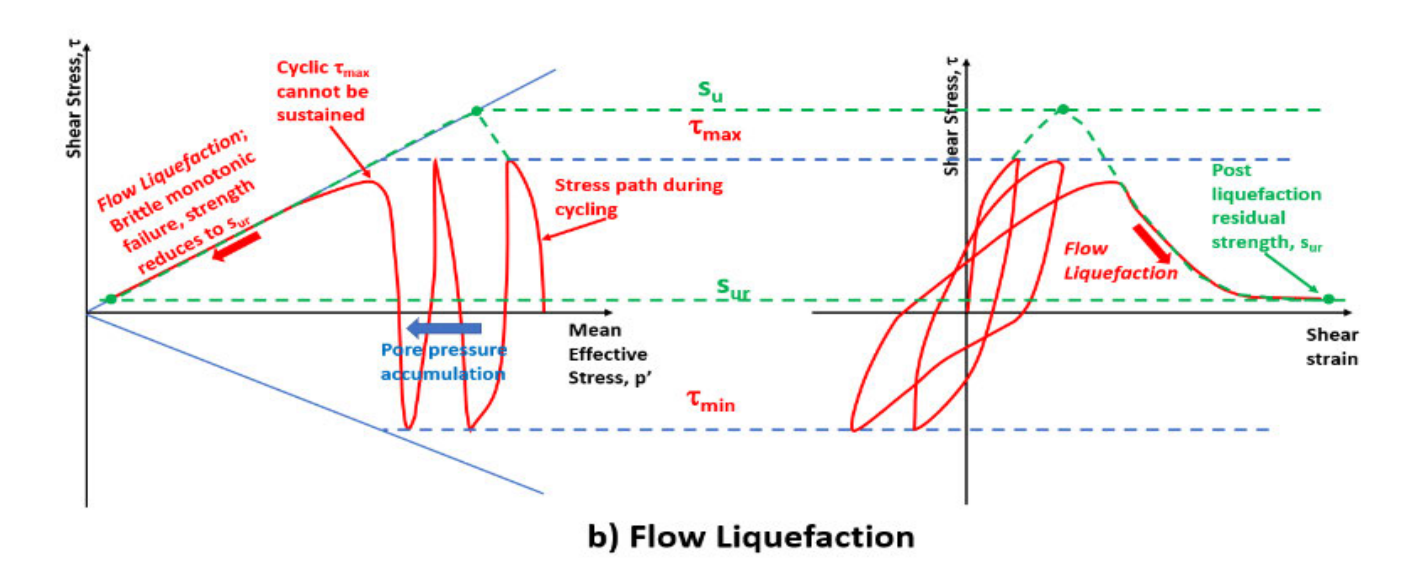
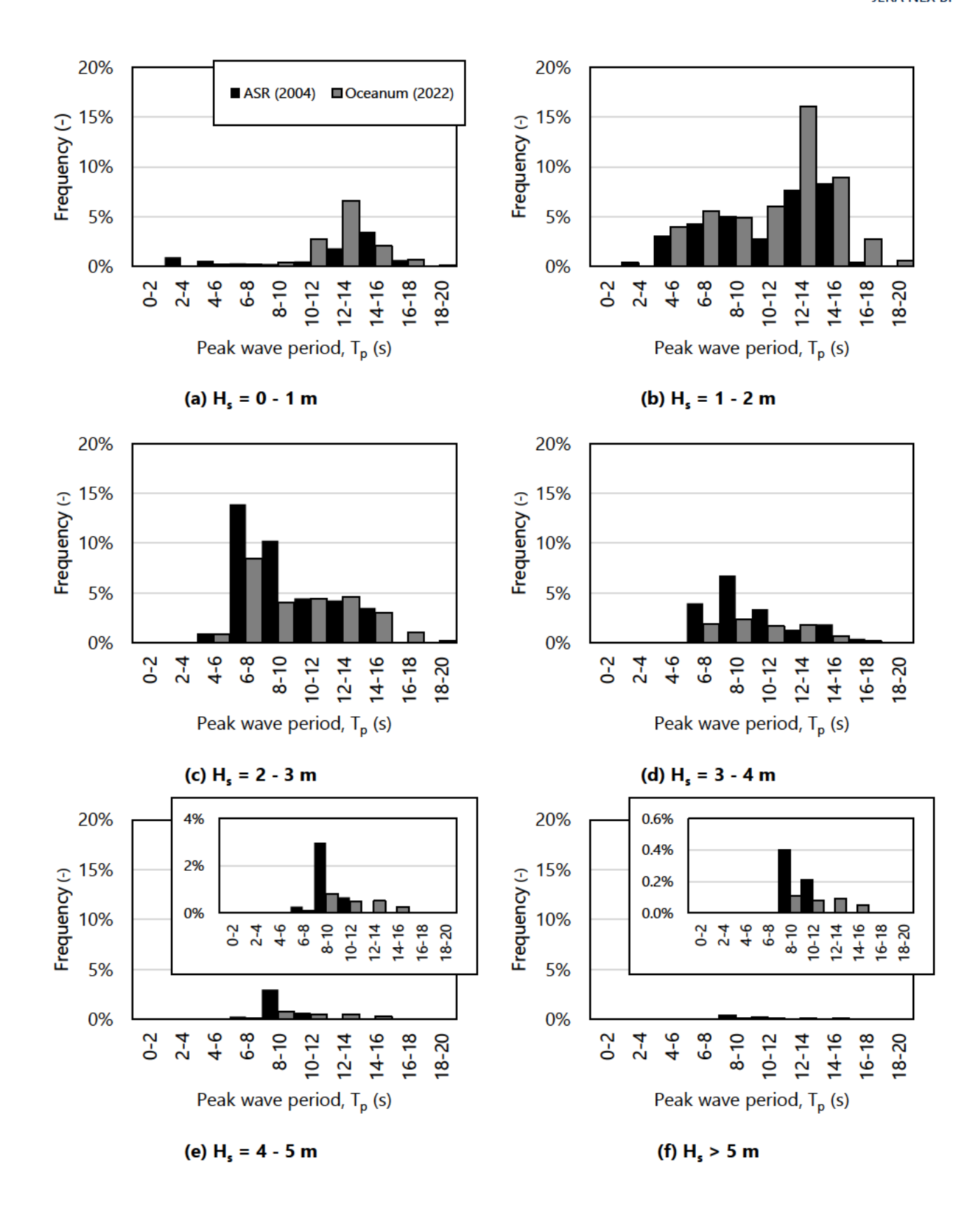
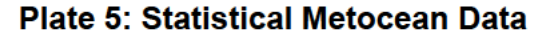


Plate 3: Cyclic Mobility and Flow Liquefaction









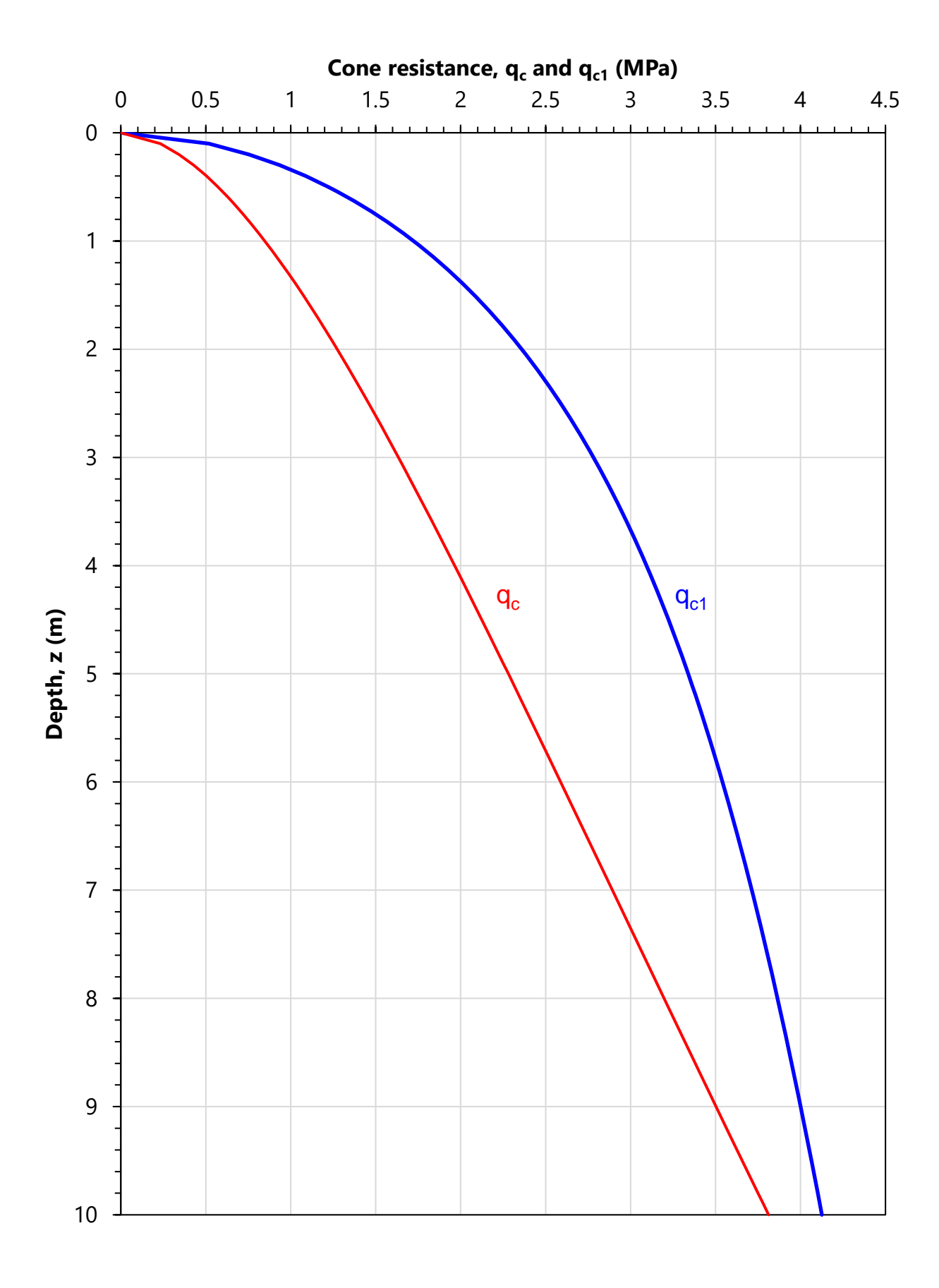
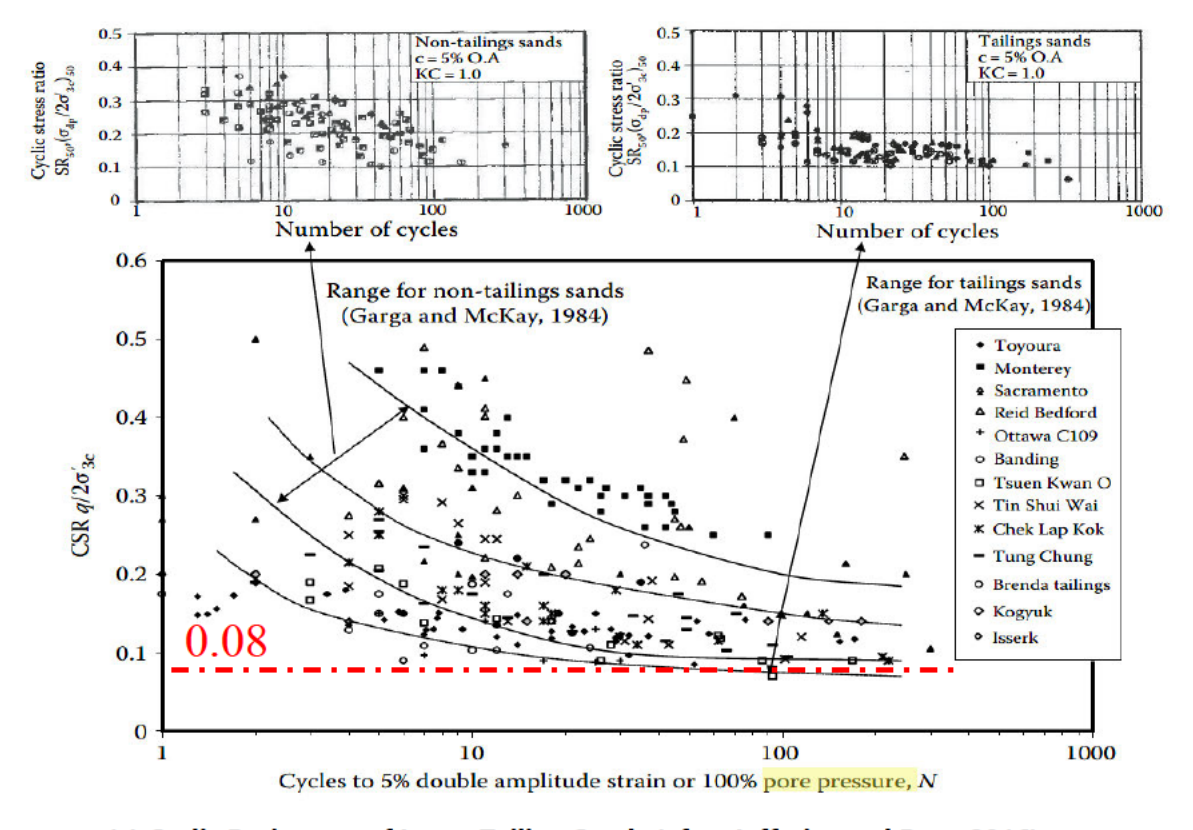


Plate 6: Estimated Cone Resistance Profile for Backfilled Sand





(a) Cyclic Resistance of Loose Tailing Sands (after Jefferies and Been 2016)

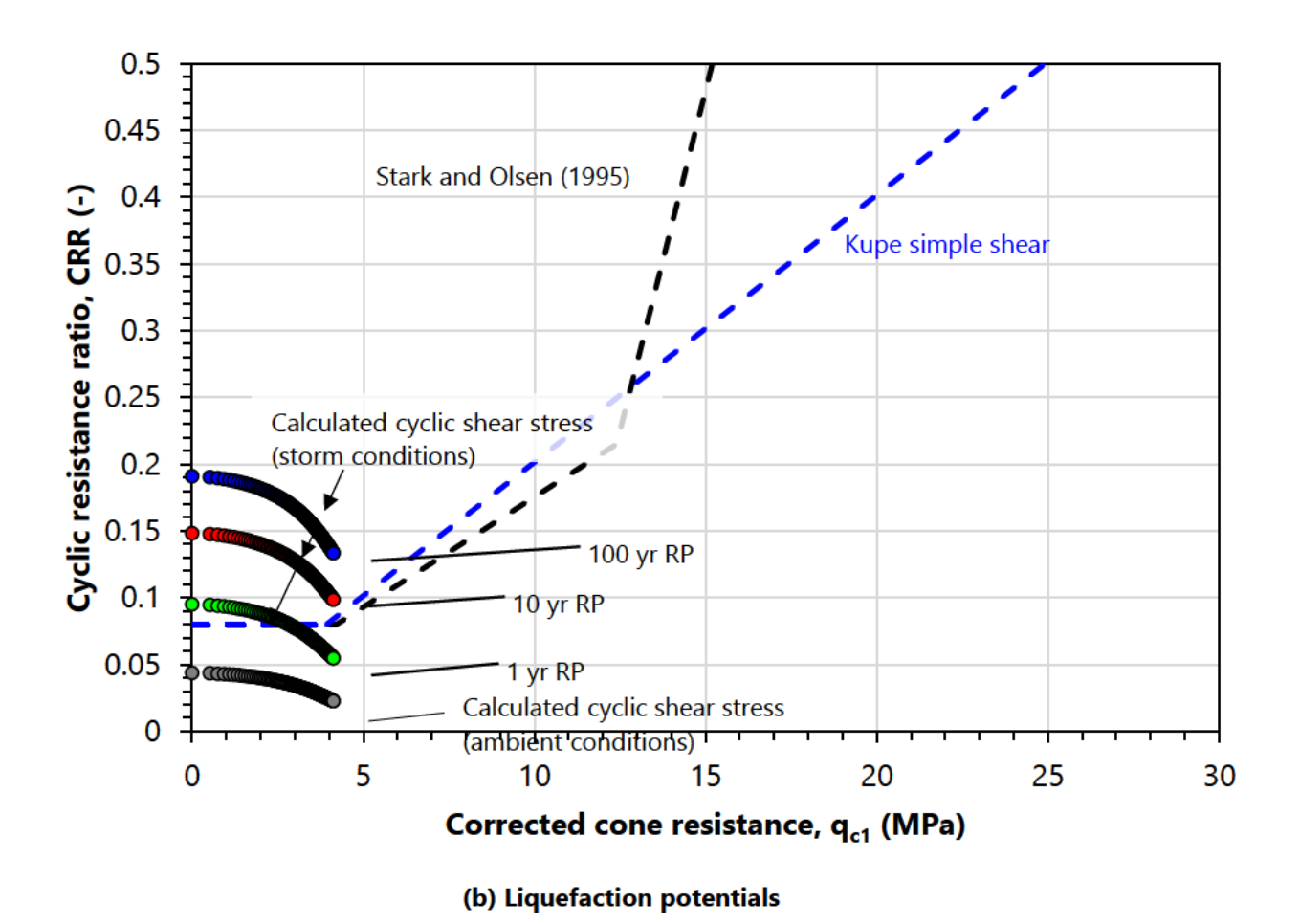


Plate 7: Liquefaction Potential for Ambient and Storm Conditions



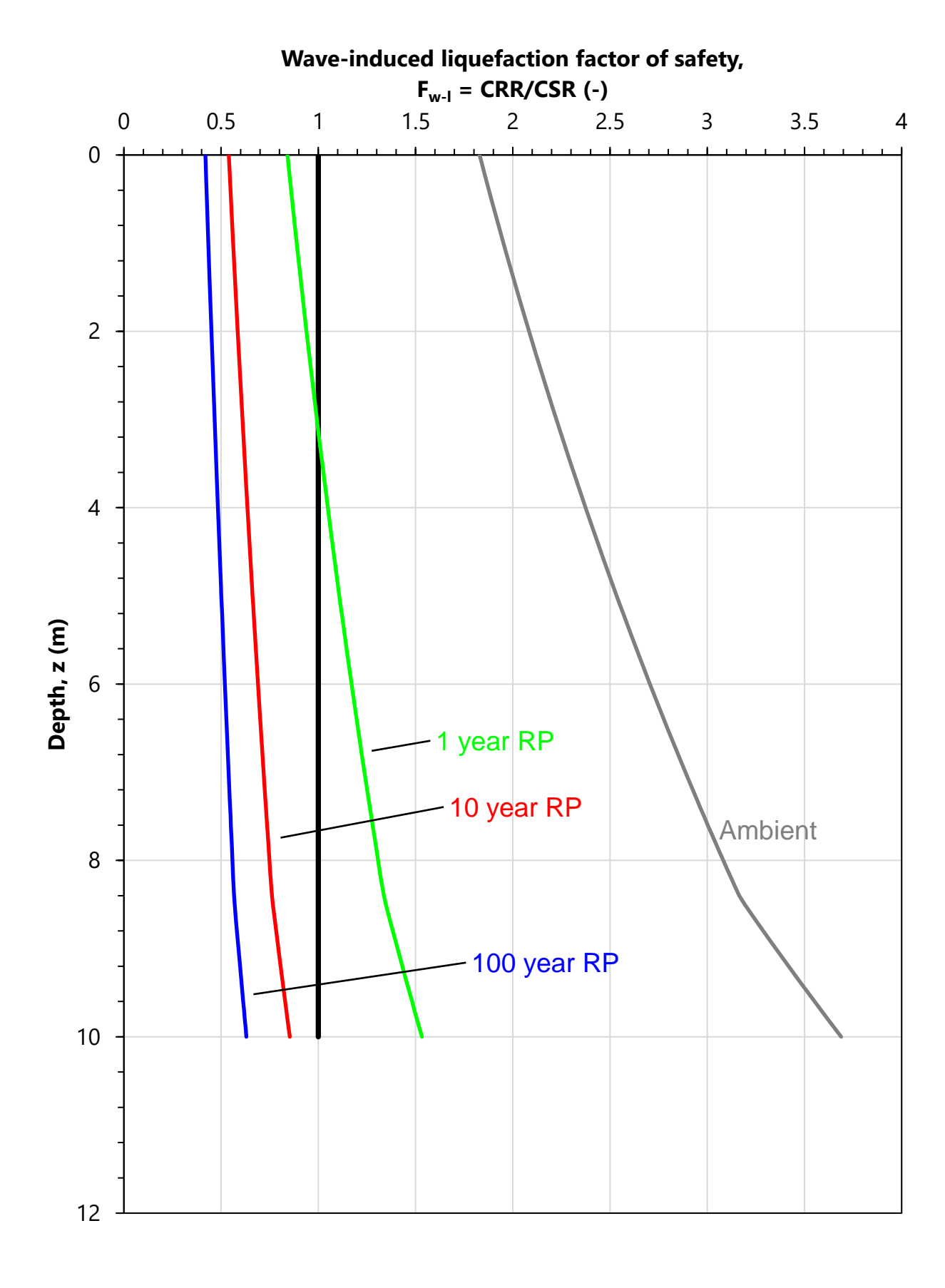


Plate 8: Factor of Safety Against Wave-induced Liquefaction



# Seismic liquefaction factor of safety, $F_{s-l} = CRR/CSR (-)$ 0 0.2 0.4 0.6 8.0 1 1.2 0 2 4 RIE Depth, z (m) - DEE 8 10 12

Plate 9: Factor of Safety Against Seismic Liquefaction



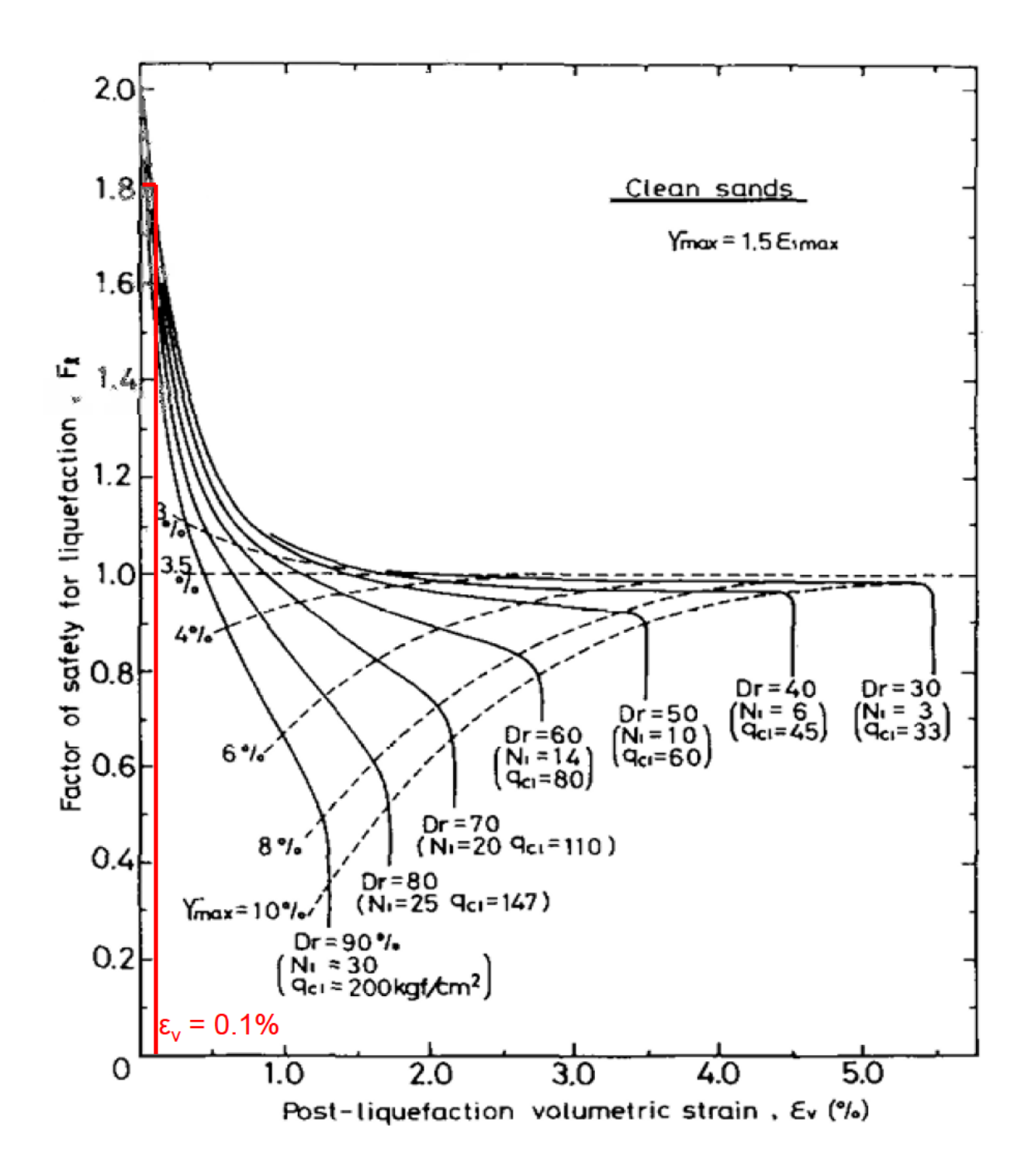


Plate 10: Assessment of Post-liquefied Volumetric Strain (after Ishihara, 1993)



Plate 11: 2018 Palu Earthquake – Flow Liquefaction at Petobo (runout 1)



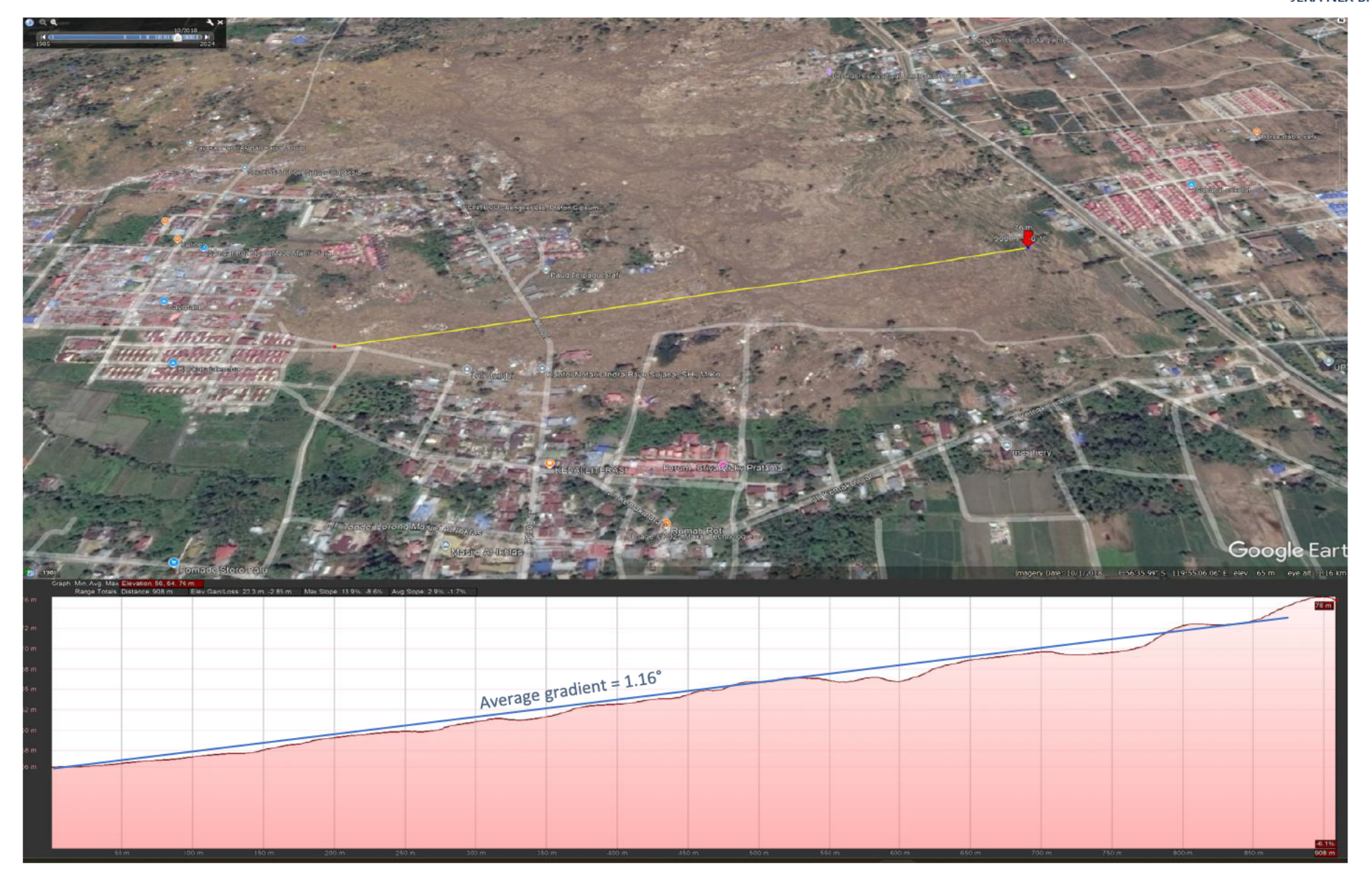


Plate 12: 2018 Palu Earthquake – Flow Liquefaction at Jono Oge (runout 2)



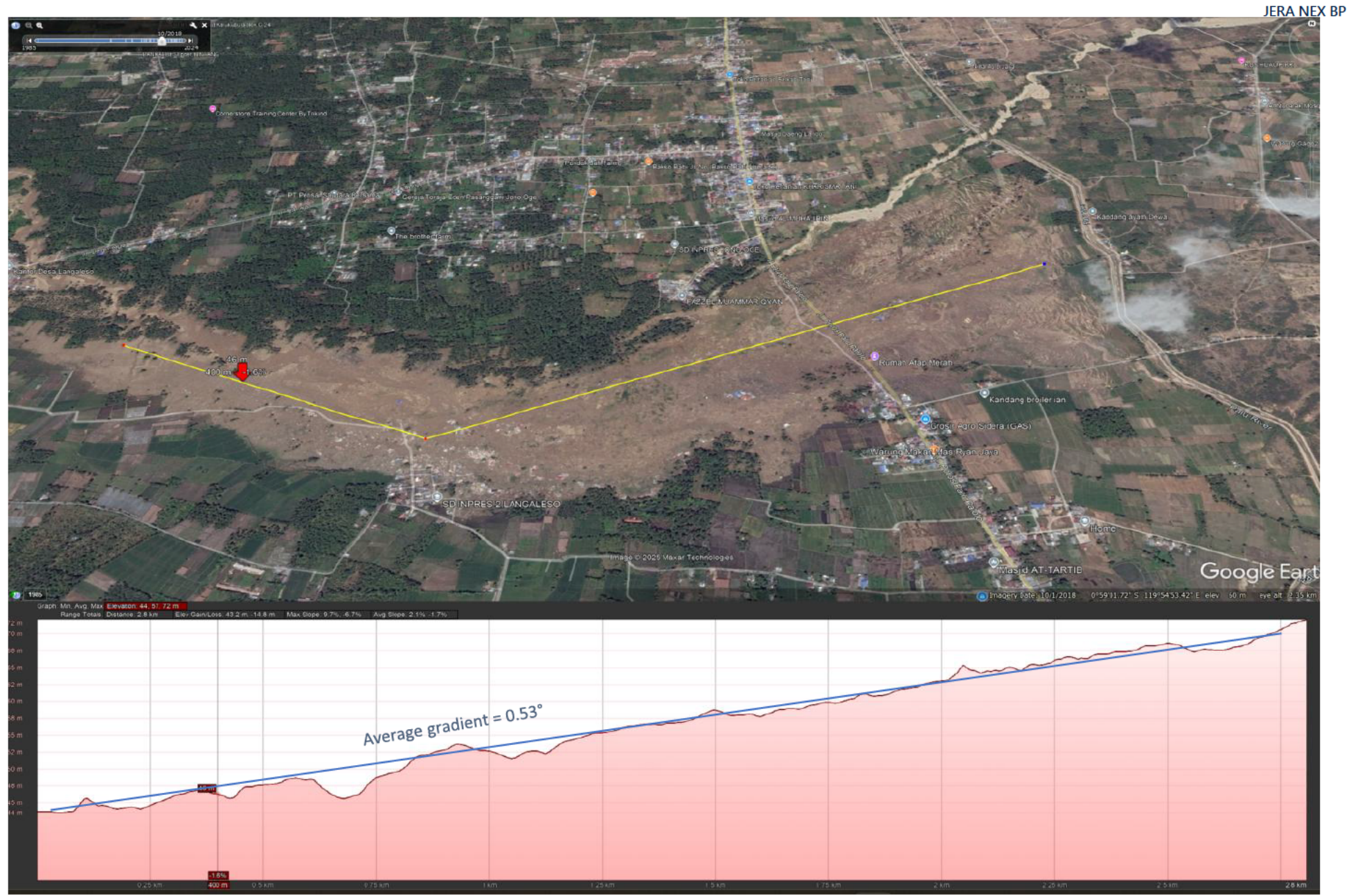


Plate 13: 2018 Palu Earthquake – Flow Liquefaction at Petobo (runout 3)



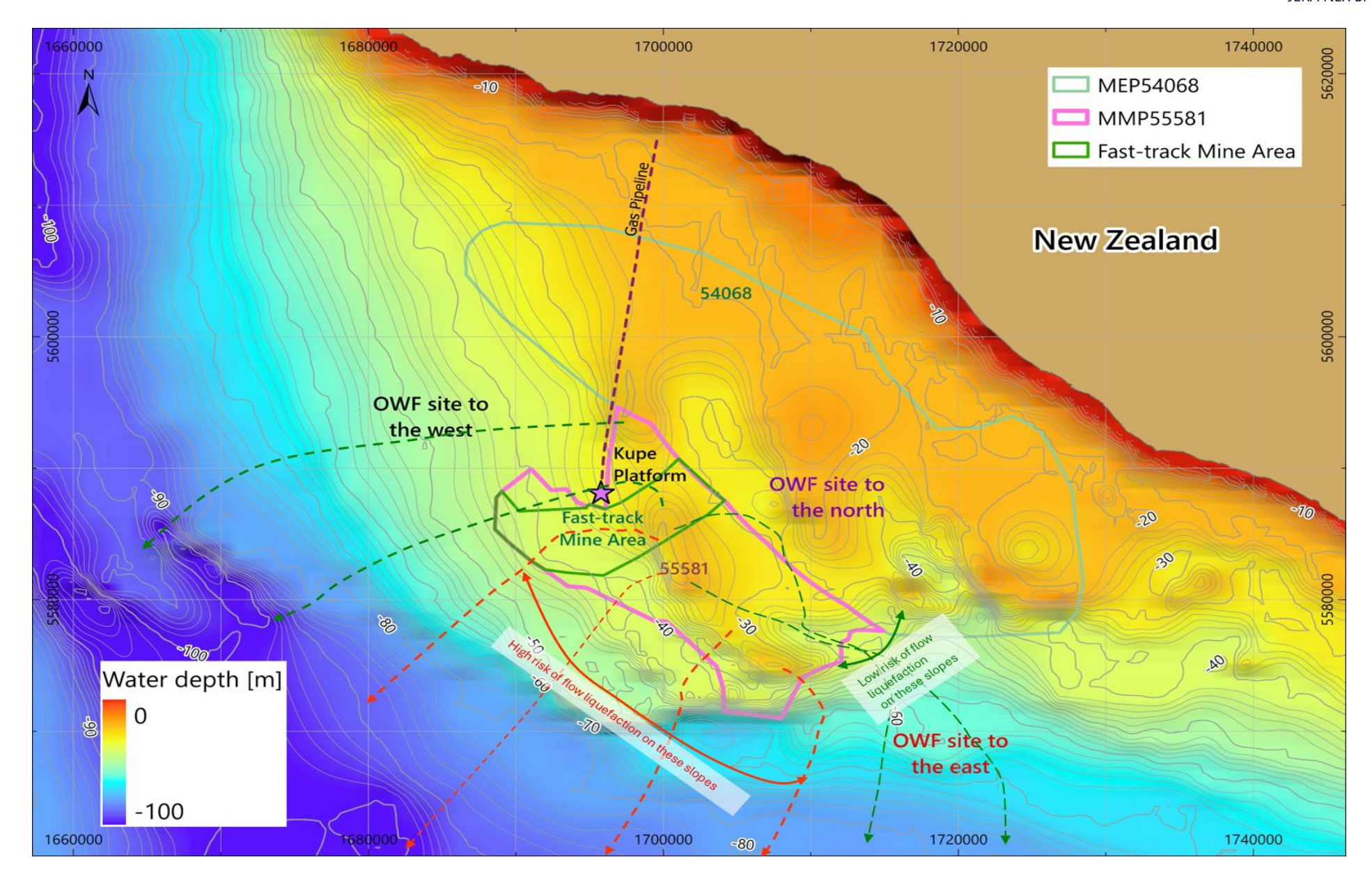


Plate 14: Potential Flow Paths from Seabed Mining Zone - Bathymetry



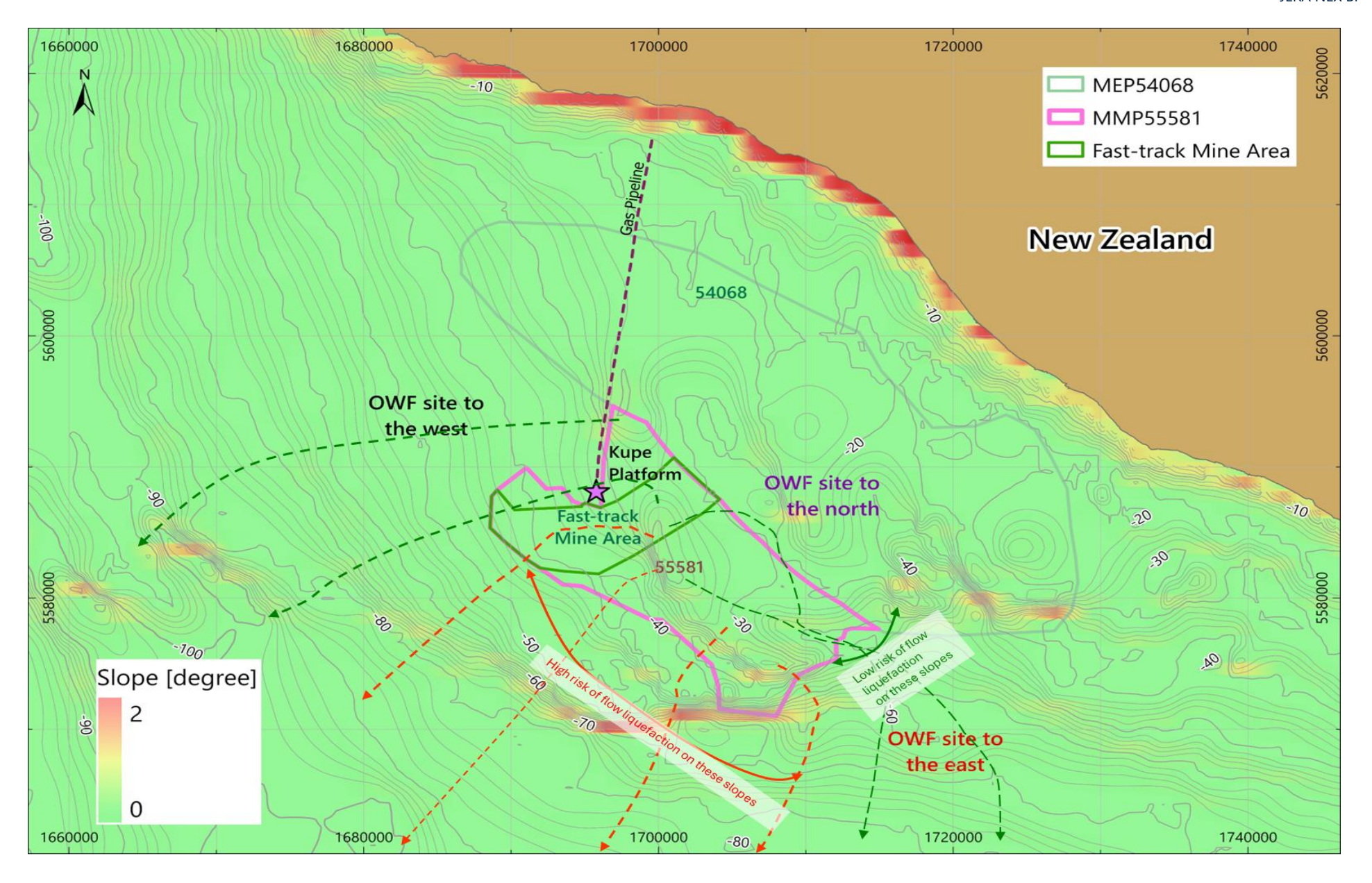


Plate 15: Potential Flow Paths from Seabed Mining Zone - Seabed Gradient



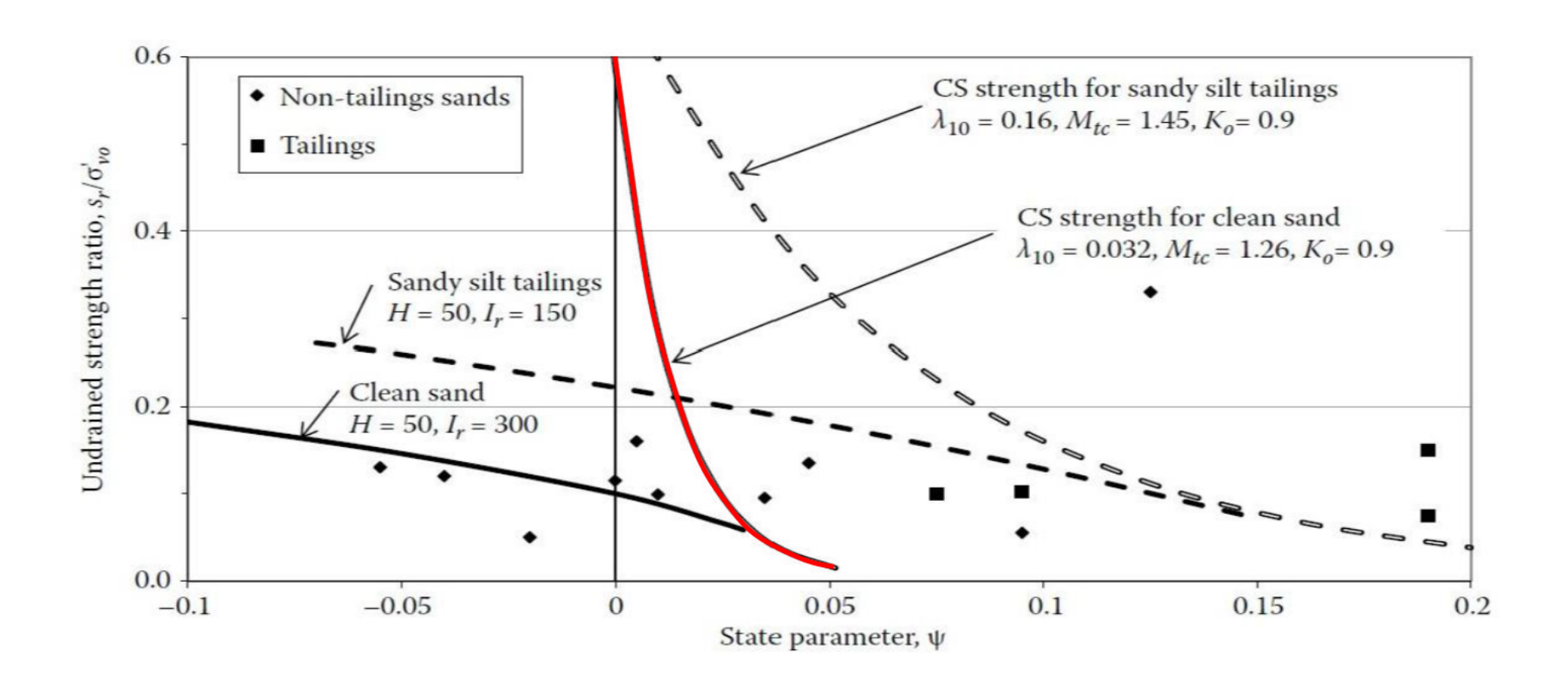


Plate 16: Residual Strength of Liquified Sands (after Jefferies and Been 2016)



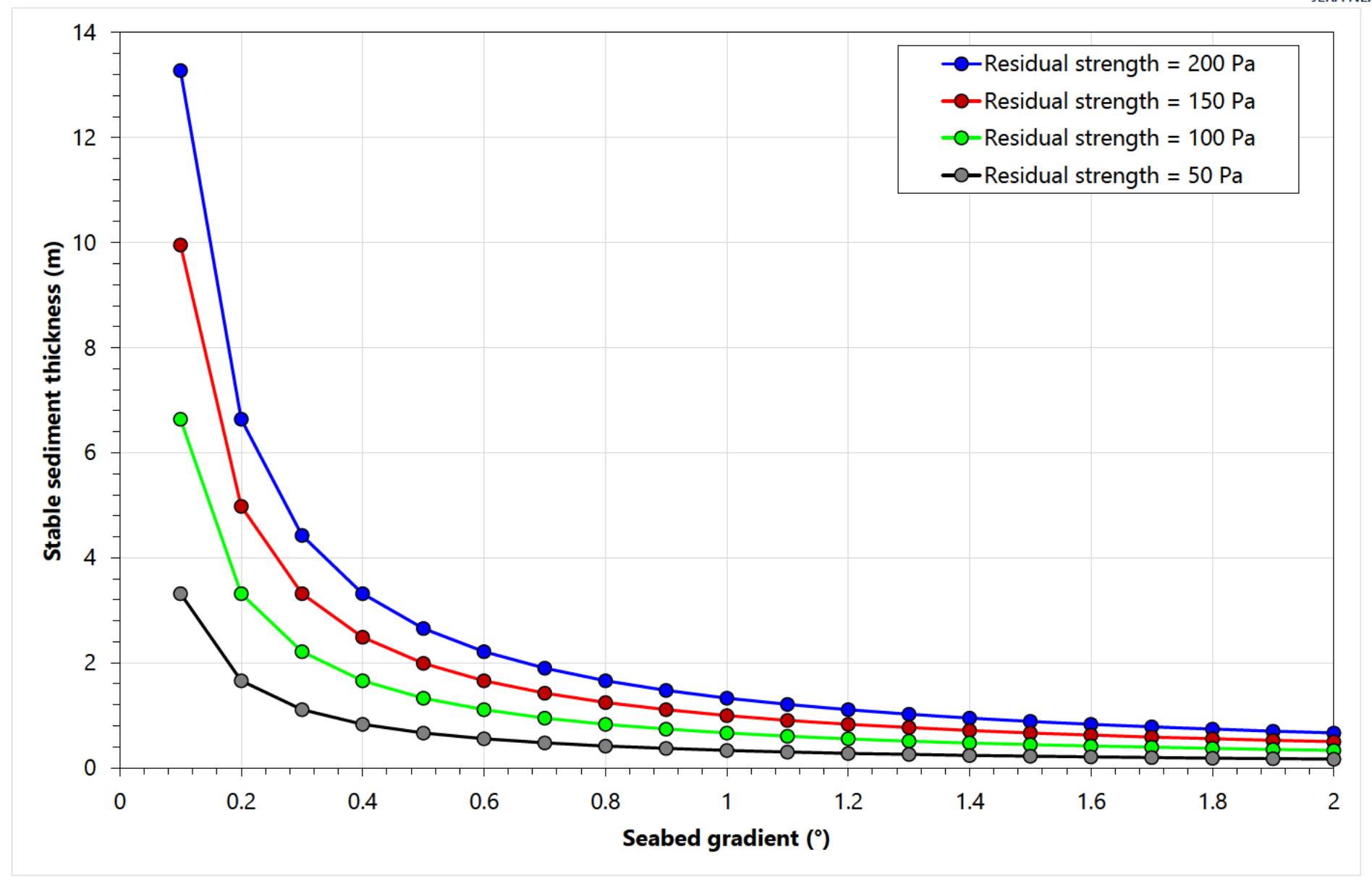
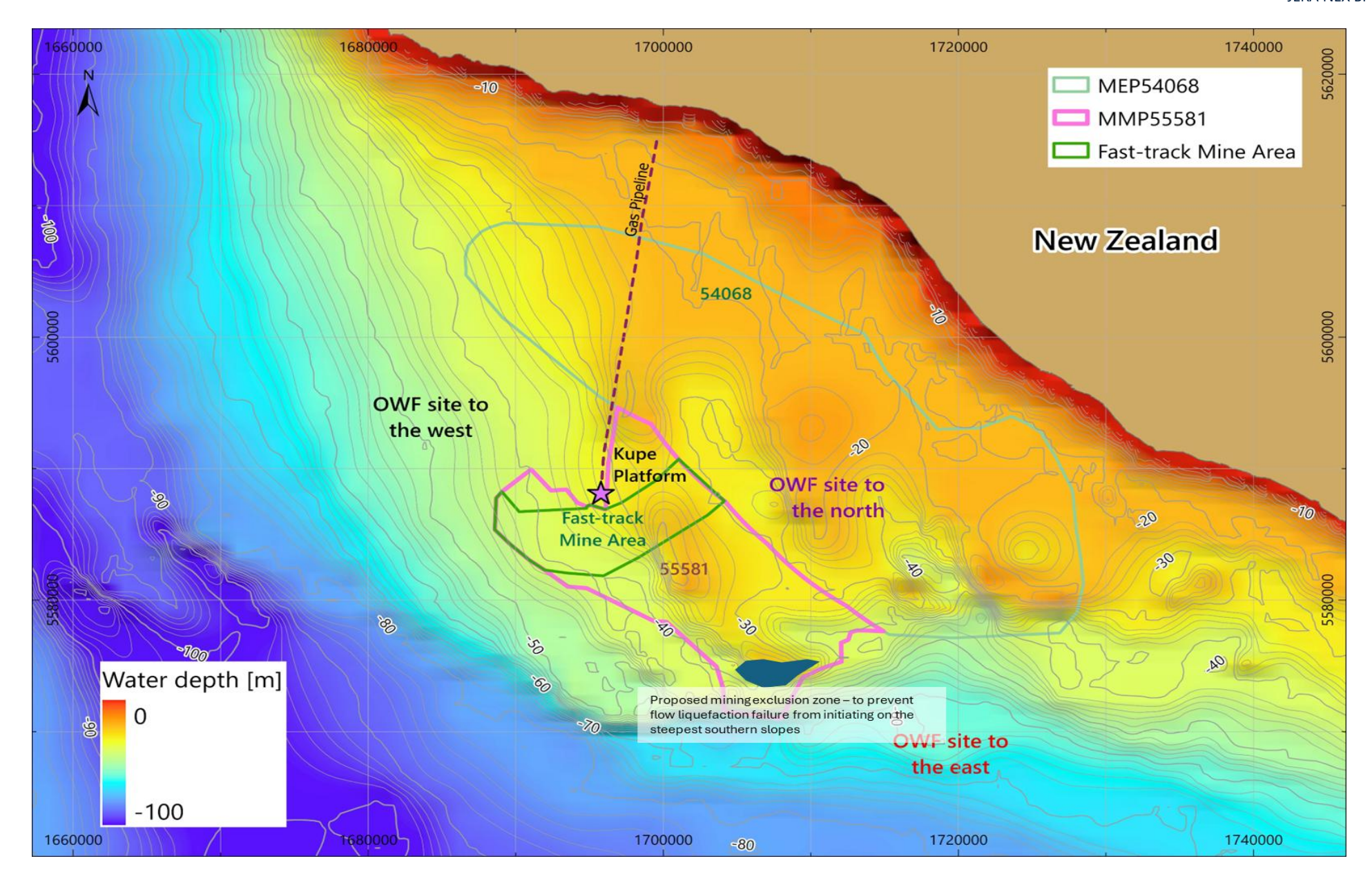


Plate 17: Stable Sediment Thickness and Seabed Gradient





**Plate 18: Proposed Mining Exclusion Zone** 



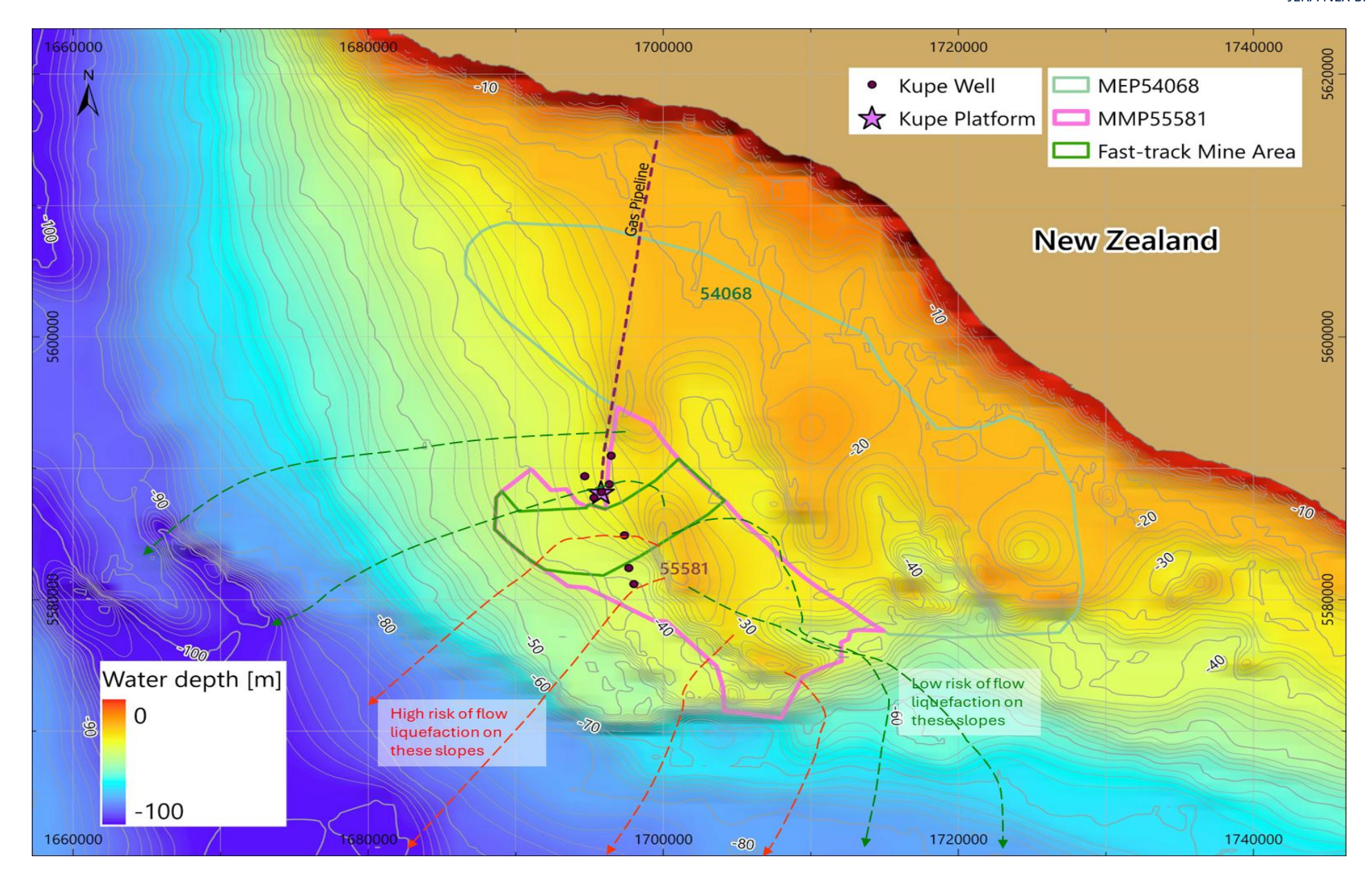


Plate 19: Potential Flow Paths from Seabed Mining Zone Around Existing Kupe Infrastructure



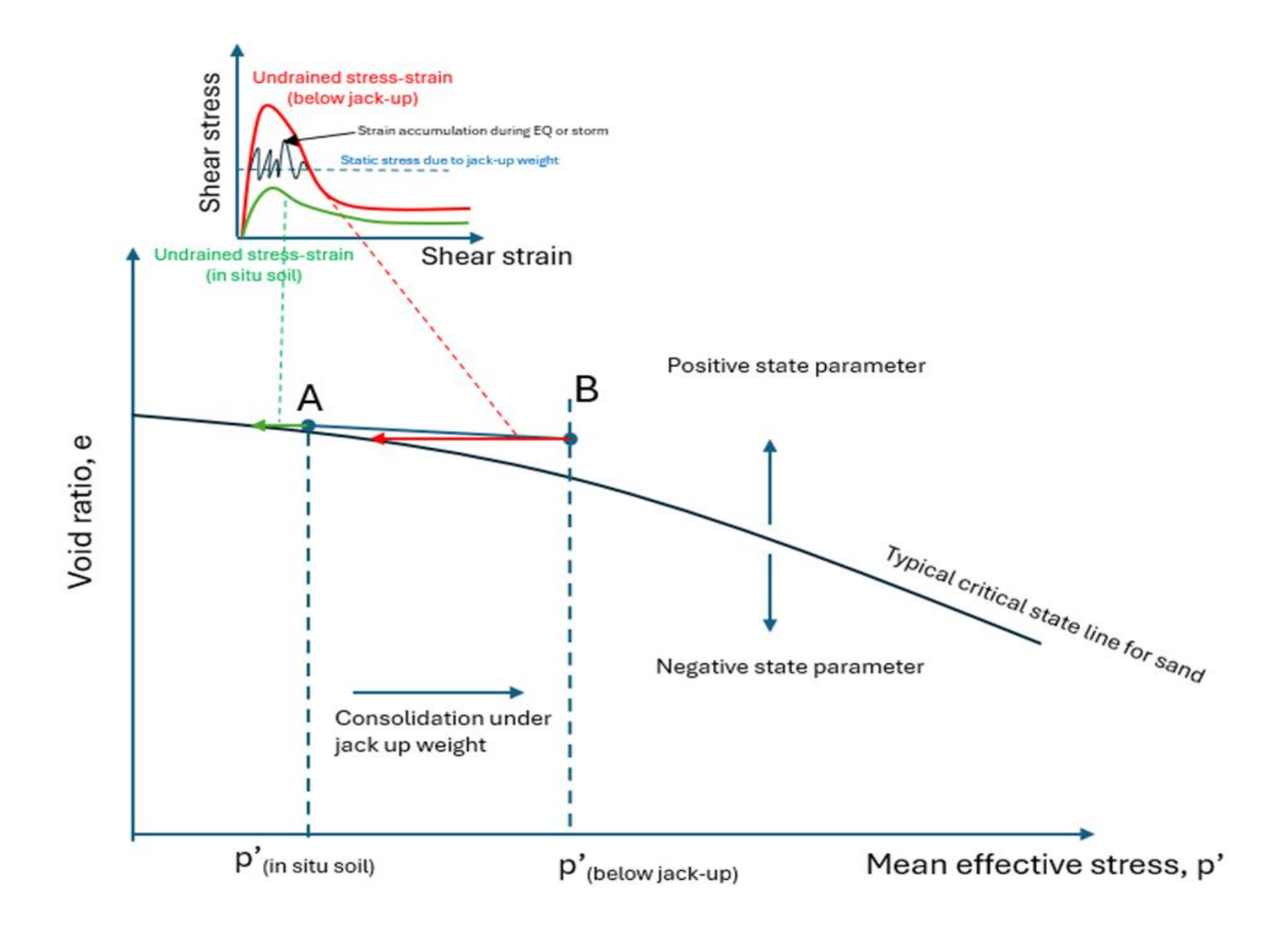
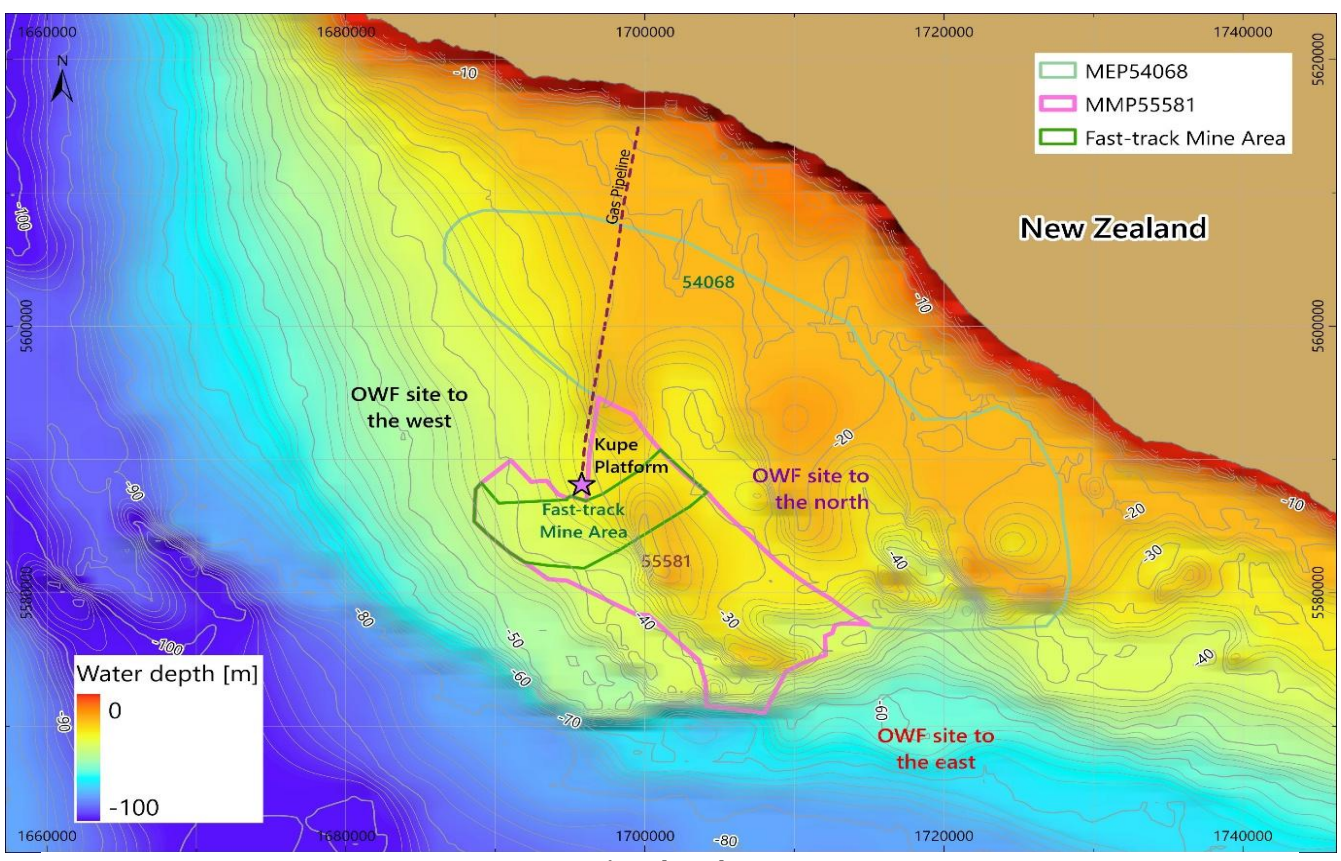
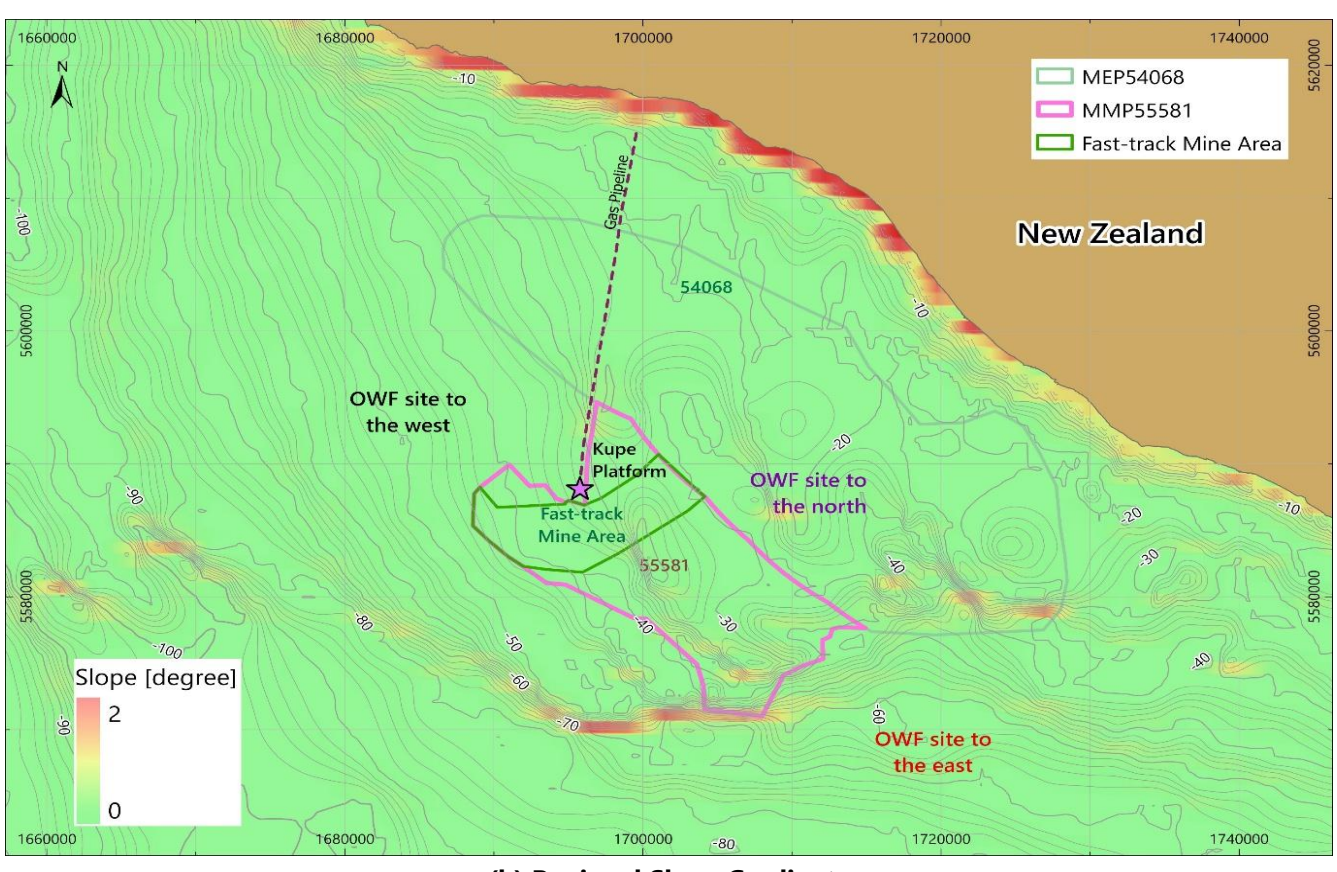


Plate 20: Loose Tailings Stress-strain Responses and Stress Paths With and Without Soil Consolidation





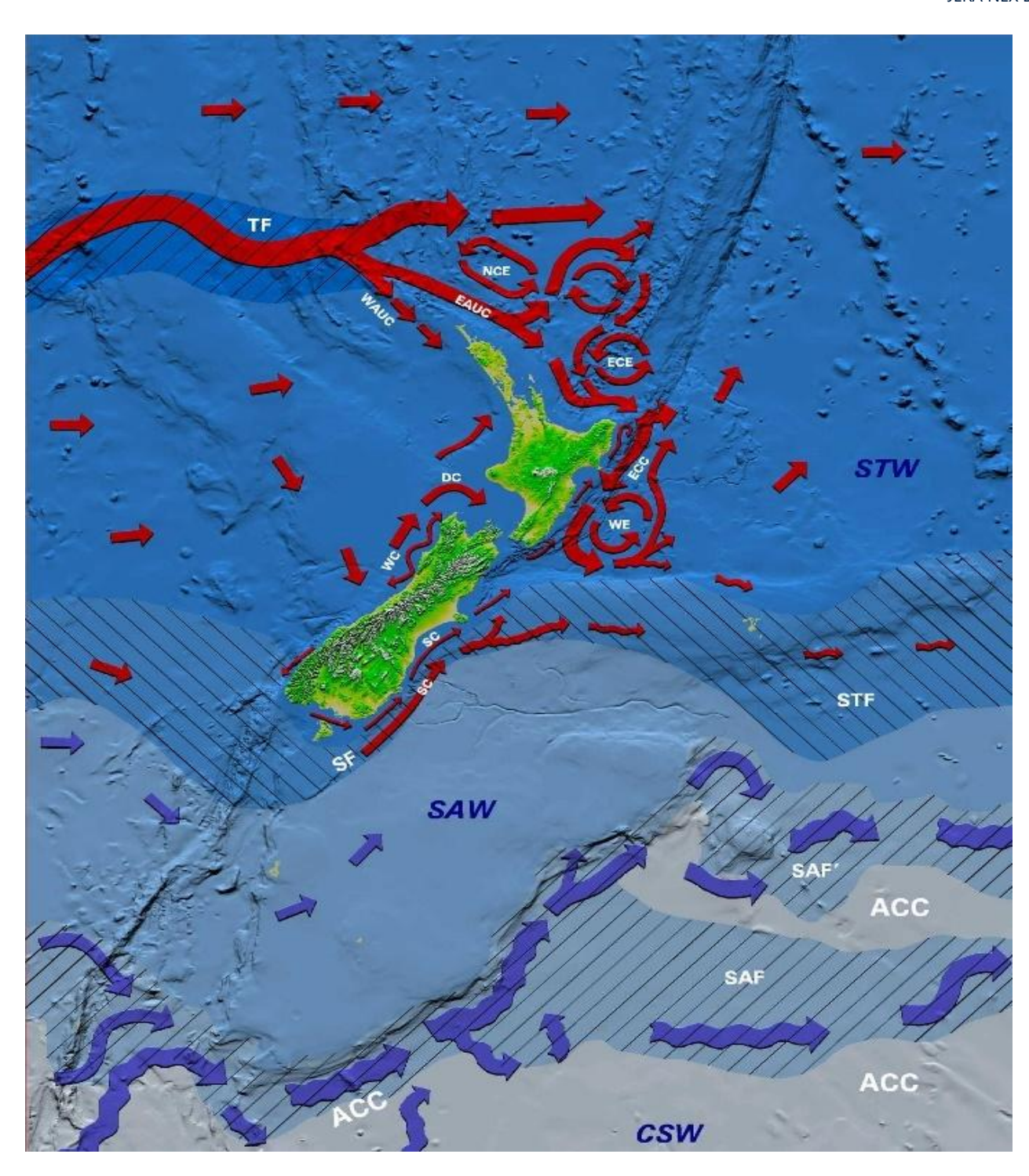
(a) Regional Bathymetry



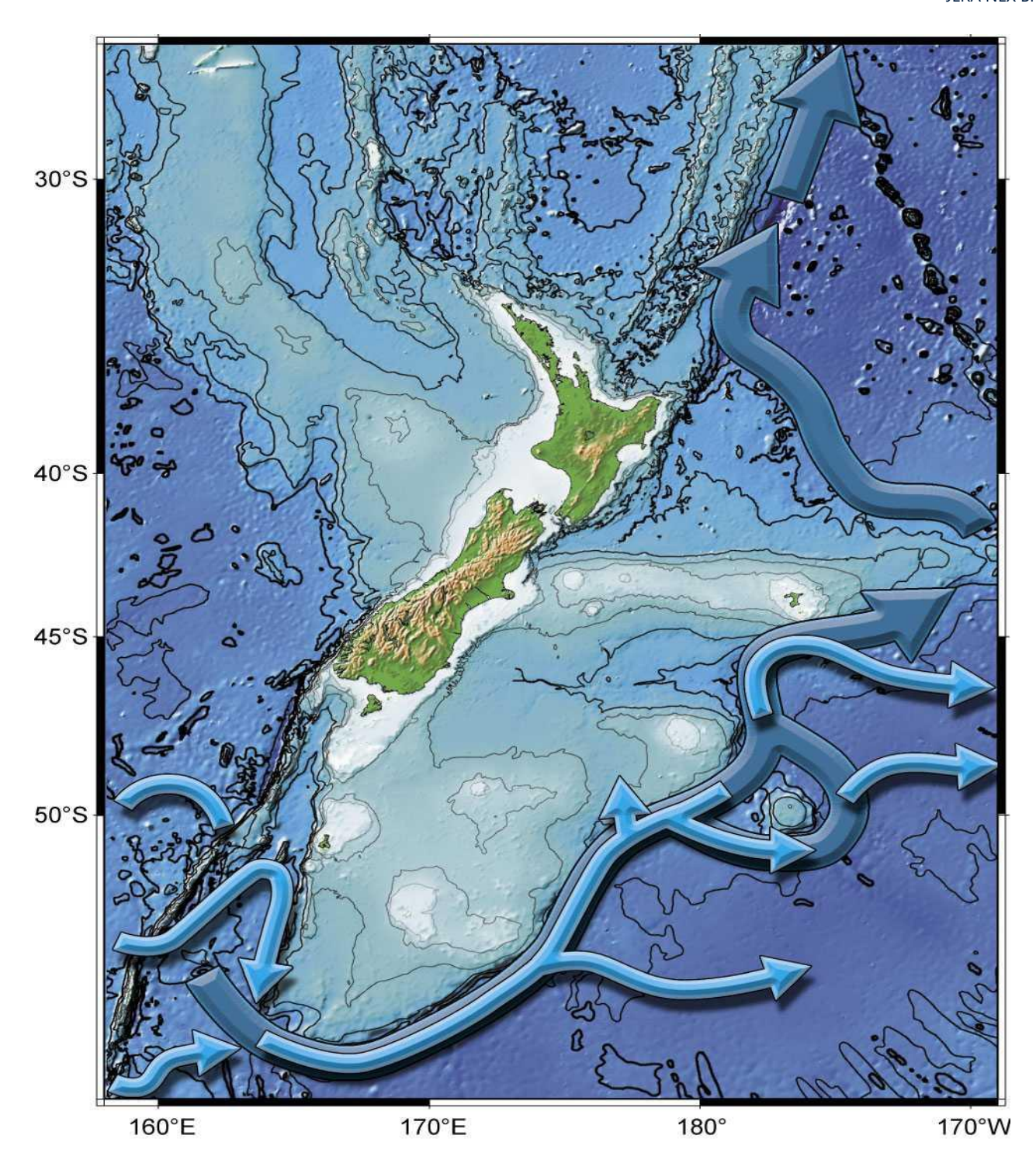
(b) Regional Slope Gradients

Plate 21: Regional Bathymetry and Slopes over Mining and Potential OWF Sites





Summary of the characteristics of the surface current systems, oceanic fronts and main water masses including Subtropical Water [STW]; Subtropical Front [STF]; Subantarctic Water [SAW]; Subantarctic Front [SAF]; Antarctic Circumpolar Current [ACC], the northern limit of which is defined by the SAF; Circumpolar Surface Water [CSW]. Currents are annotated as follows: East Australian Current [EAC]; East Auckland Current [EAUC]; North Cape Eddy [NCE]; East Cape Eddy [ECE]; East Cape Current [ECC]; Wairarapa Eddy [WE]; Southland Current [SC]; Southland Front [SF]; Westland Current [WC], and D'Urville Current [DC]; Tasman Front [TF]. Images retrieved from Project Reef South Taranaki.



Outline of the main elements of the abyssal circulation including the deep western boundary current [dark arrows] and the overlying but deep-reaching Antarctic Circumpolar Current [light blue arrows]. Images retrieved from <a href="Project Reef South Taranaki">Project Reef South Taranaki</a>.

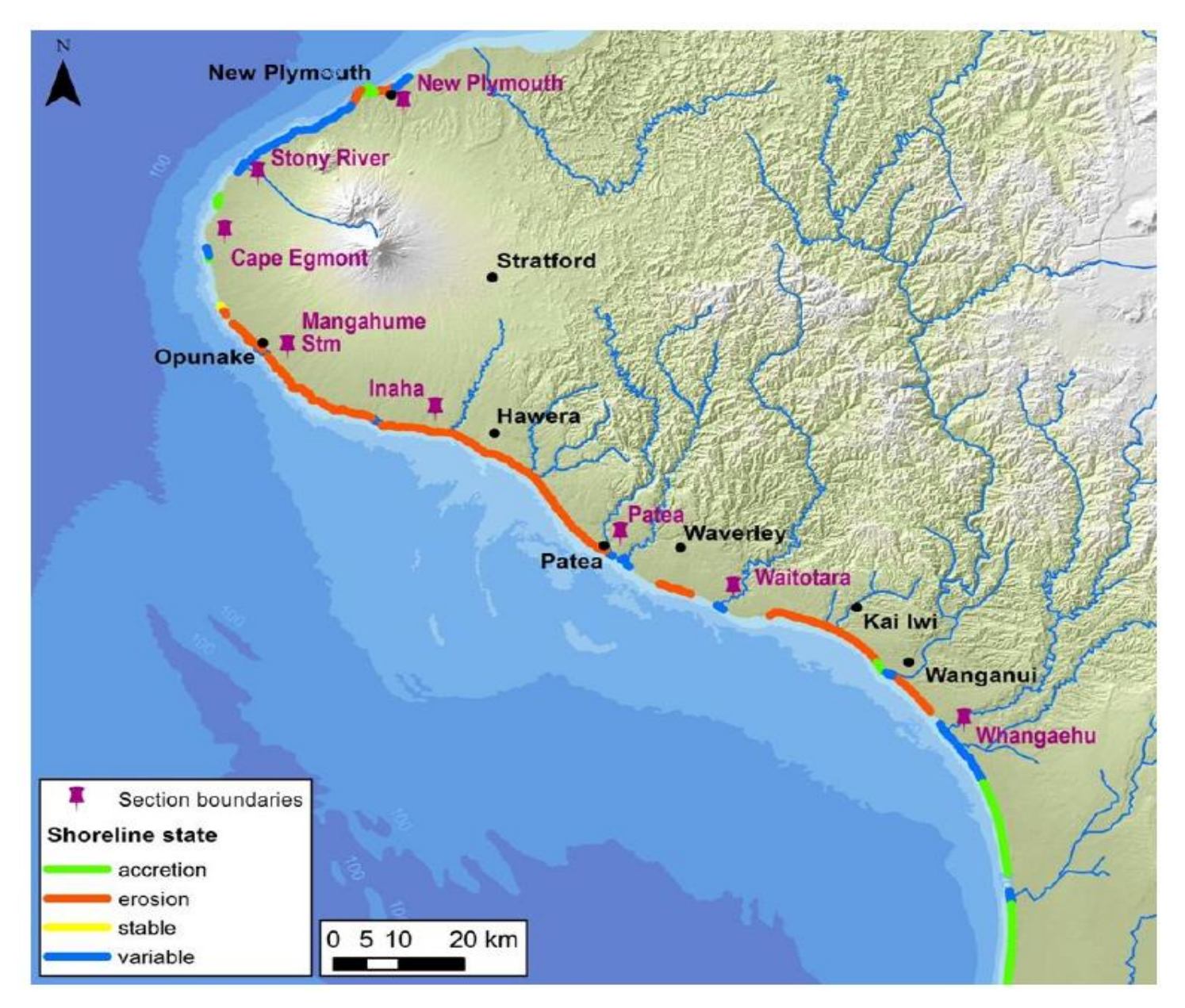


Plate 24: Shoreline Stability in South Taranaki Bight in Historical Times NIWA, 2015b)



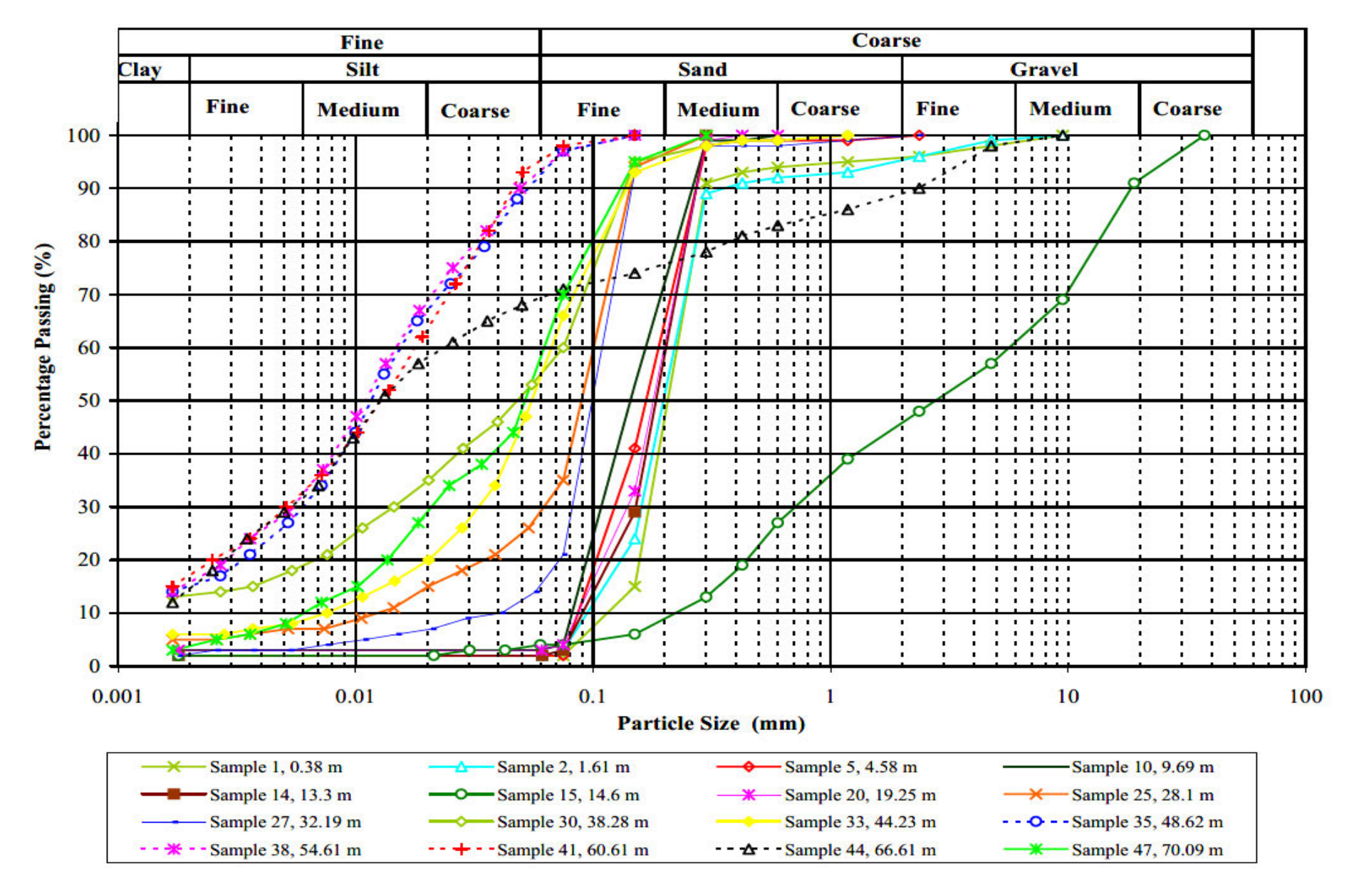
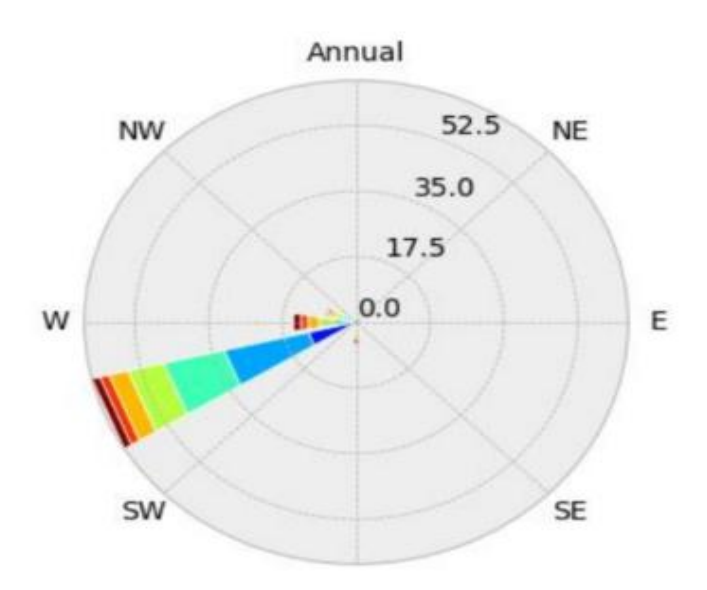
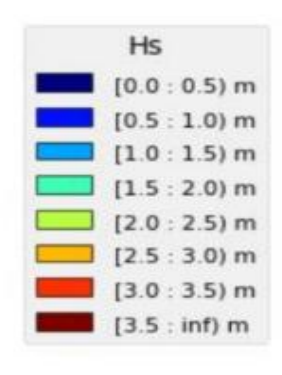


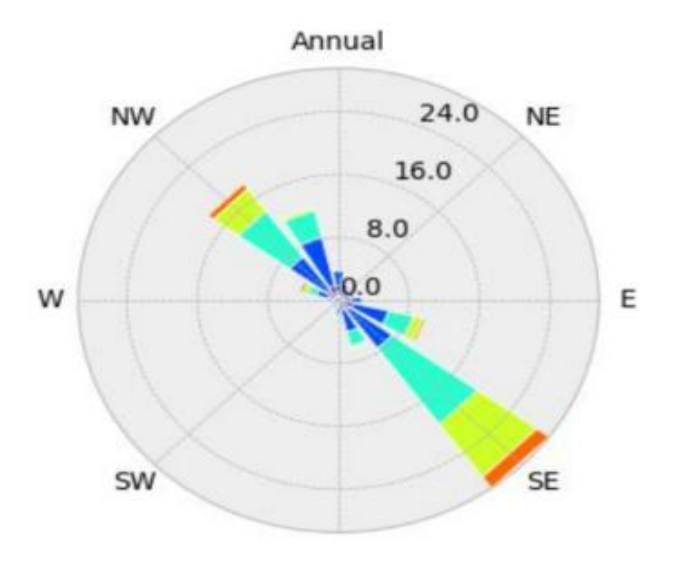
Plate 25: Particle Size Distribution Curves (Advanced Geomechanics, 2004)

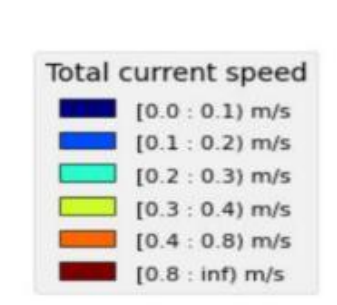






(a) Significant wave height for annual conditions (sea and swell partitions) at Kupe platform location. Directions 'coming from' (Oceanum, 2022)





(b) Depth-averaged currents for annual conditions at Kupe platform location. Directions 'going to' (Oceanum, 2022)



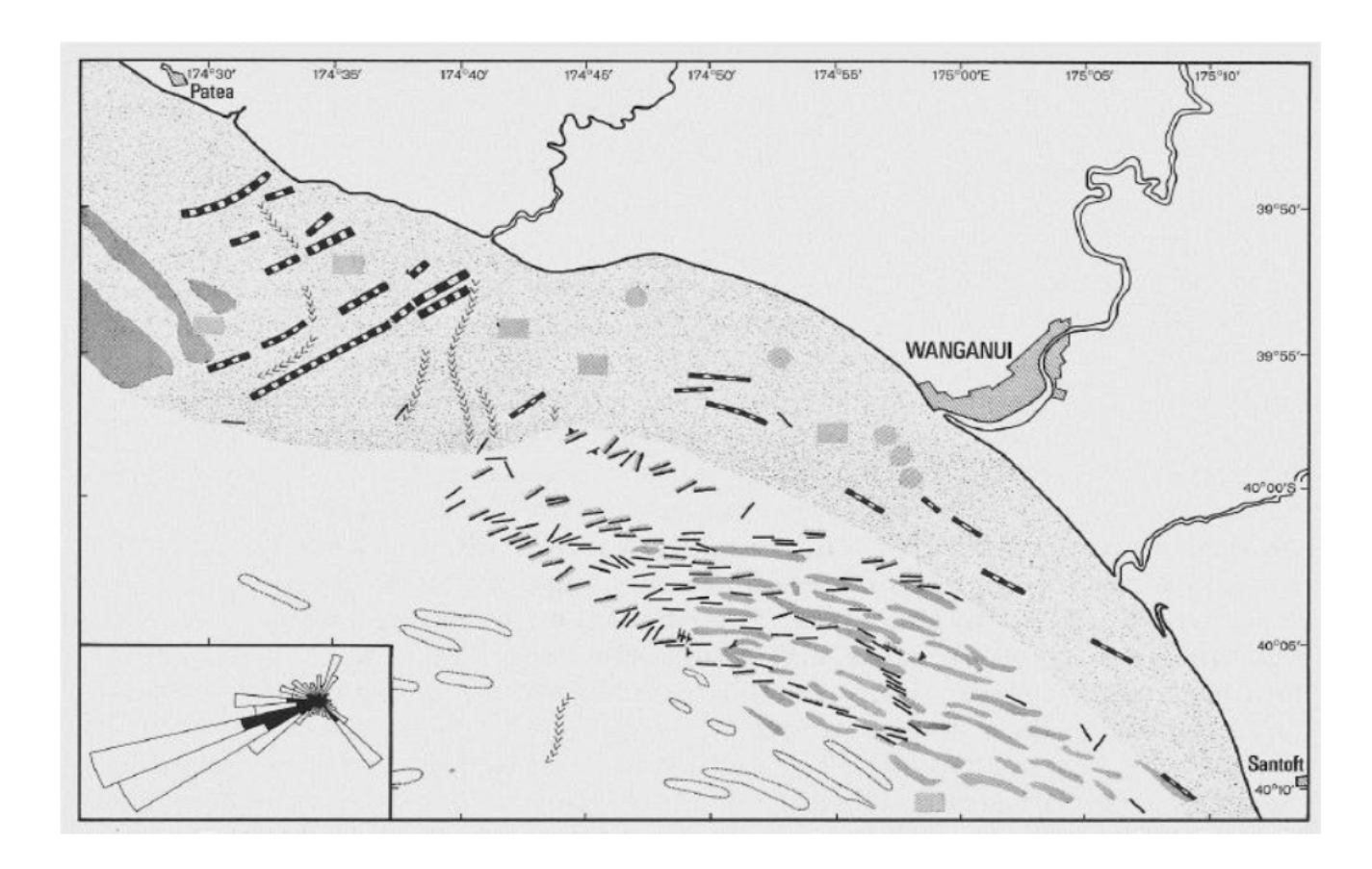
Plate 26: Significant Wave Height & Depth-averaged Current

## Mean wave energy flux (kW/m) 1979-1998 Month: ALL 25 -39 20 20 kW/m -39.515 -40 10 -40.55 -41 -41.5└ 173 0 173.5 174.5 174 175 175.5

Spatial distribution along the 50 m isobath of mean wave energy flux, averaged over 20-year hindcast record. The colour scale shows the mean of the magnitude of the energy flux, while the arrows show the vector averaged flux (NIWA, 2011).



Plate 27: Spatial Distribution along Isobath of Mean Wave Energy Flux

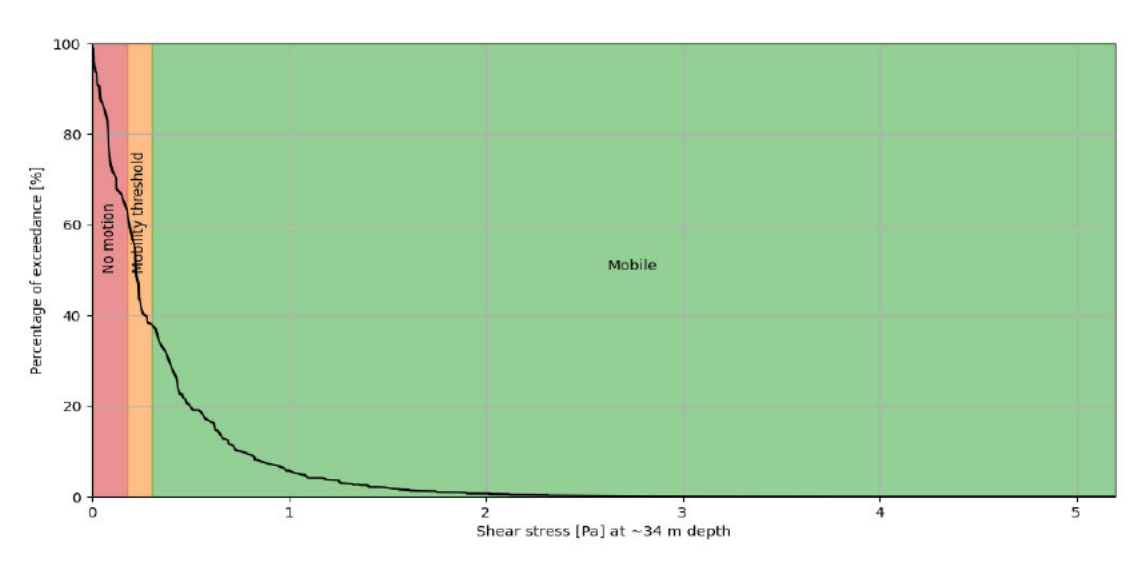


A diagrammatic summary of bedforms by Lewis (1979) determined from side-scan and high-resolution seismic reflection surveys. Legend: rock outcrops (heavy broken lines); ancient buried valleys (line of V's); ironsand ridges (grey dense stipple); sand ribbons (bold lines); symmetrical megaripples (fine lines) and sand waves (arrowed lines). The inset shows the directions of large waves stirring fine sand at 30 m (white fill) and 50 m (solid black fill). Retrieved in (NIWA, 2015a).





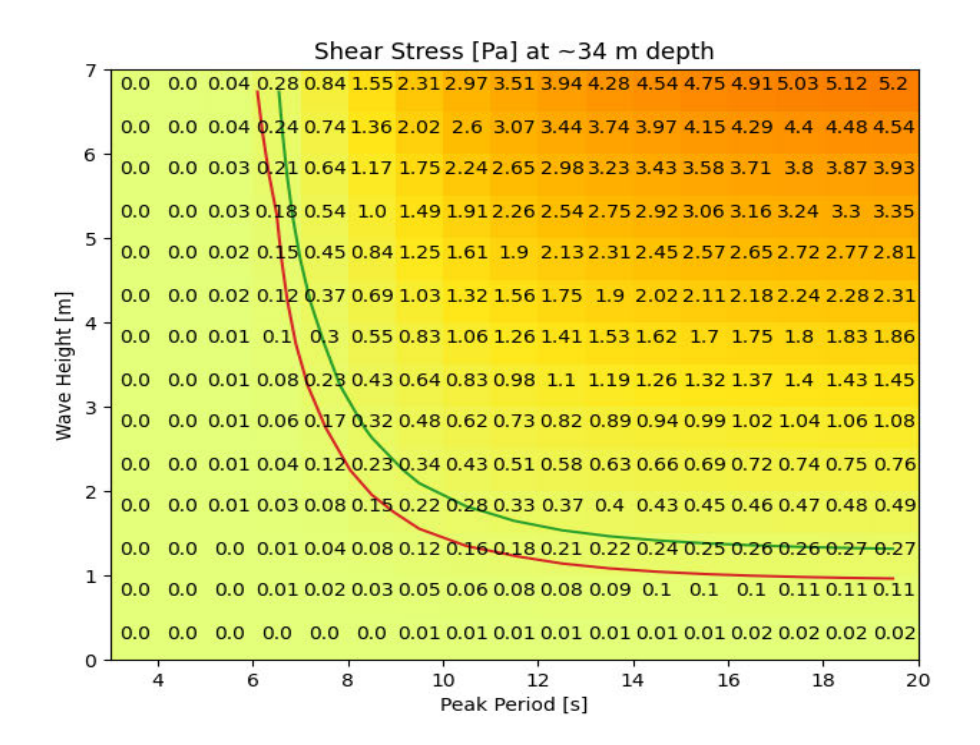
(a) Current-induced bed shear stress exceedance curve (based on Kupe platform location)

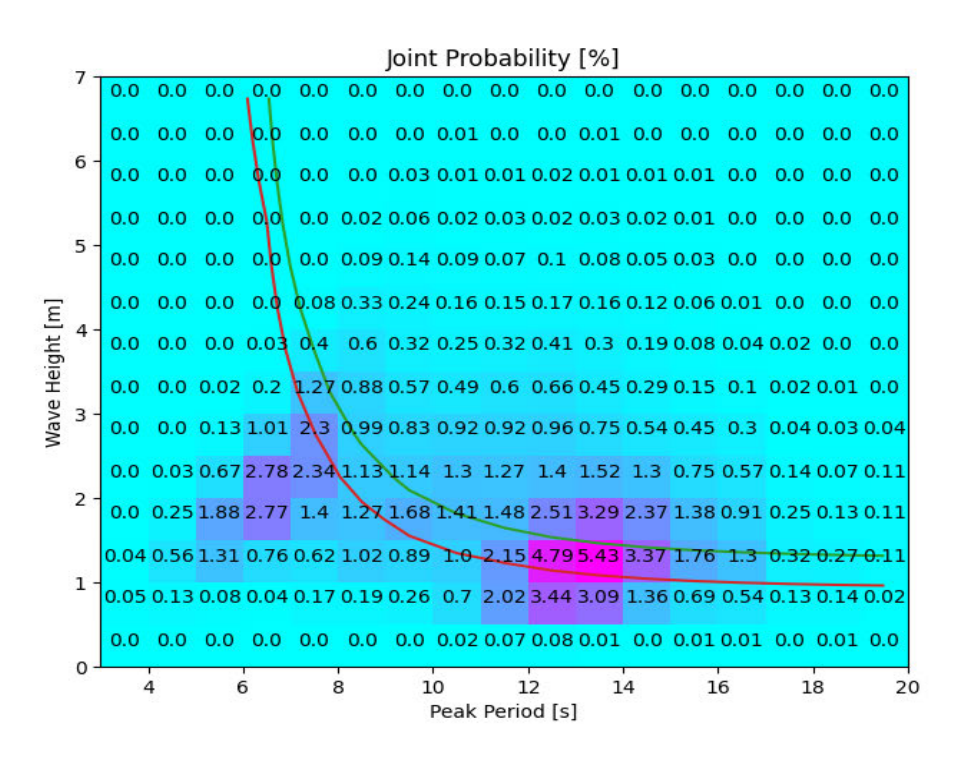


(b) Wave-induced bed shear stress exceedance curve (based on Kupe platform location)



Plate 29: Seabed Shear Stress Exceedance Curve





Left: Wave-induced bed shear stress for in situ sediment; Right: Joint probability of significant wave height and peak period. Red and green lines represent the mobility criterion for in situ and processed sediments (i.e. 0.18 Pa and 0.3 Pa respectively). Based on Kupe platform location (Oceanum, 2022).